

**ФЕДЕРАЛЬНОЕ АГЕНТСТВО НАУЧНЫХ ОРГАНИЗАЦИЙ
ФЕДЕРАЛЬНОЕ ГОСУДАРСТВЕННОЕ БЮДЖЕТНОЕ
УЧРЕЖДЕНИЕ НАУКИ
ТИХООКЕАНСКИЙ ОКЕАНОЛОГИЧЕСКИЙ ИНСТИТУТ
ИМ. В.И. ИЛЬИЧЕВА
ДАЛЬНЕВОСТОЧНОГО ОТДЕЛЕНИЯ
РОССИЙСКОЙ АКАДЕМИИ НАУК**

**V.I. IL'ICHEV PACIFIC OCEANOLOGICAL INSTITUTE
FAR EASTERN BRANCH
RUSSIAN ACADEMY OF SCIENCE**

ОКЕАНОЛОГИЧЕСКИЕ ПРОЦЕССЫ И ИЗМЕНЕНИЯ КЛИМАТА

**3-й международный российско-китайский симпозиум по морским наукам
21-23 сентября 2017 г., Владивосток, Россия**

OCEANIC PROCESS AND CLIMATE CHANGE

**The 3rd Russia-China Symposium on Marine Science
21-23 September, 2017, Vladivostok, Russia**

PROCEEDINGS

ФЕДЕРАЛЬНОЕ АГЕНТСТВО НАУЧНЫХ ОРГАНИЗАЦИЙ ФЕДЕРАЛЬНОЕ
ГОСУДАРСТВЕННОЕ БЮДЖЕТНОЕ УЧРЕЖДЕНИЕ НАУКИ
ТИХООКЕАНСКИЙ ОКЕАНОЛОГИЧЕСКИЙ ИНСТИТУТ
ИМ. В.И. ИЛЬЧЕВА
ДАЛЬНЕВОСТОЧНОГО ОТДЕЛЕНИЯ РОССИЙСКОЙ
АКАДЕМИИ НАУК

V.I. IL'ICHEV PACIFIC OCEANOLOGICAL INSTITUTE
FAR EASTERN BRANCH
RUSSIAN ACADEMY OF SCIENCE

ОКЕАНОЛОГИЧЕСКИЕ ПРОЦЕССЫ И ИЗМЕНЕНИЯ КЛИМАТА

3-й международный российско-китайский симпозиум по морским наукам

21-23 сентября 2017 г., Владивосток, Россия

Материалы докладов

OCEANIC PROCESS AND CLIMATE CHANGE

The 3rd Russia-China Symposium on Marine Science

21-23 September, 2017, Vladivostok, Russia

Proceedings

Владивосток

2017

УДК 556 (551)

Океанологические процессы и изменения климата: материалы докладов 3-го международного российско-китайского симпозиума по морским наукам, 21-23 сентября 2017 г., Владивосток, Россия – Владивосток: ДВО РАН, 2017.–118 с.

ISBN 978-5-9909943-9-3

Рассматривается широкий круг вопросов физической, химической и биологической океанологии морей Тихого океана и Арктики, включая геологическое строение океанического дна, процессы седиментации и палеоокеанологию, современную физическую океанологию и изменения климата в прошлом, минеральные морские ресурсы и процессы минералообразования, состояние морских экосистем региона.

Симпозиум проводится на базе ТОИ ДВО РАН с участием представителей ведущих научных организаций России и КНР.

Утверждено к печати ученым советом Федерального государственного бюджетного учреждения науки Тихоокеанского океанологического института им. В.И. Ильичева Дальневосточного отделения Российской академии наук (ТОИ ДВО РАН)

Oceanic process and climate change: proceedings of the 3rd Russia-China Symposium on Marine Science, 21-23 September, 2017, Vladivostok, Russia. – Vladivostok: FEB RAS, 2017. – 118 p.

ISBN 978-5-9909943-9-3

Problems of physical, chemical, and biological Pacific and Arctic oceanography were considered, including geological structure of ocean bottom, sedimentology and paleo- and modern oceanology, climate changes in the past, marine mineral resources and ecosystems.

The Symposium was held in POI FEB RAS (Vladivostok) represented by leading science organizations of Russia and China.

ISBN 978-5-9909943-9-3

© ТОИ ДВО РАН, 2017 г.



We are grateful for the support

The 3rd Russia-China Symposium on Marine Science - 2017 to:

Far Eastern Branch of the Russian Academy of Sciences

Russian Foundation for Basic Research

V.I.I'ichev Pacific Oceanological Institute

State Oceanic Administration, China (SOA)

The First Institute of Oceanography, SOA (FIO)

Chinese Arctic and Antarctic Administration (CAAA)

China Ocean Mineral Resources R & D Association (COMRA)

Russian Federation Federal Agency of Scientific Organizations

Ministry of Natural Resources and Environment of the Russian Federation

Russian Science Foundation

Organizing Committee of the 3rd Russia-China Symposium on Marine Science

Chairman:

Lobanov V.B. Director, V.I. Il'ichev Pacific Oceanological Institute, Russia
Tiegang Li Director, the First Institute of Oceanography, SOA, China

Members

Akulichev V.A. Academician of RAS, Pacific Institute of Geography, Russia
Astakhov A.S. Professor, V.I. Il'ichev Pacific Oceanological Institute, Russia
Baklanov P.Ya. Academician of RAS, Pacific Geographical Institute, Russia
Yuan Yeli Academician of the CAE, First Institute of Oceanography (FIO), SOA
Chen Yue Deputy Director, International Cooperation Department, SOA, China
Qu Tanzhou Deputy Director, Science and Technology Department, SOA, China
Dolgikh G.I. Academician of RAS, V.I. Il'ichev Pacific Oceanological Institute, Russia
Wu Jun Deputy director, Chinese Arctic and Antarctic Administration
Lei Bo Deputy director, Chinese Ocean Mineral Resources R&D association
Qiao Fangli Deputy Director, the First institute of Oceanography, SOA
Gorbarenko S.A. Professor, V.I. Il'ichev Pacific Oceanological Institute, Russia
Shi Xuefa Professor, the First institute of Oceanography, SOA
Yang Yongzeng Professor, the First institute of Oceanography, SOA
Wang Baodong Professor, the First institute of Oceanography, SOA
Li Jiabiao Academician of the CAE, the Second institute of Oceanography, SOA
Fang Guohong Academician of the CAE, First Institute of Oceanography (FIO), SOA
Wu Lixin Academician of the CAS, China Ocean University
Wang Fan Director, Institute of Oceanography, Chinese Academy of Science

**DIATOM DISTRIBUTION AND GEOCHEMICAL EVIDENCE IN THE HOLOCENE
KURILE BASIN SEDIMENTS (SEA OF OKHOTSK)**

Antonina Artemova, Valentina Sattarova, Yuriy Vasilenko

V.I. Il'ichev Pacific Oceanological Institute, Vladivostok, Russia

artemova@poi.dvo.ru

Sediments from the Kurile Basin were collected during the Russian-German deep-sea expedition SokhoBio (Sea of Okhotsk Biodiversity Studies). The abundance of biogenic and trace elements, quantitative content, and species composition of diatom assemblages in surface sediments and core samples were analyzed.

The Kurile Basin is in the southern part of the Sea of Okhotsk to the north from the Kuril Island arc (Fig. 1). The shape of the basin resembles a triangle, and its bottom is a flat abyssal plain, slightly inclined to the southeast and raised at the edges. The average depth of the basin is 3000 m, and the maximum depth reaches 3374 m. The Kuril Ridge is a natural threshold that fences the sea basin from the ocean.

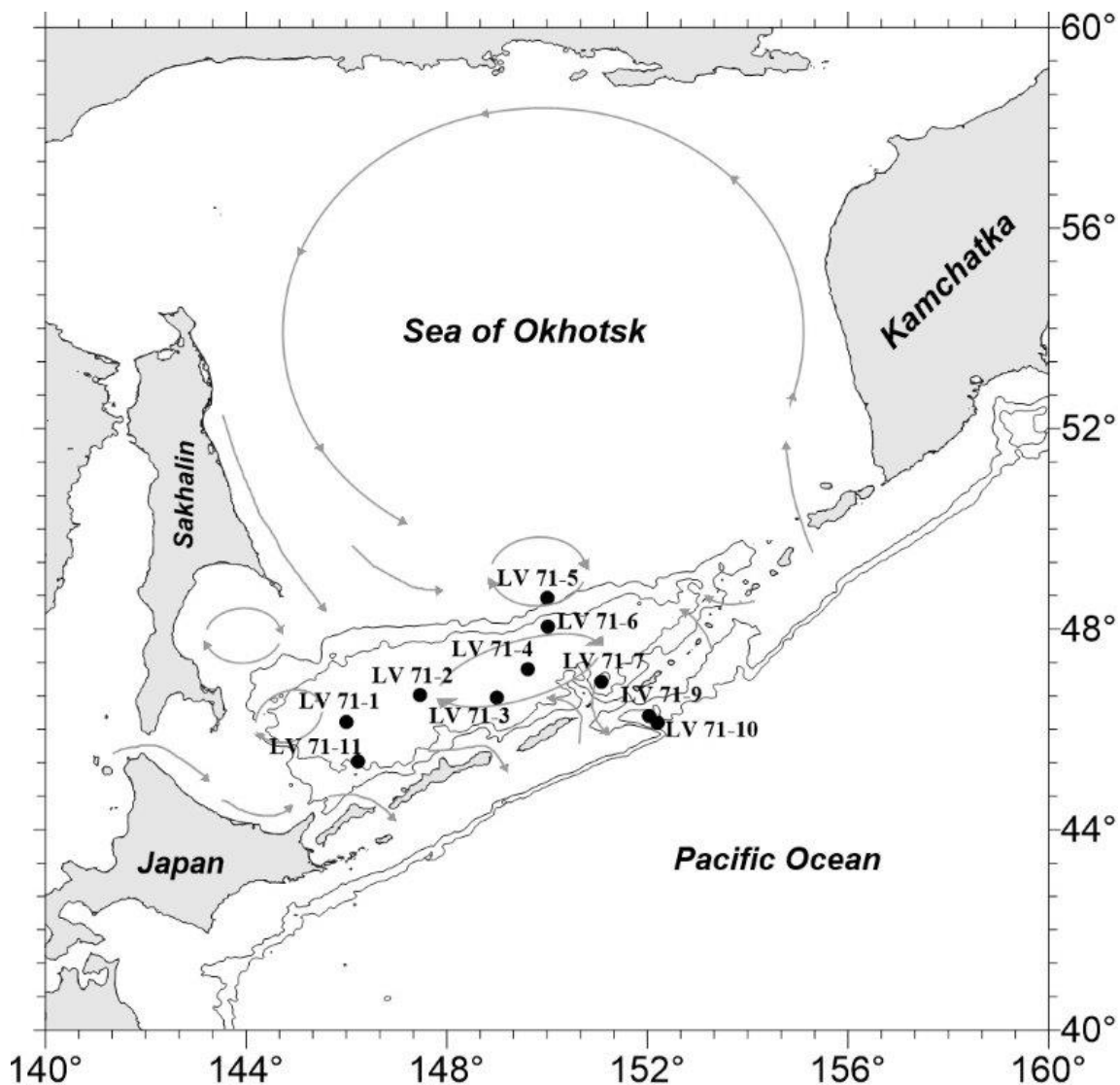


Fig. 1. Locations of sampling sediments and schematic circulation systems

The collected sediments were silt and clayey silt, with SiO_{2am} and C_{org} contents ranging from 15.85 %–36.61 % and 0.84 %–1.92 %, respectively. The spatial distribution patterns of the elements studied and the diatoms, as well as vertical profiles of the sediment cores revealed that the change in the water mass parameters and the change in the hydrological regime also affected the chemical composition of the bottom sediments over time.

The productivity and species diversity of diatoms and the chemical composition of sediments are reflections of the regional features of climatic processes.

The diatom analyses have been used for the study of the Holocene sediments in the area to the Kurile Basin. First, diatoms from the present sediments reflecting modern oceanological parameters have been studied. The key indicators reflecting climatic features were: concentration of the diatoms in the sediments and ecological structure of the diatom assemblages. Several groups of diatoms have been allocated to the description of diatom ecology in relation to a habitat and temperature.

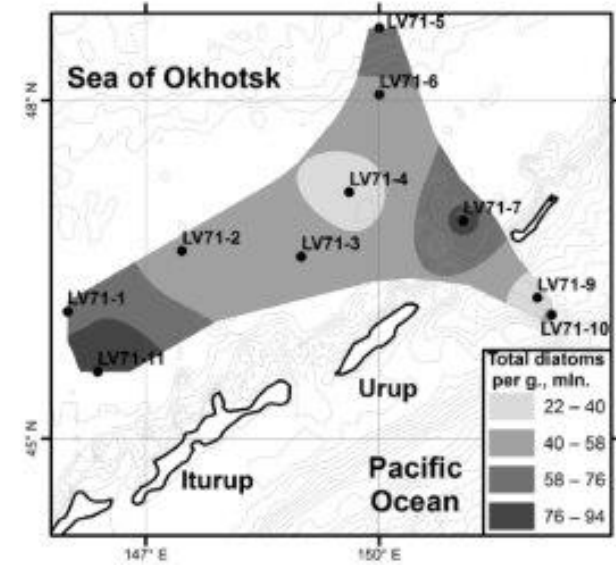
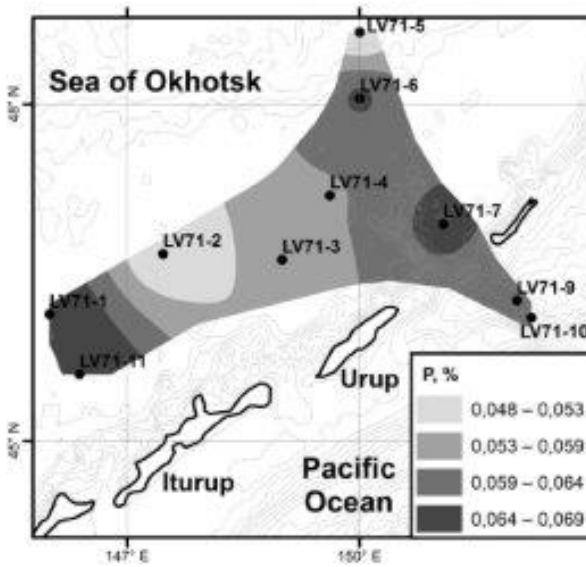
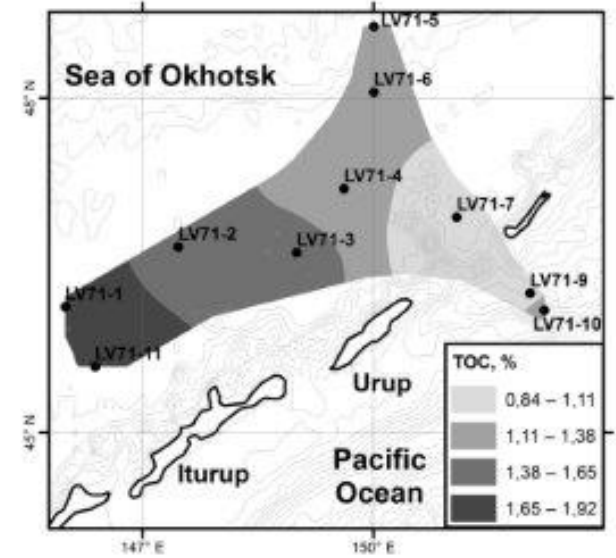
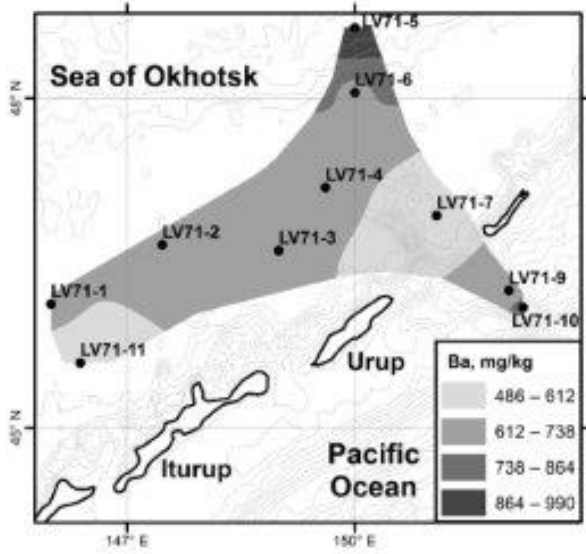
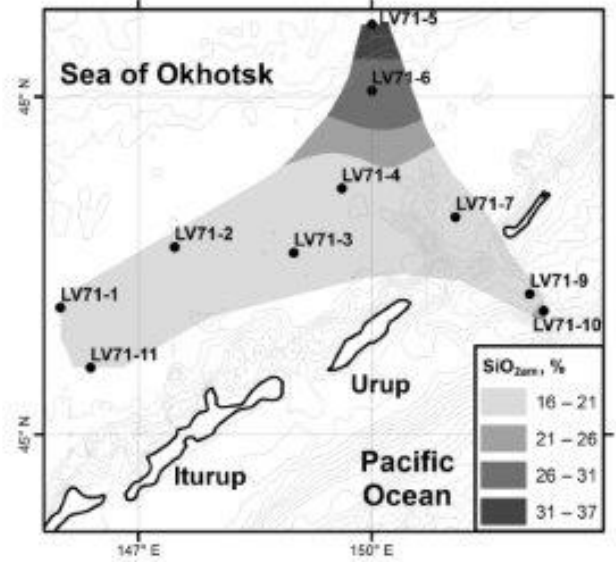
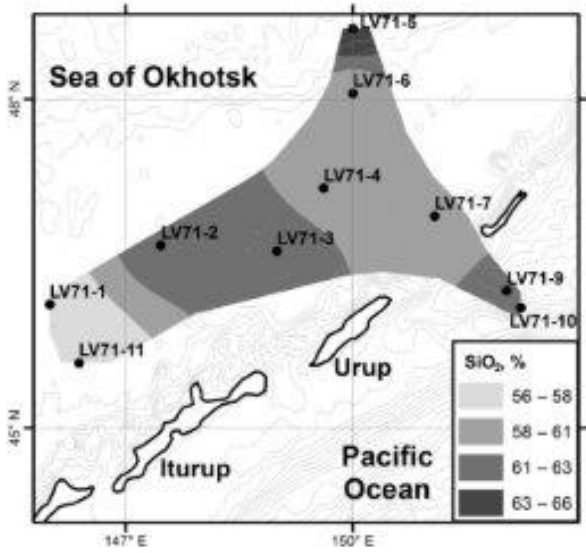
The diatoms studied are represented by 70 taxons, generally coldwater types. These taxons are open and oceanic, neritic, benthic, warm-water, coldwater, near-ice or ice species.

Quantitative distribution of diatoms in the sediments was very changeable. The largest content of the diatoms frustules was observed on the station LV71-11, LV71-7, LV71-1, assuming both high productivity of the surface waters and fragile reduction by terrigenous material. Diatoms are represented mainly by oceanic species with the best safety and longer vegetative period in comparison with the neritic species. The low amount of terrigenous material probably promoted high accumulation of the diatom frustules in these areas. The lowered abundance of the diatoms is noted at the stations LV71-4, LV71-9, and LV71-10 (Fig. 2). The stations LV71-9 and LV71-10 are in the zone of a trench of terrigenous material from the Kuril Islands and biogenic material probably streams by the sandy material.

Oceanic *Shionodiscus latimarginatus*, *Thalassiothrix longissima*, *Rhizosolenia hebetata* f. *hiemalis*, *Coscinodiscus marginatus*, *Neodenticula seminae* are dominated there.

Within each station, certain features are noted. Stations LV71-1 and LV71-11, which are nearby, differ in the predominance of oceanic species, up to 100 %. Additionally, these sediments are marked by high species content. There are dominant *S. latimarginatus* (up to 24.3 %), *Thalassionema nitzschioides* (up to 19.3 %), *N. seminae* (up to 15 %), *R. hebetata* f. *hiemalis* (up to 10 %), *Thalassiosira excentrica* (up to 11 %), *Actinocyclus curvatulus* (up to 10 %), and others.

Station LV71-2 is marked by the appearance of neritic species (up to 17 %). Oceanic species predominate (up to 85 %). The dominant species are *S. latimarginatus*, *T. longissima*, *R. hebetata* f. *hiemalis*, *Coscinodiscus oculus-iridis* Ehrenberg, *T. nitzschioides*, *Bacterosira bathyomphala*.



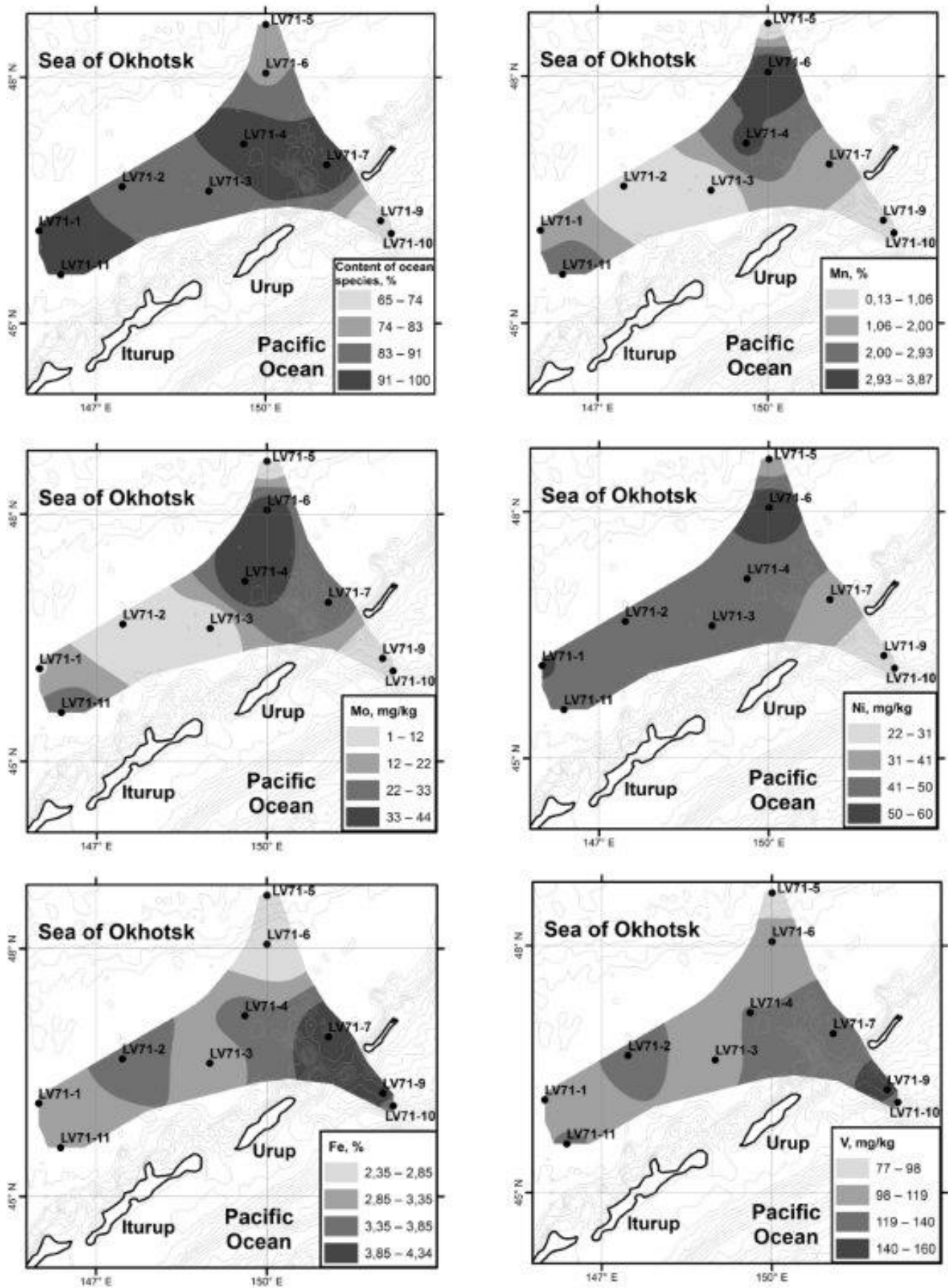


Fig. 2. Distribution of concentrations of chemical elements and diatom in surface sediment samples.

At the LV71-3 station, the guiding species are *A. curvatulus*, *N. seminae*, *R. hebetata* f. *hiemalis*, *Thalassiosira gravida*, *S. latimarginatus*, *T. longissima*. Single frustules of freshwater species of the genus *Aulacoseira* appear in the sediment, as well as a high content of silicoflagellate.

The station LV71-4 is marked by the prevalence of open oceanic species and dominant in the sediments are *T. longissima* and *R. hebetata* f. *hiemalis*. At station LV71-5 and LV71-6, an increase in the content of diatoms is noted, the share of oceanic species decreases, and the assemblage is dominated by *A. curvatulus*, *R. hebetata* f. *hiemalis*, *Thalassiosira excentrica*, and *T. gravida*.

At station LV71-7, like the previous stations of the diatom assemblages, an increase in the proportion of the species *Neodenticula seminae* was noted.

The stations LV71-9 and LV71-10, located on the Pacific side behind the Kuril Islands, are marked by the addition of neritic and benthic flora to the controlling assemblages of oceanic species, and spores of the genus *Chaetoceros* sp. and *Odontella aurita* are found in the sediment.

In general, the results obtained show the ratio of different ecological groups of diatoms in the surface sediments of the Sea of Okhotsk. The predominance of open-ocean species is observed in the sediments of the bottom of the basin, and the mixed oceanic-neritic composition of diatoms is characteristic of slope deposits. Additionally, the assemblages reflect the influence of the Pacific Ocean water masses at the stations close to the Kurile Straits and the warm waters of the Sea of Japan at the station in the Soya Current zone. The highest content of diatoms was observed in surface sediments in areas with a weak dilution of terrigenous material. Diatoms are represented here mainly by oceanic species, a longer growing season and better preservation of which, compared with the neritic ones, and a low amount of terrigenous material, probably contributes to a large accumulation of diatoms in the sediments of this area.

Modern sediments of the deep-sea basin of the Sea of Okhotsk are marked by abundant diatoms content. The number of diatoms in the sediments is affected by the location and hydrological conditions of flowering. High diatoms content is probably due to low terrigenous dilution and the formation of clayey silt. The diatom flora of the studied sediments is characterized by a high number of oceanic cold-water species.

Diatoms in the sediments of the central and western parts of the basin where the depths exceed 3 000 m are mainly represented by oceanic species (up to 100 %).

Additionally, the influence of Pacific water masses is reflected in the complexes at the stations close to the Kuril Straits and warm waters from the Japan Sea at the stations in the zone of the Soya Current. The high diatoms content is characteristic of the highly productive areas of the sea. The maximum concentrations of organic carbon, barium and partially biogenic silica and microelements are characteristic for this area, confirming the high productivity of siliceous

phytoplankton. At the same time, it should be noted that the predominance of ocean species in the sediments of the continental slope of this area may reflect the influence of Pacific waters and the longer growing season and better preservation of ocean diatoms, compared with the neritic ones (Semina, Jouse, 1959), also contributing to their greater accumulation in sediments.

The work was supported by the Russian Science Foundation (Project no. 14-50-00034), by the Russian Foundation for Basic Research (Grant no. 16-04-01431-a, 16-35-60019 mol_a_dk)

ICE CONDITIONS OF THE LAST CENTURIES IN THE NORTHERN CHUKCHI SEA: RECONSTRUCTIONS USING DETAILED VARIATION OF CHEMICAL COMPOSITION IN SHELF SEDIMENTS

Anatoly Astakhov¹, Yanguang Liu², Andrey Dar'in³, Ivan Kalugin³, Aleksandr Bosin¹, Elena Vologina⁴

¹ V.I. Il'ichev Pacific Oceanological Institute, FEB RAS, Vladivostok, Russia

² First Institute of Oceanography, SOA, Qingdao, China

³ V.S. Sobolev Institute of Geology and Mineralogy, SB RAS, Novosibirsk, Russia

⁴ Institute of the Earth's crust, SB RAS, Irkutsk, Russia

astakhov@poi.dvo.ru

In recent decades, there has been a significant increase in the area of ice-free water areas in the Arctic Ocean during the summer-autumn period. The rate of this process greatly exceeds the predictive models based on the content of greenhouse gases in the atmosphere due to human activity. Therefore, there is a necessity to develop models that take into account the cyclicity of natural processes or completely based on it. The maximum rate of change in ice conditions over the observation period was recorded in the northern part of Chukchi Sea and in the northeastern part of the East Siberian Sea (Fig. 1).

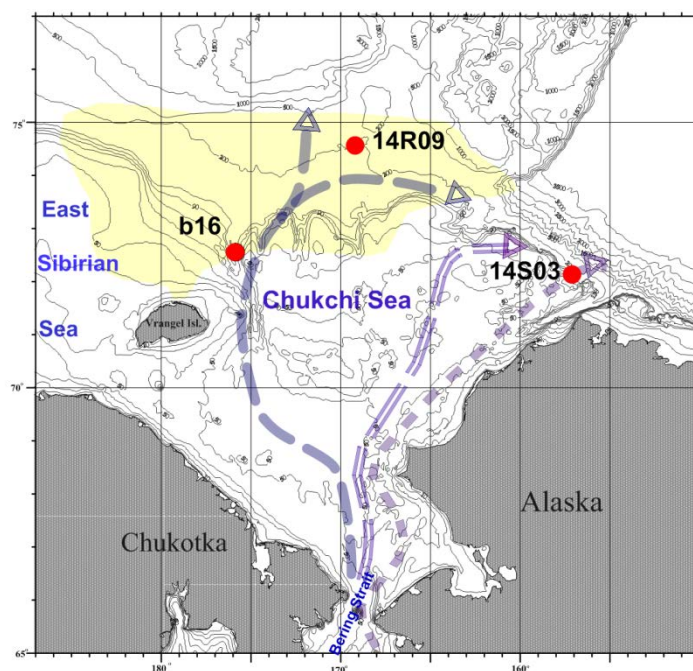


Fig. 1. Locations of studied cores.

Yellow fill shows the area of maximum changes in the concentration of ice in September 2004-2013 compared to 1980-1989 [1], dashed lines with arrows - the ways of distribution in the Chukchi Sea of various branches of warm Pacific waters (according to [2]).

It is assumed that the possible reasons for this may be: a) an increase in atmospheric heat transfer from the Bering Sea region to the north; b) a strengthening of salt and heat transfer from

Bering to the Chukchi Sea via the Bering Strait [2]; c) the rise of relatively warm intermediate Atlantic waters penetrating into the Amerasian basin along the continental slope of Eurasia [3].

Shelf sediments of the Arctic seas are substantially impoverished by biogenic components, which reduce the possibility of using them for paleoreconstructions. In this regard, the aim of this work is to determine the possibility for quantitative reconstruction of changes of the environment and ice cover of the Arctic shelf based on detailed variation in the chemical composition of the bottom sediments. The possibility of such reconstruction is determined by analysis of sediment cores accumulated during the period of instrumental observations. The data from scanning X-ray fluorescence with synchrotron radiation (XRF-SR) at 0.5-0.8 mm resolution allow us to compare chemical composition of sediment cores with measured hydrometeorological characteristics during the last 60-100 years, and to develop the calibration models linked individual hydrometeorological parameters and chemical composition of sediments using the multiple regression method [4].

For our research we chose three sediment cores recovered in the northern part of the Chukchi Sea (Fig. 1), where a significant increase in the duration of the ice-free period (IFP) over the last 20 years was noted (Fig. 2). The age models of the cores are based on sedimentation rates calculated from disequilibrium ^{210}Pb , calculated from the model of constant initial concentration [5]. In the cores b16, 14R09, and 14S03 sedimentation rates are 0.9, 0.4 and 1.7 mm / year, respectively. XRF-SR data were normalized to rubidium for elimination of the effect of different water content and grain-size composition of the sediment. The distribution of biogenic (Br, Ca, Sr, TOC, CaCO_3 , SiO_2) and redox-sensitive (Mn, Fe) elements throughout the cores (Fig. 2) is well comparable with variations in the global climate and reflects degradation of ice cover in this region over the last 20-30 years (Fig. 2).

Figure 2 presents examples of calibration models calculated from the series of geochemical data and series of observations of ice cover and average annual air temperature at the corresponding points. Developed models of the temperatures of the near-ground atmosphere show a good correlation (0.89) with instrumental data during the calibration period, as well as with the paleotemperature record [6] in the Northern Hemisphere (0.58). Models of the duration of the IFP for cores b16, 14R09, and 14S03 correlate well with observation data during 1950-1999 (0.99, 0.85, and 0.87, respectively).

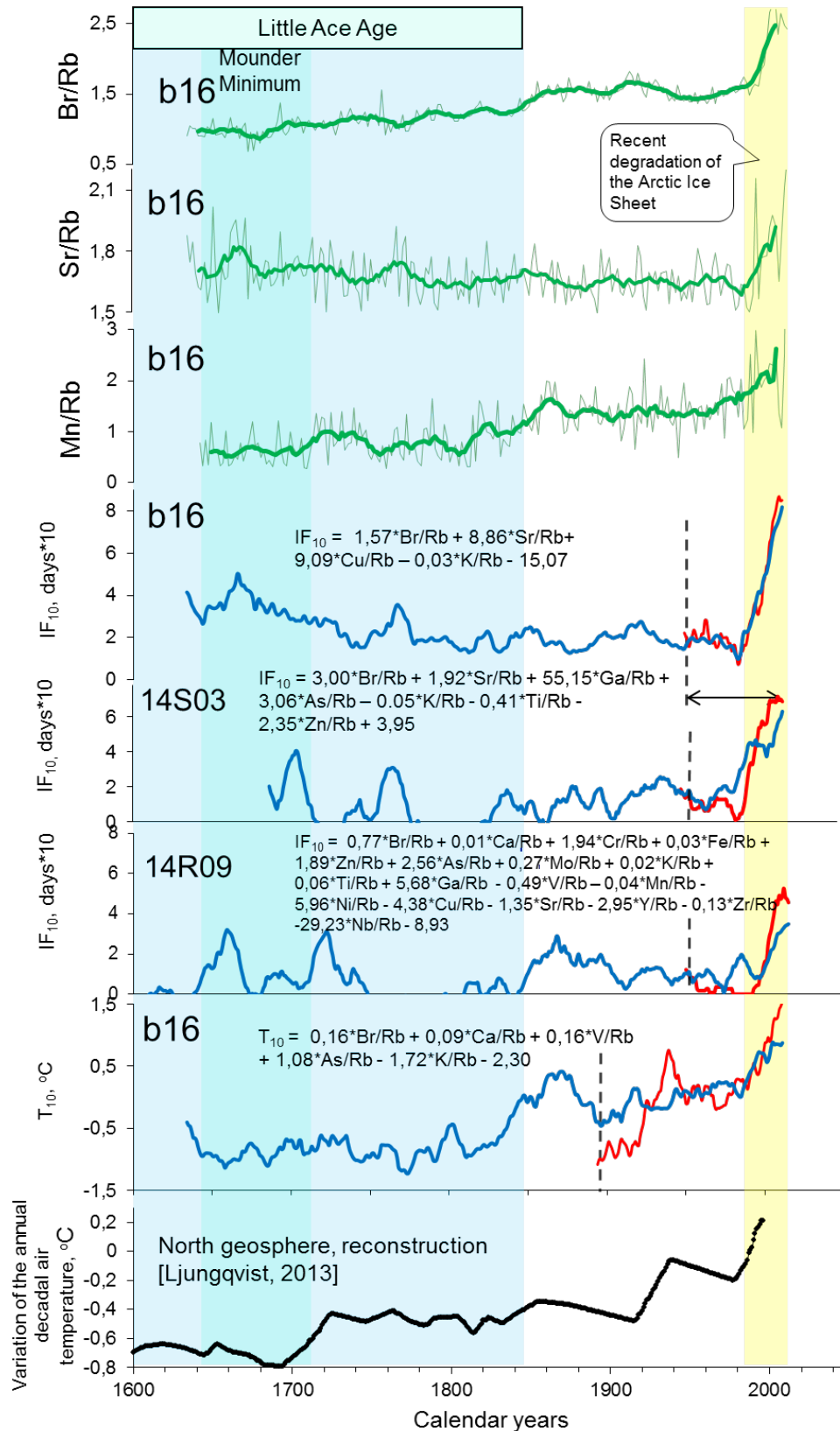


Fig. 2. Records of biogenic and redox-sensitive elements in core b16, time series of observed (red line) and reconstructed (blue line) parameters of the environment in three cores (IF₁₀ - duration of IFP, T₁₀ - average annual air temperature). Models of calculation of the environmental parameters are based on data of the chemical composition of sediment. Vertical dashed lines - the time of the beginning of observation of environmental parameters (the period used to develop the calibration model).

Reconstruction of ice conditions for the last 400 years based on three cores from the northern part of the Chukchi Sea revealed an increase in the duration of IFP during the Maunder Minimum, the main cooling period of the Little Ice Age. Taking into account the position of the studied cores, the supply of warm Pacific waters through the Bering Strait may be the possible reason for the mismatching of the ice conditions and global temperature variations. For example, the increase in the duration of IFP in the northern part of the Chukchi Sea in recent decades is well comparable to the increase in the inflow of warm Pacific waters, revealed by instrumental observations in the Bering Strait [7]. The increase in the Pacific water supply to the Arctic during the Maunder Minimum is probably caused by the balancing of decrease of Atlantic waters supply due to the slowdown of the Gulf Stream at that period.

The work was supported by the Russian Science Foundation (project No. 16-17-10109).

REFERENCES:

1. Wood K.R., Wang J., Salo S.A., Stabeno P.J. The Climate of the Pacific Arctic During the First RUSALCA Decade 2004-2013 // *Oceanography*. 2015. V. 28(3). P. 24-35.
2. Grebmeier, J.M. Biological community shifts in Pacific Arctic and sub-Arctic seas // *Annual Review of Marine Science*. 2012. V. 4. P. 63-78, doi: 10.114/annurev-marine-120710-100926.
3. Wang R., Xiao W. S., März C., Li Q. Late Quaternary paleoenvironmental changes revealed in multi-proxy records from the Chukchi Abyssal Plain, western Arctic Ocean // *Global and Planetary Change*. 2013. V. 108. P. 100–118.
4. von Gunten L., Grosjean M., Kamenik C., Fujak M., Urrutia R. Calibrating biogeochemical and physical climate proxies from non-varved lake sediments with meteorological data: methods and case studies // *Journal of Paleolimnology*. 2012. V. 47. P. 583-600.
5. Vologina, E.G., Sturm, M., Kalugin, I.A., Darin, A. V., Astakhov, A.S., Chernyaeva, G.P., Kolesnik, A.N., Bosin, A.A., 2016. Reconstruction of the conditions of Late Holocene sedimentation by integrated analysis of a core of the bottom sediments from the Chukchi Sea. *Dokl. Earth Sci.* 469, 841–845. doi:10.1134/S1028334X16080183.
6. Ljungqvist, F.C., 2010. A new reconstruction of temperature variability in the extra-tropical northern hemisphere during the last two millennia. *Geogr. Ann. Ser. A, Phys. Geogr.* 92, 339–351. doi:10.1111/j.1468-0459.2010.00399.x.
7. Woodgate R.A., Stafford K.M., Prah F.G. A Synthesis of Year-Round Interdisciplinary Mooring Measurements in the Bering Strait (1990–2014) and the RUSALCA Years (2004–2011), *Oceanography*, 2015, 28(3), 46-67.

GOLD, SILVER AND PLATINUM IN FERROMANGANESE CRUSTS FROM MARGINAL SEAS OF THE NORTHWEST PACIFIC

Nadezhda Astakhova

V.I. Il'ichev Pacific Oceanological Institute, FEB RAS, Vladivostok, Russia

n_astakhova@poi.dvo.ru

Ferromanganese mineralization is widely abundant in the marginal seas of the Northwest Pacific. Many ore crusts were collected during dredging of the slopes of most of volcanic seamounts rising above the flattened surface of the deep basins of these seas. The concentration of Mn in them, especially in the Sea of Japan, reaches 50–63%, which is significantly higher than in oceanic crusts. The concentration of nonferrous metals is low, but these FMCs contain numerous inclusions of grains of noble and nonferrous metals as native elements, intermetallic compounds, sulfides, sulfates, oxides, tungstates, molybdates, or phosphides [1–3].

The problem of noble metals in FMC of the World Ocean was not finally solved. Some researchers suggest that noble and nonferrous metals are incorporated in FMCs as a result of precipitation from water column due to sorption or microbial processes. Others relate incorporation of these metals to hydrothermal processes or fluid emanations associated with basalt.

In this paper, we compare data on the concentration of noble metals (Au, Ag, Pt, Os, Ir, and Ru) in bulk FMC samples from the Sea of Okhotsk, Sea of Japan, and Vityaz' Ridge on the oceanic slope of the Kuril island arc. Based on these data and results of microprobe analysis, we consider the problem of the sources of these metals in FMCs from the marginal seas of the Northwest Pacific (Fig.).

FMCs from the marginal seas of the Northwest Pacific are characterized by significant dispersal in the concentration of noble metals, even in samples collected at the same station. With allowance for the fact that ferromanganese mineralization in this region formed in the Late Cenozoic, i.e., all samples of FMCs are relatively young, we cannot consider seawater as the only source of these metals. Although occurrences of noble metal mineralization, mostly Au–Ag, are widely abundant on the coastal areas of these seas, we can suggest a high concentration of these metals in seawater.

Variability in the chemical composition of grains of noble metals found in FMCs from the marginal seas of the Northwest Pacific (Tables) and their chaotic distribution prevent the consideration of seawater as the only source of these metals. Ferromanganese mineralization in the marginal seas of the Northwest Pacific almost ubiquitously occurs at the top parts and calderas of volcanic seamounts. Study of gas emissions of modern volcanic systems of the Kuril–Kamchatka region shows that they introduce minor contents of many metals (Au, Ag, Pt, Bi, Te, etc.) into host

rocks. Micro- and nanosized inclusions of Au and Pt were detected in the sublimation products of these fluids [4, 5].

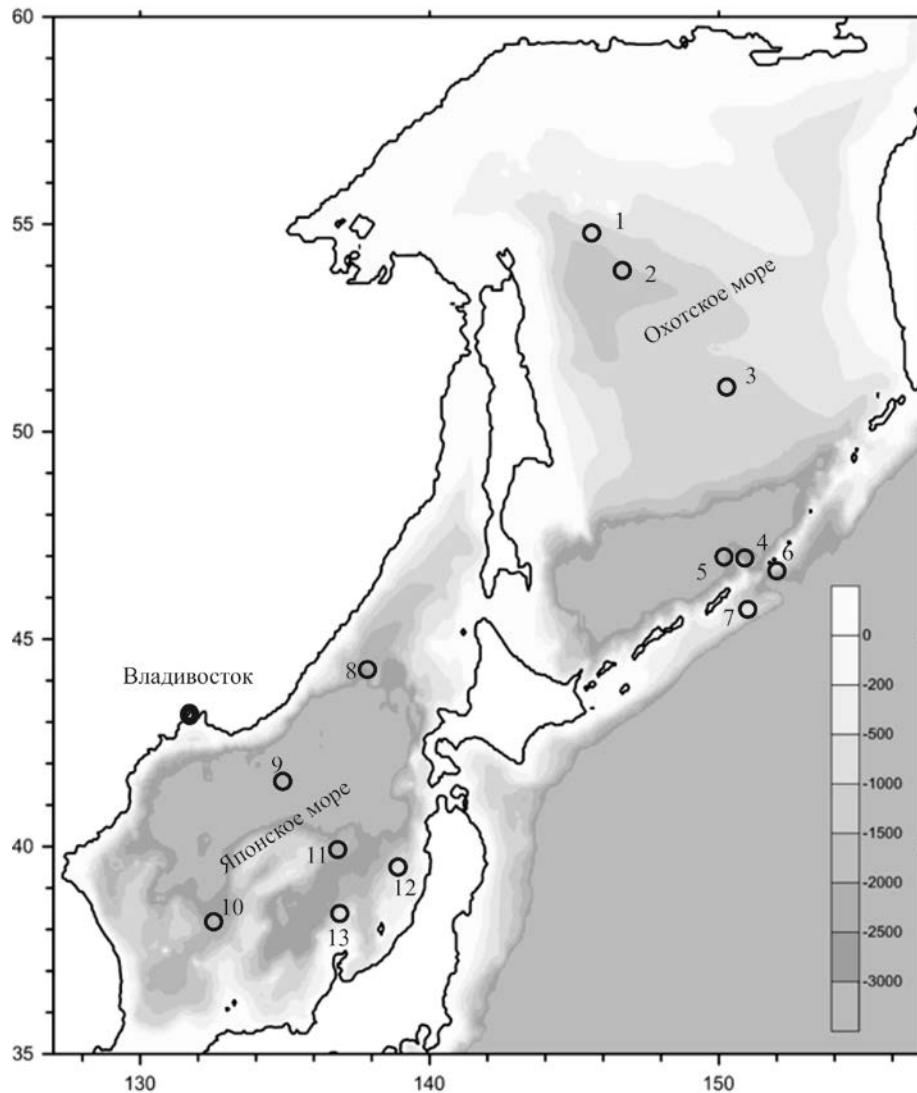


Fig. Schematic map of actual material. Circles show location of regions with ferromanganese mineralization. (1) slope of Kashevarov bank; (2) Deryugin Trough; (3) Academy of Sciences Rise; (4) Vavilov Rise; (5) Obruchev Rise; (6) Diana survey area; (7) Bussol' survey area; (8) Bezymianny Rise; (9) Belyaevskii Rise; (10) Galagan Rise; (11) superposed edifice on South Yamato Rise; (12) Matsu Rise; (13) Medvedev Rise.

Study of fluids captured by inclusions upon crystallization of minerals in modern hydrothermal fields of the Mid-Atlantic Ridge shows that, in addition to other metals, they may contain Au, Ag, Pd, and Bi [6].

Thus, we can suggest with a high degree of confidence that some noble metals were introduced with postvolcanic gaseous hydrothermal fluids that filtered through magmatic rocks and other formations of volcanic edifices and reached the surface of the floor. It is possible that some nanosized grains could have been transported with gaseous flows as aerosols; i.e., this process might be overprinted on ferromanganese mineralization. Since introduction of gaseous fluids proceeds along fractures, precipitation of introduced metals will mostly occur in porous areas.

Table. Concentration of noble metals in FMCs from marginal seas of Northwest Pacific (Au– Pt in ppb)

	Region	Au	Ag	Pt	Composition of grains of noble metals
Sea of Okhotsk					
1	1	4,9	240	864,8	Ag, Ag-S
2		0,8	150	227,9	Ag, Ag-S
3	2	0,2	16	506,9	Au, Au-Cu, Au-Cu-Ag, Ag, Ag-S, Ag-S-O
4	3	2,5	74	424,0	Ag, Ag-Rh
5	4	9,4	180	854,8	n.a.
6	5	0,4	130	484,5	n.a.
Vityaz' Ridge (oceanic slope of Kuril island arc)					
7	6	0,9	140	46,9	Ag, Ag-S, Ag-Cu, Pd-W-O
8	7	2,8	700	87,4	Au, Au-Ag, Au-Ag-Ni, Au-Ni, Ag, Ag-Te, Ag-S, Pt-Cu, Pt-Zn-Cu, Pd-Ag
Sea of Japan					
9	8	3,8	300	438,5	Ag, Ag-Cu, Pd-Pt-Cu, Pd -Bi-Cu-Pt, Pd- Cu
10	9	3,6	20	197,5	Ag
11	10	2,7	300	297,2	Ag, Pt-Pd, Pd-Pt -Cu-Bi, Pd-Pt-Cu, Pd-Cu-Ni, Pd-Cu-Zr
12		0,8	11	366,0	Ag, Ag-S
13	11	0,3	84	42,6	Ag, Ag-Cu-Zn
14	12	7,0	10	2302,1	Rh- Au-Cu-Ag, Ag, Pd-Pt-Bi-Cu , Pd-Cu-Zr
15	13	2,4	2	0	n.a.
16		1,4	22	178,3	Ag
17		5,3	22	620,8	Ag, Ag-Te, Ag-S

REFERENCES:

1. Astakhova N. V. Precious and nonferrous metals in the ferromanganese crusts of the central Sea of Okhotsk // *Oceanology* (Engl. Transl.). 2009. V. 49. № 3. P.405–417.
2. Astakhova N. V. Occurrence forms and distribution of precious and base metals in ferromanganese crusts from the Sea of Japan // *Oceanology* (Engl. Transl.). 2013. V. 53. № 6. P., 686–701.
3. Astakhova N. V. and Lelikov E. P. The specifics of ferromanganese ore formation on the submarine Vityaz' Ridge (Pacific slope of the Kuril island arc) // *Russ. Geol. Geophys.* 2013. V. 54. № 5. P. 518–525.
4. Vergasova L. P., Starova G. L., Serafimova E. K., et al. The native gold of volcanic exhalations of slag cones of the large fracture of Tolbachinskoe eruption//*Vulkanol. Seismol.* 2000. № 5. P. 19–27.
5. Distler V. V., Yudovskaya M. A., Znamenskii V. S., and Chaplygin I. V. Platinum group elements in modern fumaroles of the Kudryavyi Volcano, Iturup Island, Kuril Island arc // *Dokl. Earth Sci.* 2002. V. 387. P. 975–978.
6. Bortnikov N. S., Simonov V. A., Amplieva E. E., and Borovikov A. A. Anomalously high concentrations of metals in fluid of the Semenov modern hydrothermal system (Mid-Atlantic Ridge, 13°31' N): LA-ICP-MS study of fluid inclusions in minerals // *Dokl. Earth Sci.* 2014. V. 456. P. 714–719.

DISCOVERY AND CHARACTERIZATION OF SUBMARINE GROUNDWATER DISCHARGE IN THE BUOR-KHAYA GULF, LAPTEV SEA

Alexander Charkin^{1,2}, Michiel Rutgers van der Loeff³, Natalia Shakhova^{2,4}, Örjan Gustafsson⁵, Oleg Dudarev^{1,2}, Maxim Cherepnev², Anatoly Salyuk¹, Andrey Koshurnikov⁶, Eduard Spivak¹, Alexey Gunar⁶, Alexey Ruban², Igor Semiletov^{1,2,4}

¹. V.I. Il'ichev Pacific Oceanological Institute, FEB RAS, Vladivostok, Russia

². National Research Tomsk Polytechnic University, Russia

³. Alfred-Wegener Institute, Helmholtz Center for Polar and Marine Research, Bremerhaven, Germany

⁴. International Arctic Research Center (IARC), University of Alaska, Fairbanks, USA

⁵. Dept. of Environmental Science and Analytical Chemistry, and the Bolin Centre for Climate Research, Stockholm University, Stockholm, Sweden

⁶. Moscow State University, Russia

charkin@poi.dvo.ru

It has been suggested that increasing terrestrial water discharge to the Arctic Ocean may partly occur as submarine groundwater discharge (SGD), yet there are no direct observations of this phenomenon in the Arctic shelf seas. This study tests the hypothesis that SGD does exist in the Siberian-Arctic shelf seas, but its dynamics may be largely controlled by complicated geocryological conditions such as permafrost. The field-observational approach in the southeast Laptev Sea used a combination of hydrological (temperature, salinity), geological (bottom sediment drilling, geoelectric surveys), and geochemical (^{224}Ra , ^{223}Ra , ^{228}Ra and ^{226}Ra) techniques. Active SGD was documented in the vicinity of the Lena River delta with two different operational modes. In the first system, groundwater discharges through tectonogenic permafrost talik zones was registered in both winter and summer. The second SGD mechanism was cryogenic squeezing out of brine and water-soluble salts detected on the periphery of ice hummocks in the winter. The proposed mechanisms of groundwater transport and discharge in the arctic land-shelf system is elaborated. Through salinity versus ^{224}Ra and $^{224}\text{Ra}/^{223}\text{Ra}$ diagrams, the three main SGD-influenced water masses were identified and their end-member composition was constrained. Based on simple mass balance box models, discharge rates at site in the submarine permafrost talik zone were $1.7 \times 10^6 \text{ m}^3 \text{ d}^{-1}$ or $19.9 \text{ m}^3 \text{ s}^{-1}$, which is much higher than the April discharge of the Yana River. Further studies should apply these techniques on a broader scale with the objective of elucidating the relative importance of the SGD transport vector relative to surface freshwater discharge for both water balance and aquatic components such as dissolved organic carbon, carbon dioxide, methane, and nutrients.

EVALUATION ON ISLAND ECOLOGICAL VULNERABILITY AND ITS SPATIAL HETEROGENEITY

Yuan Chi, Honghua Shi

First Institute of Oceanography, SOA, Qingdao, China

chiyuan@fio.org.cn

The evaluation on island ecological vulnerability (IEV) can help reveal the comprehensive characteristics of the island ecosystem and provide reference for controlling human activities on islands. An IEV evaluation model which reflects the land–sea dual features, natural and anthropogenic attributes, and spatial heterogeneity of the island ecosystem was established, and the southern islands of Miaodao Archipelago in North China were taken as the study area. The IEV, its spatial heterogeneity, and its sensitivities to the evaluation elements were analyzed. Results indicated that the IEV was in status of mild vulnerability in the archipelago scale, and population pressure, ecosystem productivity, environmental quality, landscape pattern, and economic development were the sensitive elements. The IEV showed significant spatial heterogeneities both in land and surrounding waters sub-ecosystems. Construction scale control, optimization of development allocation, improvement of exploitation methods, and reasonable ecological construction are important measures to control the IEV.

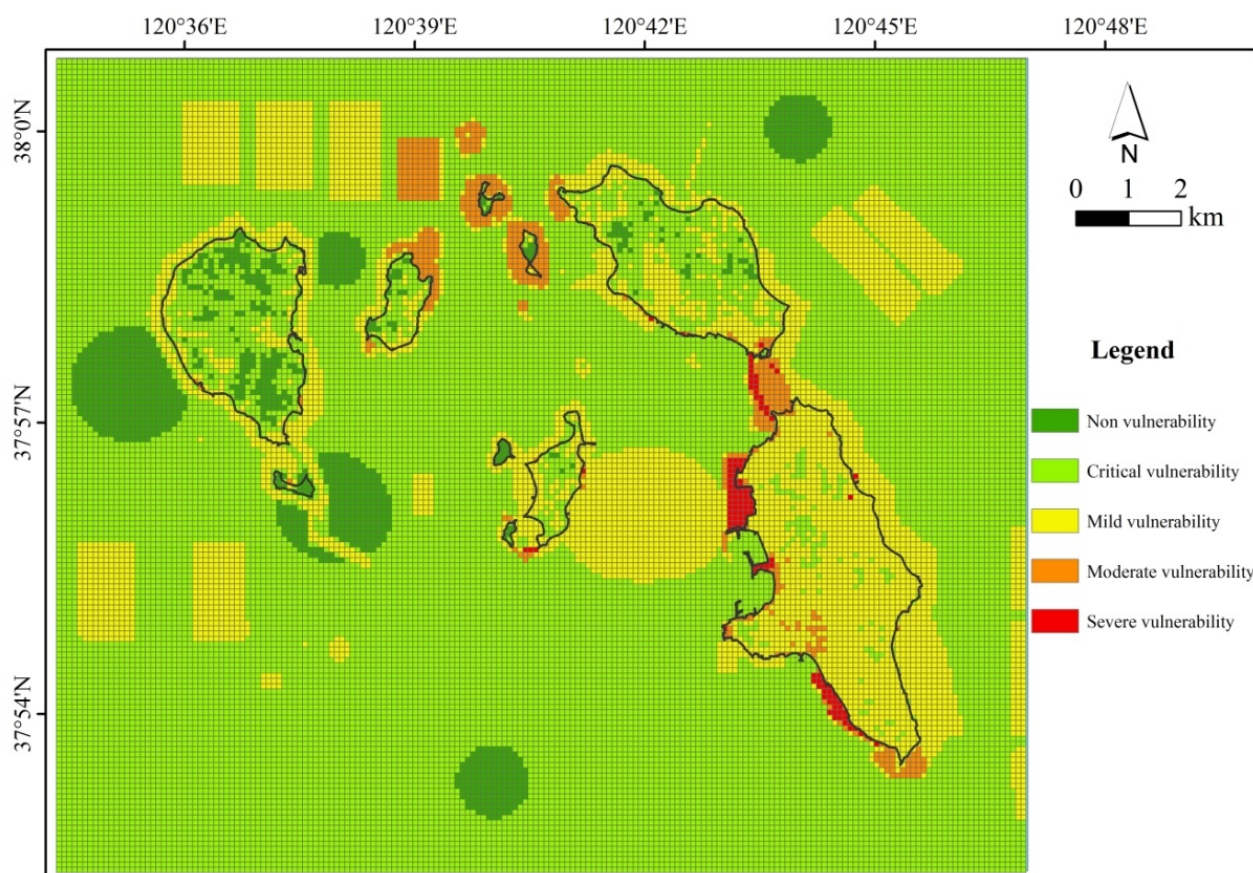


Fig. Spatial heterogeneity of IEV in southern islands of Miaodao Archipelago in North China

**NEW DATA ON TEPHROSTRATIGRAPHY OF HOLOCENE-PLEISTOCENE DEPOSITS
FROM THE NORTH-WEST PACIFIC (on the basis of the materials of 76th Cruise of the
R/V "Akademik M.A. Lavrentyev")**

**Alexander Derkachev¹, Sergey Gorbarenko¹, Maxim Portnyagin^{2,3}, Nataliya Nikolaeva¹,
Xuefa Shi⁴, Yanguang Liu⁴**

¹ V.I. Il'ichev Pacific Oceanological Institute, FEB RAS, Vladivostok, Russia

² V.I. Vernadsky Institute of Geochemistry and Analytical Chemistry, RAS, Moscow, Russia

³ GEOMAR Helmholtz Centre for Ocean Research, Wischhofstrasse, 3, Kiel, Germany

⁴ First Institute of Oceanography, SOA, Qingdao, China

derkachev@poi.dvo.ru

Volcanic ash (tephra) interlayers discovered in the land deposits as well as in the surrounding seas and ocean are one of the reliable indicators of the manifestation of large explosive volcanic eruptions within the continent-ocean transition zone. They are very effective markers for stratigraphic study of sedimentary strata and for dating of past events [1-5 and many others].

The results of expeditionary researches carried out in 2016 (76th Cruise of the R/V "Akademik M.A. Lavrentyev") in accordance with the agreement on cooperation between the Pacific Oceanological Institute of FEB RAS (POI DVO, Vladivostok, Russia) and the First Oceanographic Institute (FIO, Qingdao, PRC) were used for this report. The tephra layers were found and studied in 9 sediment cores taken in the northern part of the Emperor Range (the Detroit Rise and Tenji Rise). In sedimentary succession with the thickness of up to 8.5 m, 46 interlayers and 18 lenses of tephra were discovered.

The work was based on the results of high-quality microprobe (EPMA) chemical analyzes (785 analyzes of volcanic glasses) performed by the authors on an electronic microprobe JEOL JXA 8200 (GEOMAR-Helmholtz Center for Ocean Research, Kiel, Germany). Most of the tephra interlayers have been studied. In this report, we present preliminary results of complex study of ashes (particle morphology, chemical composition of volcanic glasses), and their age rating is given.

The data of microprobe chemical analyzes allowed with a high probability to correlate the studied sediment cores: 8 regional tephrostratigraphic marking horizons were established. The study of smear-slides under a microscope and a number of physical parameters of sediments (magnetic susceptibility, color characteristics - color b*, color intensity-CL) allowed to estimate the preliminary age of sediments in studied cores, based on the known age scales of Holocene-Pleistocene deposits in this region (ODP 882, MD01-2416, MD01-2417) [6, 7].

Schemes of the tephrostratigraphic correlation of the Holocene-Pleistocene deposits are proposed for the studied region. The conducted researches supplement the information on the strong eruptions of the volcanoes in this region; they are the basis for both the development of the

generalized tephrochronological scale of Quaternary deposits in this region, which is necessary for stratigraphic correlation of deposits, and for estimation of natural changes caused by these eruptions and for paleoceanological and paleogeographic reconstructions.

This work was supported by the Russian Foundation for Basic Research (grants 16-55-53048 and 16-05-00127), the Russian Science Foundation (grant #16-07-10035), Russian Federation budget (N. 01201363042), the International Cooperation 40, Project of Global Change and Ocean-Atmosphere Interaction (GASIGEOGE-04), the National Natural Science Foundation of NNSF of China (grants N. 41476056, 41611130042 and U1606401) and international cooperative projects in polar regions (201613), as well as by Russia-Taiwan projects (17-MHT-003).

REFERENCES:

1. Lowe D. J. Tephrochronology and its application: a review // *Quat. Geochronol.*, 2011. V. 6. P.107–153.
2. Jensen B. J., Reyes A. V., Froese D. G. and Stone, D. B. The Palisades is a key reference site for the middle Pleistocene of eastern Beringia: new evidence from paleomagnetism and regional tephrostratigraphy // *Quat. Sci. Rev.*, 2013. V. 63. P. 91–108.
3. Davies S. M., Abbott P. M., Mearns R. H., Pearce N. J. G., Austin W. E. N., Chapman M. R., et al. A North Atlantic tephrostratigraphical framework for 130–60 ka b2k: new tephra discoveries, marine-based correlations, and future challenges // *Quat. Sci. Rev.*, 2014. V. 106. P. 101–121.
4. Ponomareva V., Portnyagin M., Pevzner M., Blaauw M., Kyle Ph., Derkachev A. Tephra from andesitic Shiveluch volcano, Kamchatka, NWPacific: chronology of explosive eruptions and geochemical fingerprinting of volcanic glass // *Internat. J. Earth Scien.* 2015. V. 104. P. 1459–1482.
5. Kutterolf S., Jegen M., Mitrovica J. X., Kwasnitschka T., Freundt A. and Huybers P. J. A detection of Milankovitch frequencies in global volcanic activity // *Geology*, 2013. V. 41. P. 227–230.
6. Gebhardt H., Sarnthein M., Grootes P.M., Kiefer T., Kuehn H., Schmieder F., Roehl U. Paleonutrient and productivity records from the subarctic North Pacific for Pleistocene glacial terminations I to V// *Paleoceanography*, 2008. V. 23. PA4212.
7. WEPAMA Cruise Report – Leg 2. 2002. P. 411-423.

SEDIMENTATION ENVIRONMENTS ON THE LAPTEV SEA OUTER SHELF (NORTHERN POLYGON)

**O. Dudarev^{1,2}, A. Charkin^{1,2}, I. Semiletov^{1,2,3}, N. Shakhova^{2,3}, D. Chernykh¹, A. Ruban²,
T. Tesi⁴, O. Gustafsson⁴**

¹ V.I. Il'ichev Pacific Oceanological Institute, FEB RAS, Vladivostok, Russia

² Tomsk Polytechnic University, Tomsk, Russia

³ University of Alaska Fairbanks, International Arctic Research Center, Akasofu Building, Fairbanks, Alaska, USA

⁴ Stockholm University, Department of Applied Environmental Science and Bolin Centre for Climate Research,
Stockholm, Sweden

dudarev@poi.dvo.ru

On the outer shelf of the Laptev Sea eastern part (further names as Northern Polygon) revealed azonal to sustainable under ice accumulation lithological structure of the bottom sediments. The data obtained in the International multidisciplinary expeditions of 2008 (HV «Yakob Smimitckiy», ISSS- 2008 project: International Siberian Shelf Study-2008 project; supported by the Wallenberg Foundation, FEBRAS, NOAA, and Russian Foundation for Basic Research), 2011 (RV «Academician M.A. Lavrent'ev»), 2012 (RV «Victor Buynitskiy», projects of Russian Foundation for Basic Research; supported by FEBRAS, NOAA, NSF), 2014 (IB «Oden», SWERUS-C3 project: The Swedish - Russian - US Arctic Ocean Investigation of Climate-Cryosphere-Carbon Interactions) and 2016 (RV «Academician M.A. Lavrent'ev») (Fig.1)

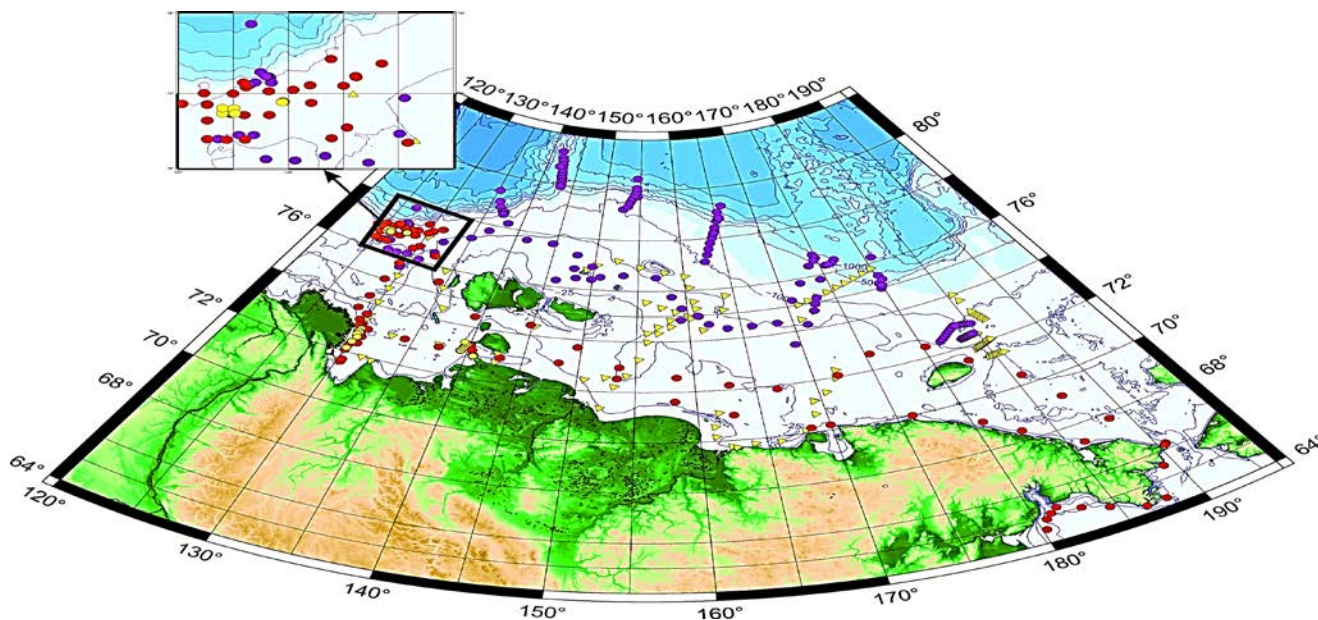


Fig. 1. Samples collected on the Northern Polygon, Laptev Sea (insert)

Sediments with variable ratio of fractions of sand, silt and clay are found among dispersed sediments in the depth range of 50-70 m. The most significant dissemination is sandy clay. The most significant is fine sand, clayey sand, sandy clay, sandy sand-silt-clay and clayey sand-silt-clay (Fig. 2). It is obvious that the transformation of the lithological composition of the bottom sediments in the area of sustainable accumulation from clay to silt and sand caused of erosion

pressure. Considered several possible mechanisms of the precipitation fields, field azonal under ice accumulation.

Formation sands areas may be due to poorly understood processes of fluid lithogenesis in the field discharge fluid flows. Numerous bubble fountains (the so-called seeps) instrumentally recorded in the range of depths from 60 to 110 m, where the periods of Late Pleistocene regression of the sea level is the ancient shorelines, instrumentally recorded [1-3] (Fig. 3). It is assumed that they are confined to areas of thawing permafrost sediment thickness [4]. Diameter some seeps up to 1 km [5], which is comparable to the size of the area of sand at a depth of 65÷70 m. The bottom surface in the areas of gas discharge fluids broken microcraters and bioturbated (Fig. 3). At the same time, the overturning character structure of the water column does not indicate the discharge of gases from the sedimentary deposits. Obviously, in this case there is a display on the East Arctic shelf lithogenesis of fluid type. Sites of concentrated discharge gas can also be traced to other facial features real-precipitation - bioturbation (Fig. 3) and authigenic carbonate formation, typical of methane.

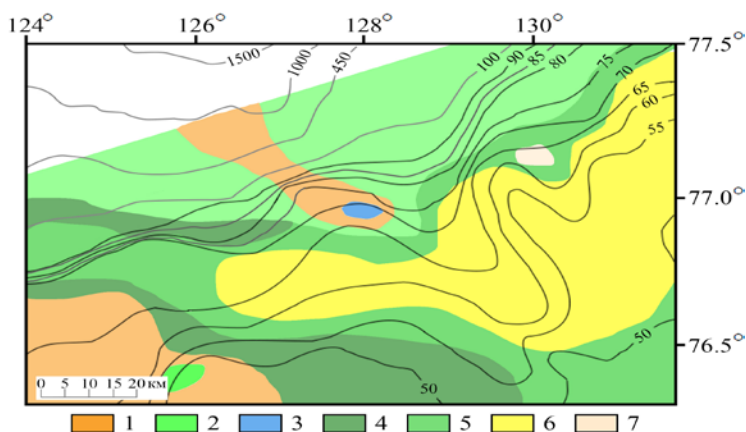


Fig. 2. Bottom sediments

(1-sandy clay, 2-clayey sand, 3-fine sand, 4-clayey silt, 5-silty clay, 6-clay, 7-clay-silt-sand (mictite))



Fig. 3. Bioturbated sediments (red circles show the escape of gas bubbles)

Perhaps the erosive effect of the underground suprapermafrost flow in areas of the island permafrost. The area is confined to the Ust-Lena Graben - fault structure meridional direction. It crosses the entire shelf and upper continental slope, and expressed paleovalleys in the relief of. Site erosion is probably marks the area of fine sand (with a content of sand fraction > 80%, silt and clay <10%) among the sandy clay (Fig. 4). At the same time, the distribution of temperature and salinity of the bottom does not favor the legality of the hypothesis.

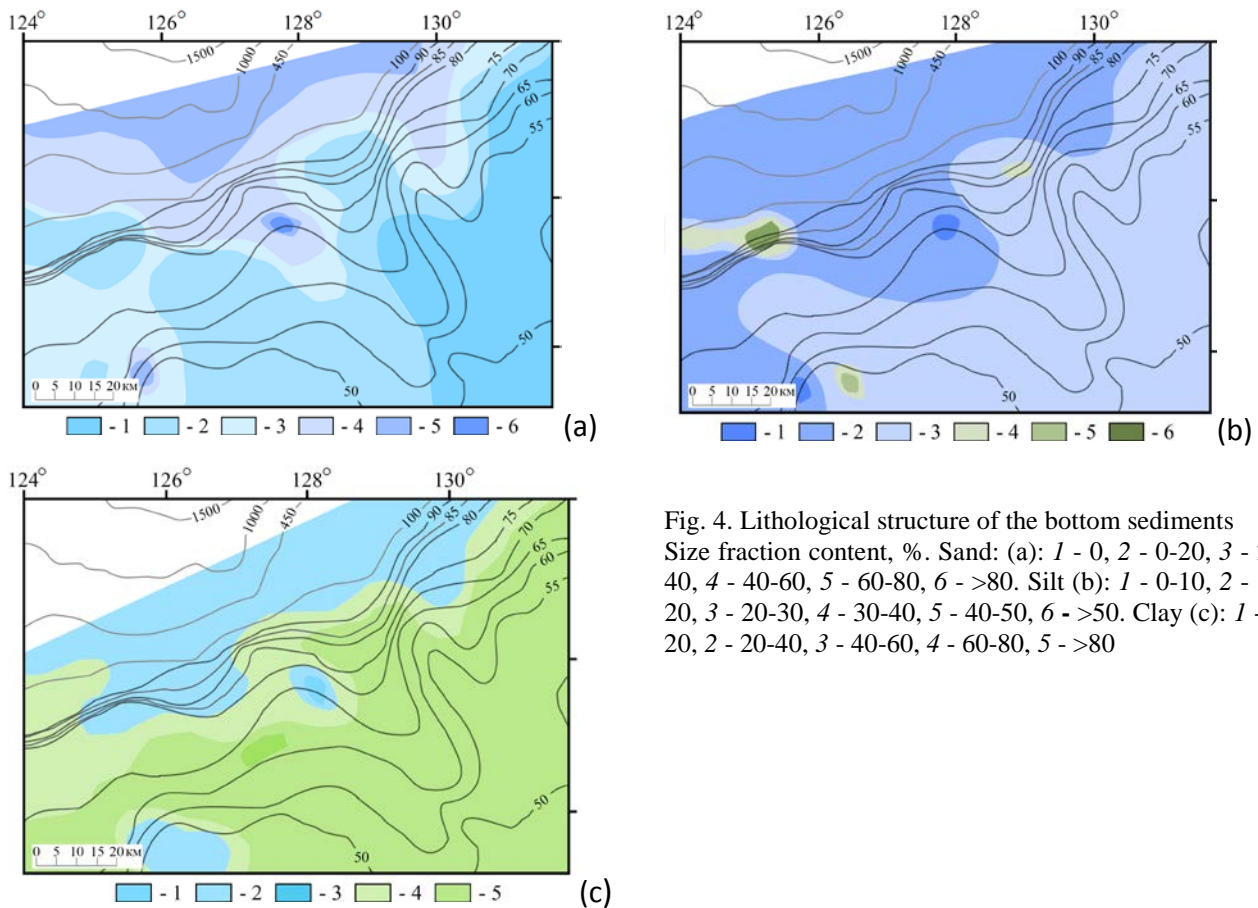


Fig. 4. Lithological structure of the bottom sediments
 Size fraction content, %. Sand: (a): 1 - 0, 2 - 0-20, 3 - 20-40, 4 - 40-60, 5 - 60-80, 6 - >80. Silt (b): 1 - 0-10, 2 - 10-20, 3 - 20-30, 4 - 30-40, 5 - 40-50, 6 - >50. Clay (c): 1 - 0-20, 2 - 20-40, 3 - 40-60, 4 - 60-80, 5 - >80

Geophysical methods at a depth of 59 m outer shelf of the Laptev and East Siberian fixed exaration furrow width of about 300 m and a depth of 4 m. These dimensions provide a glimpse of significant size and weight of a hummock, the pressure force it to the bottom of the keel. Earlier traces of ice furrows in the Arctic shelf observed at depths up to 50- 78 m [6, 7]. In the absence of information about the existence now of huge ice bodies capable plowed the bottom in deep water [8, 9], there is a question about the time of the detected exaration furrows. Its affinity to the ancient shoreline suggesting relic origin. In this case, it could be formed about 12-10 thousand years ago when the area was under consideration in the dissemination of fast ice in the inner shelf. The existence of a powerful ice thickness of up to 6-7 meters, not only in the interglacial periods of the Pleistocene, but even in the Holocene optimum, confirms the possibility of the formation of hummocks powerful at this time. Safety morphosculpture furrow to date can be attributed to two factors: (a) strong physical seal its bottom and the sides of the huge mass of the hummock and (b) a low rate of sedimentation. This area of the Laptev Sea, it is only 2-3 cm /1000 years, and the absolute weight paleoflows sedimentary material - about 0.1 g / m² / 1,000 years [10]. The thin sedimentary layer invests surface grooves, which is likely to ensure the sustainability and morphosculpture appearance in a state.

REFERENCES:

1. Semiletov, I.P. On Carbon Transport and Fate in the East Siberian Arctic Land-Shelf-Atmosphere System / I.P. Semiletov, N.E. Shakhova, V.I. Sergienko, I.I. Pipko, O.V. Dudarev // *Environmental Research Letters*. – 2012. – Vol. 7, N 1. – P. 015201. doi: 10.1088/1748-9326/7/1/015201.
2. Semiletov, I.P. Space-time dynamics of carbon and environmental parameters related to carbon dioxide emissions in the Buor-Khaya Bay and adjacent part of the Laptev Sea / I.P. Semiletov, N.E. Shakhova, I.I. Pipko [et al.] // *Biogeosciences*. – 2013. – Vol. 10, Is. 9. – P. 5977-5996. doi: 10.5194/bg-10-5977-2013.
3. Shakhova, N. Ebullition and storm-induced methane release from the East Siberian Arctic Shelf / N. Shakhova, I. Semiletov, I. Leifer [et al.] // *Nature Geoscience*. – 2014. – N 7. – P. 64-70.
4. Shakhova, N.E. Current state of subsea permafrost on the East Siberian Shelf: Tests of modeling results based on field observations / N. Shakhova, D.Y. Nicolsky, I. Semiletov // *Doklady Earth Sciences*. – 2009. – Vol. 429, N 2. – P. 1518-1521 (In Russian).
5. Sergienko, V.I. The degradation of submarine permafrost and the destruction of hydrates on the shelf of east arctic seas as a potential cause of the “Methane Catastrophe”: some results of integrated studies in 2011 / V.I. Sergienko, L.I. Lobkovskii, I.P. Semiletov, O.V. Dudarev, et al. // *Doklady Earth Sciences*. – 2012. – Vol. 466 (1). – 1132-1137 pp. (In Russian).
6. Lisitzin, A. P. Marginal filter of oceans / A.P. Lisitzin // *Oceanologia*. – 1994. – 34 (5). – 735-747 (In Russian).
7. Beaufort Sea, Alaska / P.W. Barnes, E. Reimnitz, D. Fox // *J. Sediment Petrol.* – 1982. – Vol. 52, N 2. – P. 493-502.
8. Reimnitz, E. Sediment transport by Laptev sea ice / E. Reimnitz, H. Kassens, H. Eicken // *Repts on Polar Research*. – 1995. – Vol. 176. – P. 71-77.
9. Reimnitz, E., Kempema, E.W. Dynamic ice-wallow relief in northern Alaska's nearshore / E. Reimnitz, E.W. Kempema // *Journal of Sedimentary Petrology*. – 1982. - V. 52. - № 2. – P. 451-462.
10. Kuptsov, V.M. Radiocarbon of Quaternary along shore and bottom deposits of the Lena and the Laptev Sea / V.M. Kuptsov, A.P. Lisitzin // *Marine Chemistry*. – 1996. – Vol. 53. – P. 693-703.

SEDIMENTARY ENVIRONMENT AND FRAMEWORK CHARACTERISTICS OF DIAOKOU LOBE IN THE MODERN YELLOW RIVER DELTA

Wei Gao, Ping Li, Jie Liu

¹ Key Laboratory of Marine Sedimentology and Environmental Geology, First Institute of Oceanography, SOA, Qingdao, China

² Function Laboratory for Marine Geology, National Oceanography Laboratory, Qingdao, China

gaoweigeo@fio.org.cn

Based on the data of 11 geological boreholes and sub-bottom profiles in the study area, the sedimentary environment and the framework characteristics of Diaokou lobe since Xianxian transgression were studied. Especially, The Modern Yellow River was diverted into the Diaokou River in 1964 and abandoned in 1976, which lasted 12 years and 4 months (Fig. 1). During this period, the estuary experienced a complicated evolution of sheet flooding, merging, braiding, swinging, and formed a very complex sedimentary system.

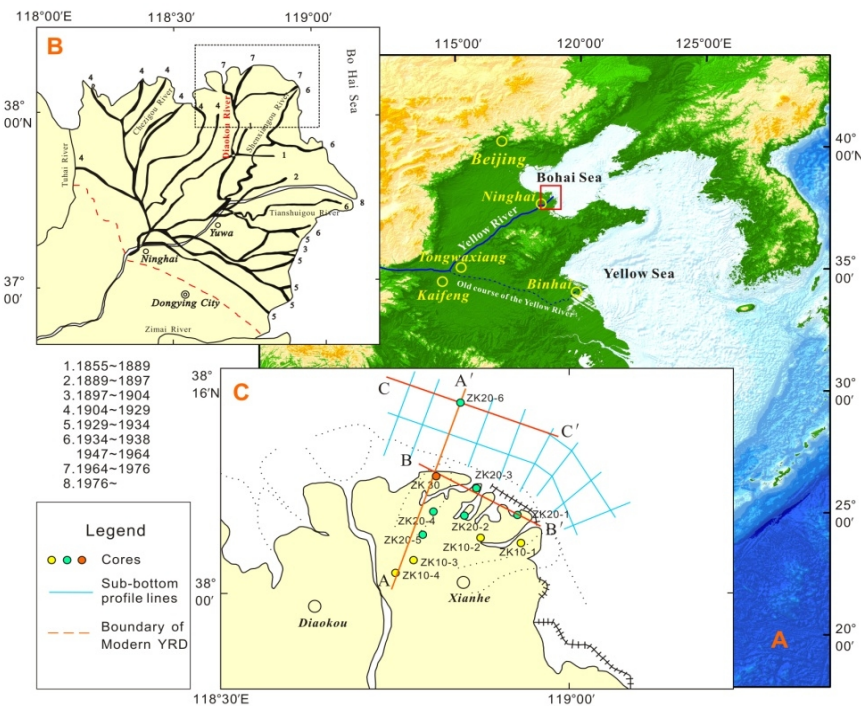


Fig. 1 A) The location of the modern Yellow River delta; B) The distribution of the modern Yellow River delta lobes in different periods and the study areas; C) The distribution of the boreholes in the Diaokou lobe and the sub-bottom profiles

The Yellow River has been brought into the sea at least 880 ka ago [1]. There was a transgression event happened here as so-called Xianxian transgression around 23~31ka BP. About 15 ka BP, the area of Modern Yellow River Delta was a bunch of dray land. As the sea level fluctuating, this area was covered by sea water, then the tidal-flat facies were developed. When the sea water retreated, some new terrestrial facies were developed, which can explain the rusty colored sediments in tidal-flat facies. As time went by, this area turned into a salt marsh land, vegetation that could stand saline-alkali environment were greatly developed here, as the 20cm peat layer

found in the sediments. Two peat layers indicates two small scales of sea level fluctuation (1.021(down)~8.8(up) ka BP). About 8 ka BP, with the sea level rising up rapidly, this area was again covered by sea water, thus intertidal deposits were developed.

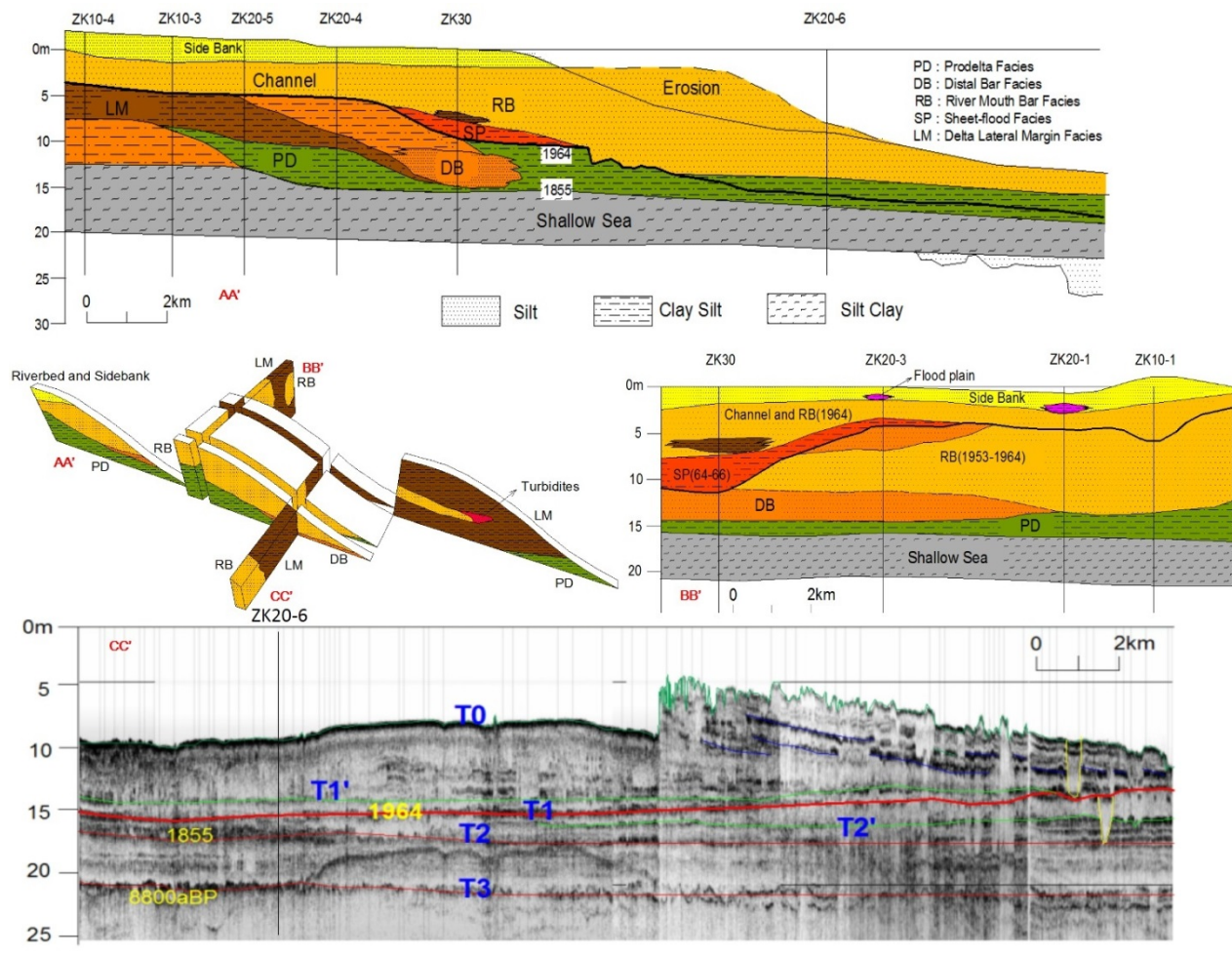


Fig. 2 Sedimentary environment evolution and framework of study area

In 1855, Yellow River changed its course into Bohai sea. Until 1889, the front delta facies were developed in study area. Well known for its frequent course changing, the Yellow River's mouth was around the location where the core drilling ZK30 was taken, which explained the existence of remote sand bar facies in the core. In 1964, the Yellow River changed its course into Diaokou channel. From 1964 to 1965, there was no stable channel, thus a pluvial facies was developed; due to the cutting effect of the flow water, a short term of several stable channel were developed years after 1965, since then a marginal delta facies was developed; from 1965 to 1971, one stable channel was developed in the area of ZK30 core, thus a large amount of sand was poured into sea, which resulted in the rapid spread of estuary sandbar; from 1972 to 1974, the channel was swayed northeastwardly and at last stayed at northwest, thus this channel became a distributary channel; in 1976, a manmade course change resulted in the abandonment of Diaokou change.

The modern Yellow River Delta basically conforms to the ternary structure of progressive delta, with coarsening upward, which is in general a regressive sedimentary sequence [2]. The

Yellow River delta is formed mainly by river sediment and large amount of sidebanks and overbanks, together with subfacies of flood plain and natural levee. The delta-front sedimentary facies is formed mainly by the river mouth bar and the distal bar with the delta lateral margin deposited on both sides. The sedimentation of the modern Yellow River delta is dominated by river sediment. The delta front is the most intense area of the interaction between the river and the sea, which is mutually controlled by the sediment condition of the Yellow River and the hydrodynamic condition of the Bohai Sea. The prodelta sediment is mainly fine particles and often affected by the hyper concentration fluid. The high sand content fluid sediment of the Yellow River is mainly graded suspension sediment, with uniform suspension sediment of subsidiary importance, and a small amount of hydrostatic suspension sediment. However, there is a large difference between the suspended sediment and the ordinary traction flow, the turbidity flow and the mud flow. The hydrodynamic condition weakens from the riverbed, the river mouth bar, the sidebank, the distal bar, the delta lateral margin, the prodelta to the flood plain. This shows that the hyper concentration flow of the Yellow River has the transporting and depositing characteristics of the gravity flow. And a complicated sedimentary system is formed after the constantly changing of the sedimentary dynamic environment.

The 30m stratigraphy reveals the environment evolution of the Yellow River delta since the Xianxian transgression. Up to 8000 years ago, rivers, lakes and salt marshes developed relatively well. Then, with the rising of sea level, tidal flat and shallow sea were developing together. After 1855, especially in 1964 ~1976, a complicated modern deltaic sedimentary system was developed.

Modern yellow river delta basically conforms with the 3-unit structure of prograding delta, which features in the growing grain size upwardly. On the whole, the sedimentary sequence is a regression type, but in the marginal area of the delta we found a positive grain size sequence with indicates a transgression history. Vertically the delta can be divided into a river mouth bar type and marginal delta type, longitudinally it can be divided into main river way type and branch type. At the delta transverse section shows the river mouth bar and marginal delta overlap each other.

This study is financially supported by the National Natural Science Foundation of China (Grant No. 41206054), the NSFC-Shandong Joint Fund for Marine Science Research Centers (Grant No. U1606401), the National Program on Global Change and Air-Sea Interaction (Grant No. GASI-GEOGE-05-3).

REFERENCES:

1. Yao Z, Shi X, Qiao S, et al. Persistent effects of the Yellow River on the Chinese marginal seas began at least ~880 ka ago//Scientific Reports. 2017. 7: 2827. P. 1-11.
2. Gao W, Li G X, Wang X D, et al. [Sedimentary characteristics of the hyperpycnal flow in the modern Yellow River Delta](#)// Indian Journal of Geo-marine Sciences. 2014.34. 8. P. 1438-1448.

MICROBIOLOGICAL DIVERSITY OF PROTEOBACTERIAS FROM SURFACE WATER OF THE GOLDEN HORN

Y. Golozubova¹, L. Buzoleva^{1,2}, E. Bogatyrenko¹

¹ Far Eastern Federal University, Vladivostok, Russia

² Somov Institute of Epidemiology and microbiology Environmental Studies, Vladivostok, Russia

know-26@mail.ru

Marine aerobic heterotrophic proteobacteria are an important component and play an important role in the biological processes of the ecosystems of oceans [3]. The Golden Horn Bay, is located in the coastal zone of Vladivostok, It is characterized by fresh and chronic faecal contamination [2]. At present, it is known that up to 99% of microorganisms can not be cultivated [1]. In this regard, the aim of the work is to investigate the microbiological diversity of surface water proteobacterias.

Samples of surface waters of the Golden Horn Bay were selected in August 2015. DNA from the samples was isolated with the help of AmpliPrime DNA-Sorb-B kit according to the protocol with modification-treatment of bacterial sediment before isolation with lysozyme solution. Fragments of the 16s rRNA gene of DNA was sequenced in the ABI 3130XL Analyzer in the Genomics Center (Novosibirsk). The data was analyzed using the Mothur software package and the Silva database.

Representatives of the proteobacteria were constituted the dominant part of the bay community (59% of the total number of sequences in all samples). Representatives of the class were dominated by representatives of uncultivated bacteria, which accounted for 36% of the total number of proteobacteria and 21% of the bacterial biodiversity of the Golden Horn Bay. The proteobacteria of the Golden Horn Bay were represented by 40 families. The family *Rhodobacteriaceae* was the most common among proteobacteria and accounted for 28% of all proteobacteria. The family is represented by such identifiable genera as *Punicebacterium* (66%), *Pacificibacter* (23%), *Pelagimonas*, *Vadicella*, *Profundibacterium*. The families of *Altermonadaceae*, *Rhodospirillaceae*, *Phyllobacteriaceae*, *Brucellaceae*, *Hyphomonadaceae*, *Hyphomicrobiaceae*, *Comamonadaceae*, *Haliaceae*, *Enterobacteriaceae*, *Litoricola*, *Oceanospirillaceae*, *Piscirickettsiaceae*, *Cellvibrionaceae* also were contributed significantly to the biodiversity of the proteobacteria of the Golden Horn Bay. The families of *Pseudoalteromonas*, *Pseudomonas*, *Vibrio*, *Colwelliaceae*, *Moraxellaceae*, *Thiotrichaceae*, *Spongibacteriaceae*, *Halomonadaceae* are represented by individual representatives.

The work was financially supported by the Russian Science Foundation (agreement no.14-50-00034).

REFERENCES:

1. Amann R.I., Ludwig W., Schleifer K.H. Phylogenetic identification and in situ detection of individual microbial cells without cultivation // *Microb. Rev.* 1995. V. 59. P. 143–169.

2. Buzoleva L.S., Kalitina E.G., Bezverbnaya I.P., Krivosheeva A.M. Microbial communities in the coastal surface waters of Zolotoi Rog bay under the conditions of strong anthropogenic pollution //Oceanologia. 2008. №6(48) P. 882-888
3. Romanenko L.A. Taxonomic characteristics and biological features of new taxa of marine aerobic heterotrophic gammaproteobacteria .Vladivostok. 2004. P. 221 p

**ADVANCES IN THE RESEARCH OF PALEOCEANOGRAPHY AND CLIMATE
CHANGES IN THE NORTHERN PACIFIC AND MARGINAL SEAS AS A RESULT OF
THE CHINESE-RUSSIAN COOPERATION DURING LAST DECADE**

Sergey Gorbarenko¹, Xuefa Shi^{2,3}

¹ V.I. Il'ichev Pacific Oceanological Institute, FEB RAS, Vladivostok, Russia

² Key Laboratory of Marine Sedimentology and Environmental Geology, First Institute of Oceanography, SOA,
Qingdao, China

³ Laboratory for Marine Geology, Qingdao National Laboratory for Marine Science and Technology, Qingdao, China
gorbarenko@poi.dvo.ru

An excellent progress was achieved in research of paleoceanography and climate changes of the Northern Pacific and marginal seas as a result of cooperative efforts of the First Institute of Oceanography of State Oceanic Administration (FIO), and the V.I. Il'ichev Pacific Oceanological Institute of the Far Eastern Branch of RAS (POI) since 2007. Within the framework of cooperative FIO and POI agreements, the fruitful and substantial achievements have been made including several joint research cruises to the marginal seas and northwestern (NW) Pacific and Arctic Ocean, cooperative investigation, scientific conferences and scientist exchanges.

Four joint scientific cruises using R/V «Academik M.A. Lavrentyev» were successfully organized and performed in the Japan, Okhotsk and Bering Seas and the NW Pacific: cruise 53, year 2010; cruise 55, 2011; cruises 63, 2013 and 67, year 2016. During each of cruises, a wide spectrum of investigations was provided in the fields of physical oceanography, sedimentology, paleoceanography, seismic stratigraphy and modern productivity. As a result, more 120 sediment cores with length of 3-10 m were put into the Depositary of the FIO and nearly same number of cores into the POI Depositary, which were used for cooperative Chinese-Russian study of paleoceanography and climate changes in the NW Pacific and its marginal seas. As a result, several joint papers were prepared and published in peer reviewed international journals.

“Fine structure of dark layers in the central Japan Sea and their relationship with the abrupt climate and sea level changes over the last 75 ka inferred from lithophysical, geochemical and pollen results”, S. Gorbarenko, X. Shi, Y. et al., Rybiakova, A. Bosin, M. Malakhov, J. Zou, J. Liu, T. Velivetskaya, A. Derkachev, Y. Wu, F. Shi. *Journal of Asian Earth Sciences*, 2015.

For the first time it was established that the long-lasting, millennial scale Greenland/Chinese Interstadials (GI/CI) 14, 12 and 8 of the Dansgaard-Oeschger (DO) cycles (NGRIP members, 1994; Wang et al., 2008) led to the accumulation in the Japan Sea a sequence of enriched in organic matter sediments with sub-millennial variability which may be accompanied by formation of several related dark layers.

A. Bosin, S. Gorbarenko, X. Shi, Y. Liu, J. Zou. Regionalized primary paleoproduction variability in the Sea of Okhotsk during the late Pleistocene and Holocene. *Journal of Asian Earth Sciences*, 2015.

Spatial and temporal history of paleoproductivity changes in the Okhotsk Sea during the last 160 kyr was obtained as a result of investigation of 11 early studied sediment cores retrieved in various parts of the Sea. Broad pattern shows that the paleoproductivity in the Okhotsk Sea was depressed during glacial stages and increased during interglacials. As a result of spatial correlation of the productivity records, we identified three main regions in the Sea of Okhotsk with specific environmental conditions. Productivity in the central region is low as compared to that in other regions due to nutrient limitation.

Yu. Vasilenko, S. Gorbarenko, A. Bosin, X. Shi, J. Zou, Y. Liu. 2017. Millennial mode of variability of sea ice conditions in the Okhotsk Sea during the last glaciation (MIS 4–MIS 2). *Quaternary International*, accepted, 2017.

Coarse fraction (CF) content, used as ice rafted debris (IRD), grain-size distribution and roundness of CF were studied in sediments of the eastern Okhotsk Sea core LV28-44-4 with established age model. Results show that sea ice was the main transport agent for the IRD delivery to the eastern and other parts of the Sea. The 19 peaks of IRD, mostly coincided with DO Stadials (DOSs) were found in the eastern Okhotsk Sea during Marine Isotope Stages (MIS) 4, 3, and 2. Significant strengthening of north-eastern and eastern winds during DOSs of MIS 3 was established, contrary to the dominated northern and north-western winds during MIS 2.

Gorbarenko, S.A., Shi, X., Malakhova, G.Y., Bosin, A.A., Zou, J., Liu, J., Chen, M-T., 2017. Centennial to millennial climate variability in the far northwestern Pacific (off Kamchatka) and its linkage to the East Asian monsoon and North Atlantic from the Last Glacial Maximum to the Early Holocene. *Clim. Past*, 13, 1063-1080, <https://doi.org/10.5194/cp-13-1063-2017>

High resolution reconstructions based on productivity proxies and magnetic properties of the dated core LV63-41-2 (off Kamchatka) reveal a prevailing centennial productivity/climate variability in the NW Pacific during last 19 kyr which occurred synchronously with the well dated East Asian Summer Monsoon sub-interstadials. Remarkable similarity of increased productivity events in the NW Pacific with the EASM sub-interstadials implies that the Siberian High is a strong and common driver responding to the centennial variations in productivity of the NW Pacific and they may be used as template for high resolution paleoceanography and sedimentology in the NW Pacific.

Based on the results obtained we intent to discuss and launch several highlight investigations, paramount for the deep understanding of the North Pacific and marginal Seas environment and paleoceanography changing in the past and forecasting in the future.

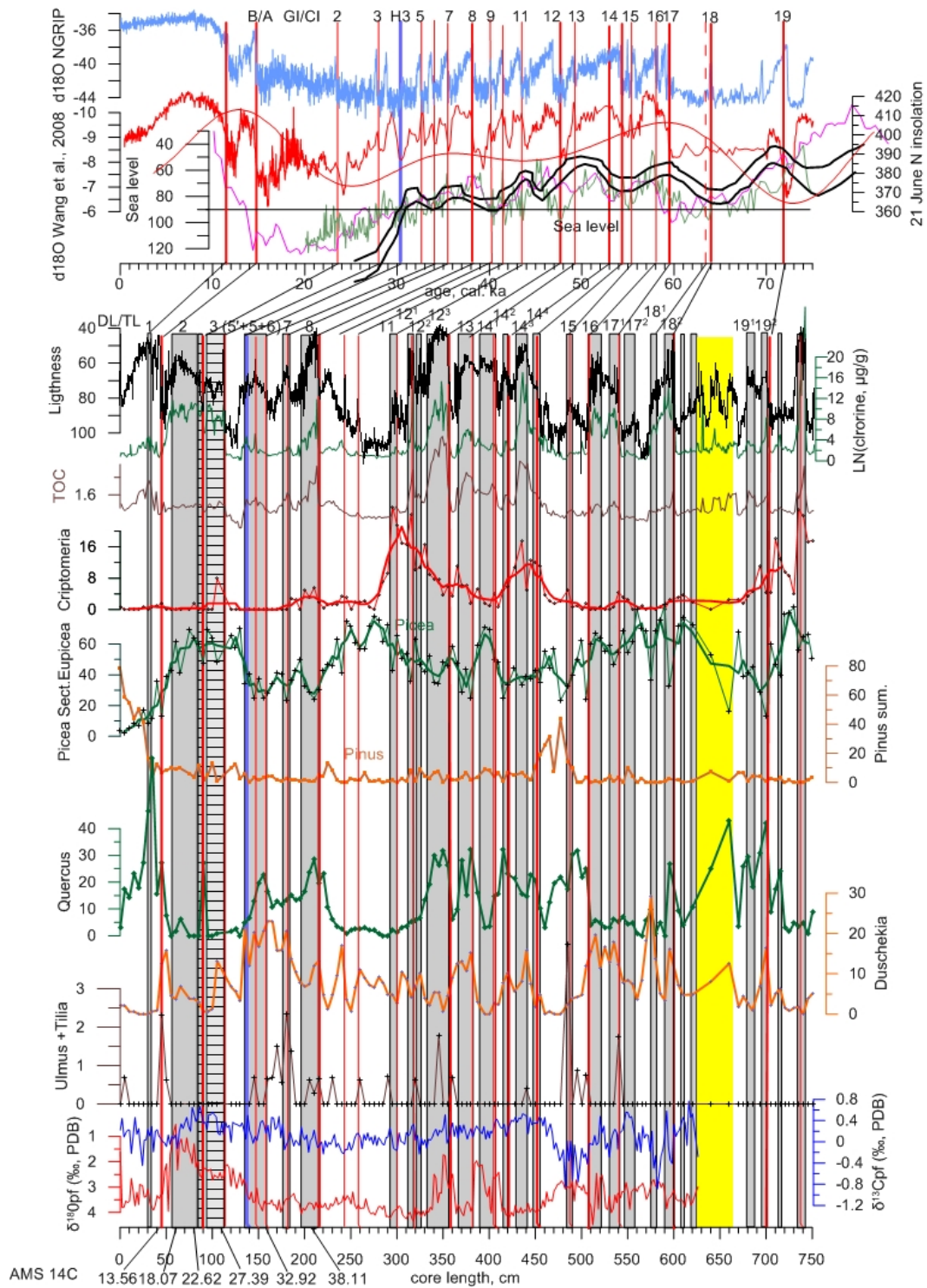


Fig. 1. Correlation of the millennial scale vegetation changes of surrounded land according to pollen results and variability in the main productivity proxies (color lightness, chlorin and TOC), $\delta^{18}\text{O}$ and $\delta^{13}\text{C}$ of planktonic foraminifera *N. pachyderma* (s.) and Dark-Layers locations (shaded bars) in sediments of core LV53-23-1 versus core depth with GI/CI in $\delta^{18}\text{O}$ records of Greenland ice core [1] and of China cave stalagmite [2] and sea level changes versus age. Pollen data show percentage changes of dominated broadleaved and conifer species in pollen assemblages: *Tilia and Ulmus*, *Duschekia*, *Quercus*, sum of *Pinus s/g Diploxylon and Pinus s/g Haploxylon*, *Picea sect. Eupicea and Criptomeria*. Thick red vertical lines show initiation of pronounced vegetation/climate amelioration and fine structure of DO cycles. Thin red lines show sharp increase in productivity correlated with G/CIs. Yellow bar shows interval of turbidity in sedimentation.

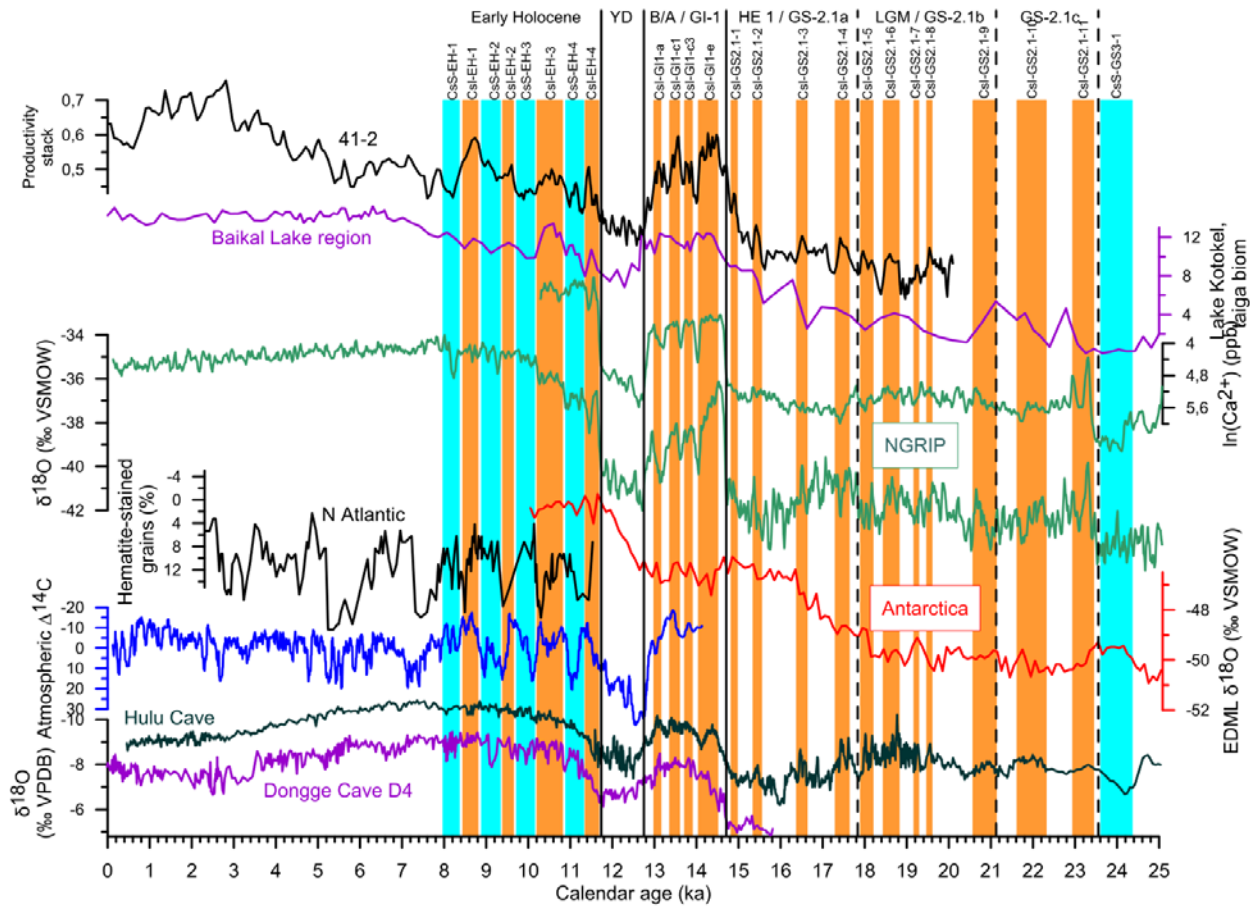


Fig. 2. Compilations of N-S hemisphere climate records, solar activity, NW Pacific productivity events, and vegetation records from the southern Siberia during the last 25 ka. From bottom to top: $\delta^{18}\text{O}$ calcite of Chinese cave stalagmites [2]; residual atmospheric $\Delta^{14}\text{C}$ record [3]; $\delta^{18}\text{O}$ Antarctic EDML records [4]; petrologic tracer of drift ice in the N Atlantic [5]; $\delta^{18}\text{O}$ and Ca^{2+} records in the Greenland NGRIP ice core [6], pollen reconstructed Southern Siberia environment changes [7] and productivity stack for NW Pacific core LV 63-41-2. Orange and blue bars are the NW Pacific centennial events with increased and decreased productivity respectively. Centennial events with increased productivity are associated with sub-interstadial of the EASM and with increasing input of solar irradiance during the LGM-B/A and EH short-term warmings, respectively.

This research work was supported by the RFBR projects (№16-55-53048 and 16-05-00127), Russian Federation budget (01201363042), the International Cooperation 40, Project of Global Change and Ocean-Atmosphere Interaction (GASIGEOGE-04), the National Natural Science Foundation of NNSF of China (41476056, 41611130042 and U1606401), international cooperative projects in polar regions (201613) and by Russia-Taiwan project (17-MHT-003).

REFERENCES:

1. North GRIP (Greenland Ice Core Project Members), 2004. High resolution climate record of the Northern Hemisphere reaching into the last interglacial period. *Nature* 431, 147–151.
2. Wang, Y.J., Cheng, H., Edwards, R.L., 2008. Millennial- and orbital-scale changes in the East Asian monsoon over the past 224,000 years. *Nature* 451, 1090-1093.
3. Reimer, P. J., Baillie, M. G. L., Bard, E., Bayliss, A., Warren Beck, J., Bertrand, C. J. H., ... Weyhenmeyer, C. E. (2004). IntCal04 terrestrial radiocarbon age calibration, 0-26 cal kyr BP. *Radiocarbon*, 46(3), 1029-1058.

4. EPICA Community Members, One-to-one coupling of glacial climate variability in Greenland and Antarctica. *Nature* 444, 195 (2006). doi: 10.1038/nature05301
5. Bond, G., Kromer, B., Beer, J., Muscheler, R., Evans, M., Showers, W., Hoffmann, S., Lotti-Bond, R., Hajdas, I., Bonani, G., 2001. Persistent solar influence on North Atlantic climate during the Holocene. *Science* 294, 2130 – 2136.
6. Rasmussen S.O., Bigler M., Blockley S.P., Blunier T., Buchardt S.L., Clausen H.B., Cvijanovic I., Dahl-Jensen D., Johnsen S.J., Fischer H., Gkinis V., Guillevic M., Hoek W.Z., Lowe J.J., Pedro J.B., Popp T., Seierstad I.K., Steffensen J.P., Svensson A.M., Vallelonga P., Vinther B.M., Walker M.J.C., Wheatley J.J., Winstrup M. A stratigraphic framework for abrupt climatic changes during the Last Glacial period based on three synchronized Greenland ice-core records: refining and extending the INTIMATE event stratigraphy. *Quat. Sci. Rev.*, 106 (2014), pp. 14-28.
7. Bezrukova, E.V., Tarasov, P.E., Kulagina, N.V., Abzaeva, A.A., Letunova, P.P., Kostrova, S.S., 2011. Palynological study of Lake Kotokel' bottom sediments. *Russian Geology and Geophysics* 52, 457e464.

RECONSTRUCTION OF THE PALEO-BOTTOM WATER TEMPERATURES USING SEEP CARBONATES

Xiqiu Han

Key laboratory of Submarine Geosciences & Second Institute of Oceanography, SOA, Hangzhou, China

xqhan@sio.org.cn

Authigenic carbonates formed at seep sites are archives of seepage history and record paleo-environmental conditions when they formed. Based on U/Th dating of seep carbonates and seep bivalve fragments, we obtained the ages of the seep carbonates and the timing of past methane release events at the northeastern slope of the South China Sea from three sites located at 22°02'–22°09'N, 118°43'–118°52'E (water depths from 473 to 785 m). Using a criterion consists of mineralogy, redox-sensitive trace elements and U/Th-isotope systematics, those carbonates formed in contact with bottom water with negligible influence of deep fluid were screened. Then the equilibrium temperatures were calculated using the corresponding past $\delta^{18}\text{O}$ of seawater and the $\delta^{18}\text{O}$ of the selected samples to reconstruct the past bottom water temperatures at the ages when they formed. Our results show that all methane release events occurred between 11.5 ± 0.2 and 144.5 ± 12.7 ka, when sea level was about 62–104 m lower than today. The calculated past bottom water temperature at one site (Site 3; water depth: 767–771 m) during low sea-level stands 11.5 and 65 ka ago ranges from 3.3 to 4.0 °C, i.e., 1.3 to 2.2 °C colder than at present. The reliability of $\delta^{18}\text{O}$ of seep carbonates and bivalve shells as a proxy for bottom water temperatures is critically assessed in light of ^{18}O -enriched fluids that might be emitted from gas hydrate and/or clay dehydration. Our results provide for the first time an independent estimate of past bottom water temperatures of the upper continental slope of the South China Sea. This approach can be applied to the seep sites on the continental margins of the World Ocean to obtain the information of the paleo-temperatures of intermediate water.

REFERENCE:

1. Han X, Suess E, Liebetrau V, Eisenhauer A, Huang Y. Past methane release events and environmental conditions at the upper continental slope of the South China Sea: constraints by seep carbonates. *International Journal of Earth Sciences*, 2014, 103(7):1873-1887.

THE SEDIMENTARY RESPONSE OF ORGANIC MATTER TO NATURAL FORCING IN THE BERING SEA: SEA-ICE VARIABILITY AND REGIME SHIFT FOR THE PAST CENTURY

Limin Hu¹, Xuefa Shi¹, Yanguang Liu¹, Jianjun Zou¹, Kirsten Fahl², Xun Gong²

¹Key Laboratory of Marine Sedimentology and Environmental Geology, First Institute of Oceanography, SOA, Qingdao, China

²Alfred Wegener Institute for Polar and Marine Research, Bremerhaven, Germany

hulimin@fio.org.cn

Recent observation from the Bering Sea indicates a significant decadal shift in climate (e.g. sea ice and SST) as well as the ecosystem systems. However, due to the limit time-scale of instrumental observation records, there exist a lack of continuous high resolution data in the past centuries, which could hamper the further understanding of the mechanism of the relation between climate and ecological systems. In the present study, we use several ²¹⁰Pb well-dated multi-cores in the western Bering Sea shelf to reconstruct the sedimentary records of the recent sea ice change and evolution of ecosystem community in the subarctic region by the bulk TOC-based geochemical proxies (e.g., TOC, TN, $\delta^{13}\text{C}$, $\delta^{15}\text{N}$) and typical biomarkers (IP₂₅ and sterols), in order to examine the sedimentary response in the Bering Sea towards the natural forcing (e.g., sea-ice and ecosystem) in the past century. The results showed that there existed a good correlation between the TOC and TN, suggesting a consistent provenance for the sedimentary organic components. TOC and phytoplankton biomarkers show a fluctuated but increased trend since 1900s, with an obvious decrease and/or pause between the late 1940s and 1970s, and a gradual increase in the late 1970s. The presence of IP₂₅ in the multi-cores in the Bering Sea suggested sea ice reduction for the past century, which may pose the regional ecological regime shift, especially since the late 1970s. The multi-decadal ecosystem evolution and the nitrate utilization in the Bering Sea for the past 150 years were revealed based on the biomarker and isotopic records, indicating a potential link to the sea ice condition and water column stratification, which may pose the regional ecological regime shift. The relatively higher sequestration of TOC in the study area were also assessed in this work, which could be constrained by the higher marine productivity, quick POC export from the upper water column, effective metabolic processing and higher sedimentation rates.

**SR, ND AND PB ISOTOPES AS TRACERS OF THE MIDDLE OKINAWA TROUGH
DETRITAL SEDIMENTS: PALEOENVIRONMENTAL IMPLICATION**

Ningjing Hu^{1,3}, Peng Huang^{2,3}, Jihua Liu^{1,3}, Xuefa Shi^{1,3}, Hui Zhang^{1,3}

¹ First Institute of Oceanography, SOA, Qingdao, China

² Institute of Oceanology, Chinese Academy of Sciences, Qingdao, China

³ Laboratory for Marine Geology, Qingdao National Laboratory for Marine Science and Technology, Qingdao, China

High-resolution records of detrital elemental compositions and Sr-Nd-Pb isotopes from sediment core OKI01, in the middle Okinawa Trough, are used to trace sediment provenances and their responses to paleoenvironmental changes during the last 16 ka BP. Sediment provenance exhibits large variations with five phases, as indicated by detrital-origin elements and Sr–Nd–Pb isotope system, suggest the influences of environment related to sea level fluctuation, Kuroshio Current variability and East Asia monsoon dynamic. Between 16.0 and 13.9 ka BP, sediment was overwhelmed from Changjiang and Huanghe, associated with the low sea level and strengthened winter monsoon, particularly in the cold Heinrich 1 period. With sea level rise and the reenter of Kuroshio Current at around 13.9 ka BP, exception of Changjiang- and Huanghe-sources, Taiwan-derived sediment became another source in the trough. The changes in provenance at 11.6 ka BP reflect the enhanced fluvial input from Changjiang in the period of maximum summer monsoon, weakened Kuroshio Current and sea level high-stand approximated the present position. Sediments originated from Changjiang and Taiwan, particularly from Taiwan, dominated the sedimentation in the middle Okinawa Trough during the maximum strengthened Kuroshio Current period at 7.3–5.2 ka. However, a prominent decline in Taiwan-derived sediments from 5.2 ka BP accompanied with a weakening Kuroshio Current. These changes reveal that the modern surface circulation in the East China Sea was finally established at around 7.3 ka. Additionally, the tephra layer in the core has distinct geochemical and isotopic compositions that correlate well with the volcanic eruption at 7.3 ka in southern Japan.

**MEASUREMENTS OF MERCURY CONCENTRATIONS IN AIR AND SEAWATER
DURING THE FIRST RUSSIAN-CHINESE ARCTIC RESEARCH EXPEDITION
ABOARD THE R/V "AKADEMIK M.A. LAVRENTEV"**

Viktor Kalinchuk

V.I. Il'ichev Pacific Oceanological Institute, FEB RAS, Vladivostok, Russia

viktor_v@poi.dvo.ru

Interest in studying the behavior of mercury in the environment is primarily determined by its toxic properties and high migration ability. The Far Eastern seas of Russia and the seas of the eastern Arctic are characterized by poor knowledge of the processes occurring with mercury in these environments. Thus, the aim of the study was to consider the features of mercury distribution in the surface layer of the atmosphere and in the seawater and to determine the factors that cause them.

The research was conducted in the First Russian-Chinese Arctic Research Expedition aboard the R/V "Akademik M.A. Lavrentev" in August-September 2016 in the in the Bering Sea, Chukchi Sea, the East Siberian Sea and the Laptev Sea. The concentration of elemental gaseous mercury (GEM) in the air was determined using an atomic absorption spectrometer RA-915M (Ltd Lumex, St. Petersburg), with a detection limit of 0.3 ng/m³ [1]. The ambient air was taken from the bow of the vessel at a height of about 2 m above the water surface. Simultaneously, with the help of the Davis Vantage Pro meteorological station (Davis Instruments Corp., USA), various meteorological parameters were recorded.

Also during the cruise, concentrations of total mercury in sea water samples were measured. Sampling was carried out both in vertical sections (at hydrological stations) and in the surface layer (4 m) with the help of the underway system. The samples were not preserved, the measurements were carried out in several hours after the sampling. The concentration of total mercury was determined by the "cold vapour" method using the RA-915 + analyzer and the RP-91 attachment with a detection limit of 0.3 ng/l [1]. The reduction of mercury in the samples was carried out with an alkaline solution of tin dichloride.

During the cruise the GEM concentrations in the air varied from 0.3 to 2.4 ng/m³, the average was 0.9±0.3ng/m³ (N = 6711) (Fig.1). The average value was lower than typical background concentrations of GEM in the surface atmosphere of the Northern Hemisphere (1.5 – 1.7 ng/m³ [2]) and background concentrations of the Southern Hemisphere (1.1 – 1.3 ng/m³ [3]). Maximum concentrations of GEM were recorded in the Kamchatka sector of the Pacific Ocean and in the Bering Sea (September 19-21), in the Chukchi Sea (September 25-28). Analysis of backward trajectories of air mass movement showed that during these periods, the air masses came to the study area almost from the center of the Pacific Ocean and took their origin from the north-east

trade-winds. It is known that after entering the atmosphere, GEM can remain in this environment for a long time (according to various data from 0.5 to 2 years) until as a result of its oxidation and/or binding with atmospheric particles does not lead to precipitation on the Earth's surface. The possible cause of recorded increases was emission of GEM into the atmosphere from Latin America characterized by significant global anthropogenic emissions of GEM [4], and the subsequent transport of contaminated air masses first by the north-east trade winds, and then by other atmospheric currents to the study areas. Earlier similar long-range atmospheric transport of GEM by westerlies from anthropogenic sources located in East Asia was recorded in North America [5].

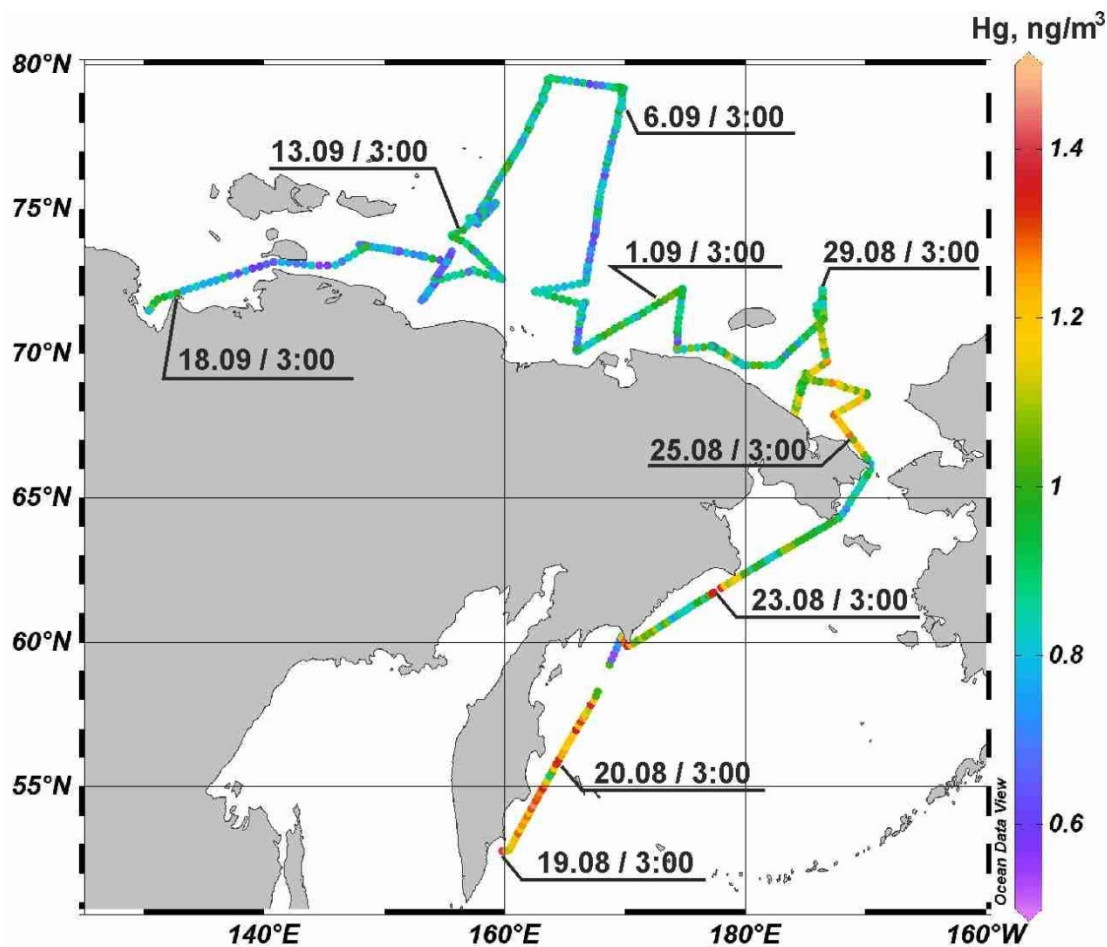


Fig. Spatial distribution of GEM in the surface layer of the atmosphere, as measured from the R/V Akademik M.A. Lavrentev in August-September 2016. Day of month and time are in UTC.

The concentrations of total mercury in seawater sampled both at offshore and at deep water hydrological stations were generally below the detection limit. Exceptions were water samples collected at offshore stations in the southwestern part of the East Siberian Sea, as well as samples from the surface layer of sea water selected in the southern part of the Laptev Sea. In these samples, the mercury concentration varied from 0.3 to 0.9 ng/l. Such concentrations are slightly elevated relative to background values. For example, in the World Ocean, the concentration of total mercury is usually in the range of 0.02 to 0.5 ng/l [6]. The likely reason for the increase in the total mercury concentration in seawater in the above-mentioned areas was the input of various forms of mercury

with the waters of Siberian Rivers, such as Lena, Yana and Indigirka. It should be noted that in areas with increased concentrations of mercury in water, an increase in the GEM concentration in the air (up to 1.2 ng/m³) was also recorded. Perhaps this was due to the GEM flux from the sea to the atmosphere.

Mercury measurements were performed during joint Russian-Chinese cruise partly funded by National Natural Science Foundation of China projects (No. 41420104005, 40710069004, 40431002); data processing and interpretation was supported by Russian Science Foundation (Project No. 16-17-10109).

REFERENCES:

1. Sholupov S., Pogarev S., Ryzhov V., Mashyanov N., Stroganov A., 2004. Zeeman atomic absorption spectrometer RA-915+ for direct determination of mercury in air and complex matrix samples // *Fuel Process. Technol.* V.85. P. 473–485.
2. Lindberg S., Bullock R., Ebinghaus R., Engstrom D., Feng X., Fitzgerald W., Pirrone N., Prestbo E., Seigneur C. A synthesis of progress and uncertainties in attributing the sources of mercury in deposition // *Ambio.* 2007. V.36(1). P. 19–32.
3. Slemr F., Brunke E.G., Ebinghaus R., Temme C., Munthe J., Wangberg W.H., Schroeder W.H., Steffen A., Berg T. Worldwide trend of atmospheric mercury since 1977 // *Geophysical Research Letters.* 2003. V.30. №10.
4. AMAP/UNEP, 2013. Technical Background Report for the Global Mercury Assessment 2013., in: Norway/UNEP ChemicalsBranch (Ed.), Arctic Monitoring and Assessment Programme. Geneva, Oslo, p. 263.
5. Jaffe D., Prestbo E., Swartzendruber P., Weiss-Penzias P., Kato S., Takami A., Hatakeyama S., Kajii Y. Export of atmospheric mercury from Asia // *Atmos. Environ.* 2005. V. 39(17). P. 3029–3038.
6. Douglas T.A., Loseto L.L., Macdonald R.W., Outridge P., Dommergue A., Poulain A. et al., The fate of mercury in Arctic terrestrial and aquatic ecosystems, a review // *Environmental Chemistry.* 2012. V. 9. P. 321–355.

**THE UNIQUE OCEANOGRAPHIC MEASUREMENTS OF CLIMATIC EFFECTS
OBSERVED DURING THE JOINT RUSSIAN-CHINESE CRUISES OF 2010-2016 TO THE
NORTH-EAST ASIAN MARGINAL SEAS FROM SURFACE TO BOTTOM**

**Dmitry Kaplunenko¹, Vyacheslav Lobanov¹, Pavel Tischenko¹, Sergey Sagalaev¹, Maria
Shetsova¹, Xuefa Shi², Yanguang Liu²**

¹ V.I. Il'ichev Pacific Oceanological Institute, FEB RAS, Vladivostok, Russia

² First Institute of Oceanography, SOA, Qingdao, China

dimkap@poi.dvo.ru

In this report we describe our results, obtained during the execution of 7-year program of collaboration between POI and SOI in the marginal seas of North-East Asia related to oceanography research. It was made a series of surveys using CTD-unit for observing basic water mass characteristics (e.g., temperature, salinity, dissolved oxygen content, nutrients content). The area of these research have covered the Japan, Okhotsk, Bering seas and North-Western part of Pacific ocean. The survey in these areas were held by R/V "Akademik M.A. Lavrentyev" during the joint Russian-Chinese cruises, and are part of a project that studies paleo and modern climate of marginal North East Asian seas and North-Western Pacific, started in the 2010. The aim of this study is to characterize the variability of observed parameters during the last 7 years, and to compare our results with other existing data (e.g. eWOCE atlas of Schlitzer, 2000). The most valuable results of these cruise are continuing monitoring shelf off processes within marginal seas of North-Asia and North-Western Pacific. It has been confirmed a presence of temperature and horizontal gradients of oceanographic characteristics increasing within the bottom layer, showing a weakening of ventilating processes in the second half of the current decade of the 21st century not only in the Japan sea, but also in the North-Western Pacific. The most region of our interest demonstrate the presence of a slope zone of the oxygen minimum in the area of a continental slope and area connected with mesoscale eddy activities and subpolar front. It should be noted that results of CTD-observations were checked and confirmed by the hydrochemical analysis of water-sampling. Due to this analysis it was possible to compare obtained results with the data, provided by eWOCE Atlas. As the result, our data, obtained in the cruises is good matched to historical observations. Also, during the cruises the unique result of hydrochemical analysis of nutrients for water column (all areas) and sediments pore water (the North-Western Pacific and Bering Sea areas) were obtained. The one of result of these researches is observed maximum concentrations of ammonium in the Bering Sea that corresponds to the mechanism of heterotrophic denitrification in the sediments in the absence of oxygen. It should be also noted that the ammonium concentration in the sediments in the study area at most stations exceeds the concentration of nitrate (Bering Sea, shelf area of the northwestern Pacific). This mechanism of nitrogen "binding" corresponds to the scheme of the oxygen "exhaustion" given in (Capone, 2008).

THE LATE NEOGENE (?) VOLCANIC ACTIVITY ON THE PERVENETS RISE: COMBINATION OF HIGH RESOLUTION SEISMIC PROFILING AND MULTYBEAM SURVEY

Victor Karnaukh¹, Xuefa Shi², Evgeny Sukhoveev¹, Andrey Koptev¹

¹ V.I. Il'ichev Pacific Oceanological Institute, FEB RAS, Vladivostok, Russia

² First Institute of Oceanography, SOA, Qingdao, China

karnaukh@poi.dvo.ru

The Pervenets Rise is located in the northern part of the Japan Basin (Japan Sea) south of Peter the Great Bay. The Pervenets Rise differs from the other positive structures in the basin by its size and its relatively thick sedimentary cover [1]. In 1973–1982, the basement and the sedimentary cover were sampled at 34 dredging stations [2]. Geological and gravimetric studies show that the Pervenets Rise is underlain by the continental earth's crust [2].

During Russian-Chinese expeditions in 2010 the Pervenets Rise was investigated by using high resolution seismic profiling. The numerous small cone-like edifices were recognized on seismic profiles. The height of those structures are 100–200 m. Normally, those objects pierce the Middle Miocene-Holocene sedimentary cover and are deprived of the recent sediments. In 2015 the eastern part of the Rise was investigated in the POI FEB RAS expedition by using the SeaBeam 3050 multibeam system. The numerous cone-like edifices can be recognized on the bathymetric map (Fig.). Sometimes, the narrow gentle ridges are adjacent to edifices. Based on these observations we conclude that the cone-like edifice corresponds to a single volcano. The gentle ridges near the volcano can be lava flows. Those facts in combination with the missing of recent sediments on the volcano slope indicate on the young age of those edifices, presumably Late Neogene-Quaternary.

REFERENCES:

- 1 V. N. Karnaukh, B. Ya. Karp, and I. B. Tsoy. Seismic stratigraphy of the sedimentary cover and the sedimentation on the Pervenets Rise and in the adjacent areas (the Japan Sea) // *Oceanology*, Vol. 45, No. 1, 2005, pp. 118–129.
- 2 I. I. Bersenev, E. P. Lelikov, V. L. Bezverkhniy, et al. *Geology of the Japan Sea* (DVNTS Akad. Nauk SSSR, Vladivostok, 1987).

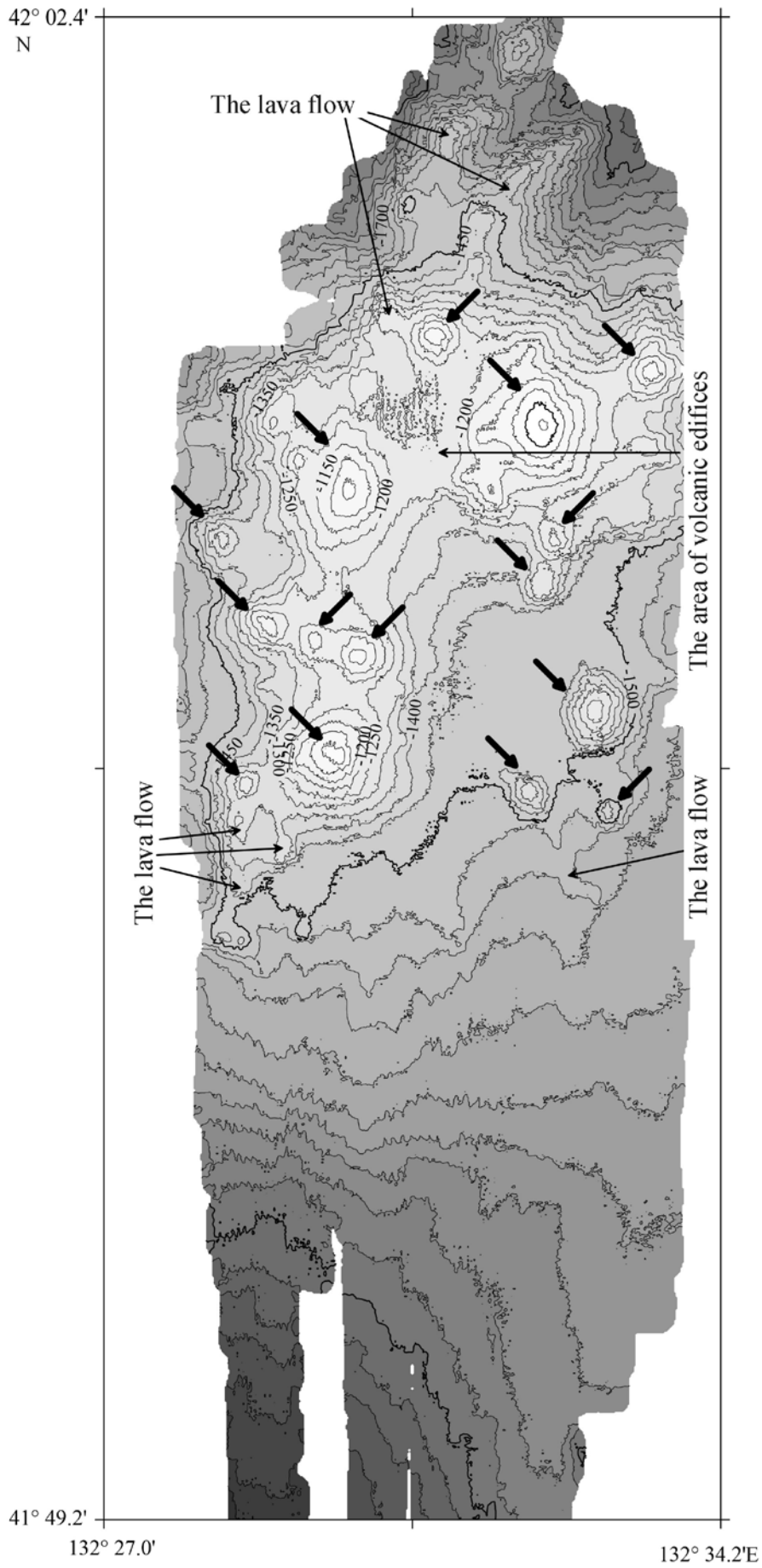


Fig. Bathymetric map of the eastern part of the Pervenets Rise. The arrows indicate location the Late Neogene (?) volcanic edifice.

SEDIMENTARY STRUCTURES AND CHEMICAL ELEMENTS DISTRIBUTION OF THE SUBMARINE LANDSLIDE IN THE NORTHERN CONTINENTAL SLOPE, SOUTH CHINA SEA

Ping Li^{1,2}, Yuanqin Xu^{1,2}, Lejun Liu¹, Hang Zhou¹, Wei Gao^{1,2}, Jie Liu^{1,2}

¹ Laboratory for Marine Geology and Geophysics, First Institute of Oceanography, SOA, Qingdao, China

² Function Laboratory for Marine Geology, National Oceanography Laboratory, Qingdao, China

liping@fio.org.cn

We take DLW3101 core obtained at the top of the canyon (no landslide area) and DLW3102 core obtained at the bottom of the canyon (landslide area) on the northern continental slope of the South China Sea as research objects. The chronostratigraphic framework of DLW3101 core and elemental strata of DLW3101 core and DLW3102 core since MIS5 are established by analyzing oxygen isotope, calcium carbonate content and XRF scanning elements. Based on the information obtained by analyzing the sedimentary structure and chemical elements in the landslide deposition. The main conclusion were drawn as follow:

(1) Through the analysis of sedimentary structures, there are four symbolic landslide layers in DLW3102 core since MIS5. L1 (2.15-2.44m) is characterized by color mutation, convolute bedding, groove contact with lower layer. L2 (15.48-16.00m) has the characteristic of high water content, silt clumps. L3 (19.00-20.90m): the upper part(19.00-20.00m) has high water content, contains hard clay clumps locally; the lower part (20.00-20.90m) is slightly light in color. L4 (22.93-24.27m): the upper part(22.93-23.50m) has obviously high water content; the lower part (23.50-24.27m) contains intrusions, intraformational folds, tilted lamina and convolute bedding.

(2) Through the detailed comparison of element strata of DLW3101 and DLW3102 core, the landslide layers identified by the sedimentary structure reflect an anomalous enrichment in Si, K, Ti and Fe which indicating terrigenous debris sources, confirming that the four strata are landslide sediments. Among which, L1 occurred in MIS1; L2, L3 and L4 occurred in MIS5.

(3) L1 (2.15-2.44m) is a slump layer with small sliding distance and scale. L2 (15.48-16.00m) is a debris flow layer with scale and sliding distance greater than L1. The upper part (19.00-20.00m) of L3 is a debris flow layer, the lower part (20.00-20.90m) is a slide layer, and the landslide scale is large. The upper part (22.93-23.50m) of L4 is a turbidity layer, the lower part (23.50-24.27m) is a slump layer, its thickness is thinner than L3, but its sliding distance is longer than L3, L4 is also a large landslide.

**WIDESPREAD OCCURRENCE OF GREIGITE (Fe₃S₄) IN THE SEDIMENTS OF THE
CENTRAL SOUTH YELLOW SEA: IMPLICATIONS FOR MID-PLEISTOCENE
PALAEOENVIRONMENTAL CHANGES**

Jianxing Liu¹, Xi Mei², Xuefa Shi¹, Qingsong Liu³

¹ First Institute of Oceanography, SOA, Qingdao, China

² Qingdao Institute of Marine Geology, Qingdao, China

³ Southern University of Science and Technology, Shenzhen, China

jxliu@fio.org.cn

Sediments from continental shelves are sensitive to changes in both oceanic and terrestrial conditions, and, therefore, magnetic minerals in such sediments are affected strongly by depositional and diagenetic processes. Here we systematically investigated a N-S transect of three sediment cores from the central South Yellow Sea muddy area. Rock magnetic data indicate the presence of a horizontally distributed thick greigite-bearing layer. Constrained by a published magnetostratigraphy and accelerator mass spectrometry (AMS) ¹⁴C dating ages, this layer was deposited within marine isotope stages (MIS) 17-13, following an enhanced anoxic period over MIS 21-19 when the Yellow Sea Warm Current and the associated Yellow Sea Cold Water Mass were strong and where underlying sediments have higher total organic carbon (TOC) and sulphur (TS) and trace element molybdenum (Mo) contents. Trace element cadmium (Cd) enrichment in the greigite-bearing layers is documented for the first time, which indicates that a suboxic (i.e., no detectable O₂ with trace levels of free H₂S also below typical detection) environment was initially established before a sulphidic (anoxic) environment where the limited porewaters H₂S was exhausted by greigite formation during early diagenesis. We propose that organic matter supply was controlled by an extended period with moderate primary productivity. The combined effects of palaeoclimate and local tectonic subsidence were crucial for the formation and preservation of the thick identified greigite layer. Our study improves our understanding of the formation and preservation mechanisms of greigite in continental shelf sediments and reveals mid-Pleistocene palaeoenvironmental changes in the South Yellow Sea.

MARINE SEDIMENTARY ENVIRONMENT EVOLUTION OF THE SOUTHERN LAIZHOU BAY UNDER THE IMPACT OF PORT PROJECTS

Jie Liu¹, Ping Li¹, Wei Gao¹, Xiao Liu²

¹ First Institute of Oceanography, SOA, Qingdao, China

² Ocean University of China, Qingdao, China

liujie@fio.org.cn

Marine hydrodynamic and sedimentary environment in the southern Laizhou Bay has changed under the influence of large-scale port project construction in recent years. Weifang Newport, located on the south side of Laizhou Bay, began its construction in May 1996, and constituted the largest marine engineering project in the southern Laizhou Bay in 2009. In this paper, evolution of hydrodynamic environment, sediment deposition rate, and geochemical characteristics was studied, in order to analyze the influence of Weifang Port on marine environment evolution.

The two cores were drilled by gravity core sampler. Core WF1 (300 cm long) was collected at the depth of 1.6 m on the west side of Weifang port (built in 1996~1997), and Core WF2 (300 cm long) was collected at the depth of 2.8 m on the east side of the port. The position of study area and drill holes are shown in Fig.1. Sediment deposition rate was studied by ²¹⁰Pb dating method and calculated by Constant Initial Concentration Model. The grain-size of the sediments was measured by Mastersizer 2000 grain size analyzer. Major geochemical element analyses were performed directly on the surface of split cores with 1 cm intervals by ITRAX Core Scanner.

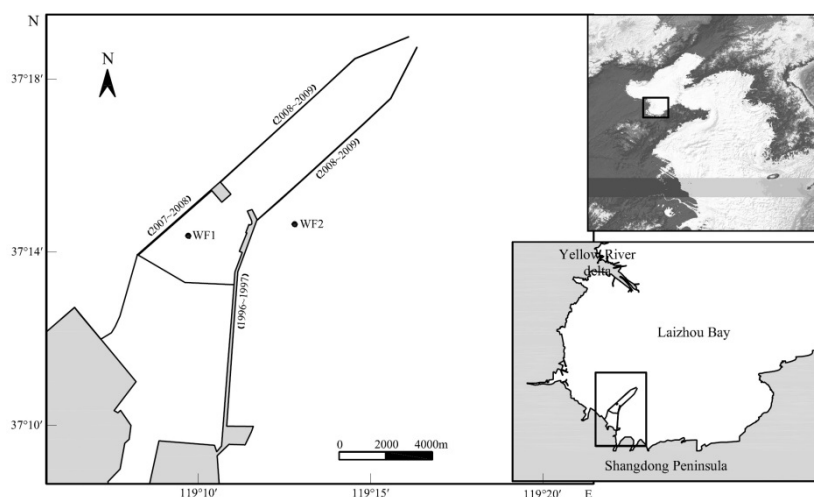


Fig.1 Positions of the study area and drill holes

Deposition age of the cores WF1 and WF2 is shown in Fig.2, and the differences of sedimentary environment evolution and deposition rate mainly appeared after 1997. The sedimentary thickness of WF1 and WF2 between 1997 and 2007 was 63 cm and 45 cm respectively. WF2 was closer to the breakwater gap with stronger hydrodynamic forcing conditions, while the embankment had better protection to WF1. The sedimentary thickness of WF1 and WF2

between 2007 and 2011 was 22 cm and 58 cm respectively. This was mainly because that the extension project of Weifang Port required it to be extended in NE for 10 km and to form a shield for the southeast waters, leading to increased deposition rate. The core WF1 was located within the encircling breakwater which was completed in 2007, and the deposition rate declined significantly due to the shield effect and lack of sediment sources.

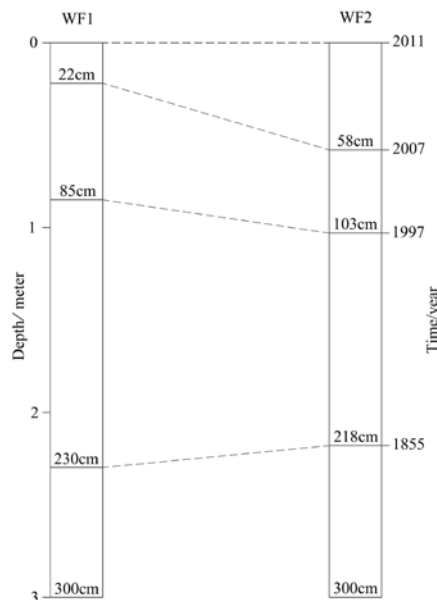


Fig.2 Deposition age of cores WF1 and WF2

The content of element Ca was influenced by sediment grain size, and Al was taken as the reference element in order to eliminate the influence, because of the chemical activity of Al being relatively stable during deposition. Taking WF1 for example, vertical distributions of mean grain size, Ca/Al, Fe, Ni are shown in Fig.3. Lots of peak values of Ca/Al existed in the sediments above 230 cm, corresponding to the position of thin layers of fine sediments. High ratio of Ca/Al in the thin layers of fine sediments indicated that the sediment was derived from the modern Yellow River, owing to characteristics of high content of Ca and Ca/Al in sediments from the Yellow River.

Ni was taken as a typical element to analyze the variation of sedimentary environmental pollution in the past one hundred years. The content of Ni in sediment was at 0-200 cps, and the content above 200 cm had a slight trend of increase, while it was stable between 200 and 300 cm. Content of heavy metals in sediments had no significant change in the vertical, indicating that the heavy metals in sediments were less affected by human activity and there was no obvious accumulation in the study area.

The Yellow River flowed into the Yellow Sea in Subei before 1855 (230-300 cm in the core WF1, and 218-300 cm in the core WF2), and the sedimentary environment of Laizhou Bay was stable due to absence of large river and single provenance.

The modern Yellow River delta was formed since the suspended sediment of the Yellow River was deposited within the modern active delta in 1855 (85-230 cm in the core WF1, and 103-

218 cm in the core WF2). The fine fraction of sediments from the Yellow River was brought and deposited in the south side of Laizhou Bay under the impact of storm surge and other extreme weathers, leading to 2-5 cm-thick layers of fine-grained and poorly graded sediments. The average annual deposition rate was at 0.3-0.5 cm.

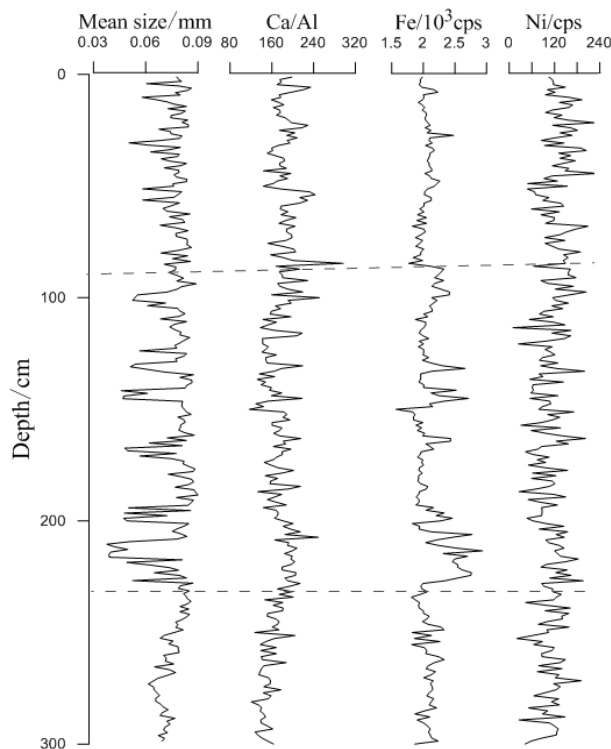


Fig.3 Vertical distributions of mean grain size, Ca/Al, Fe, Ni in the core WF1

Construction of Weifang Port since 1997 had great impact on sedimentary environment of the surrounding waters (22-85 cm in the core WF1, and 58-103 cm in the core WF2). The deposition rate significantly increased, and the average annual deposition rates of the core WF1 and WF2 were 5.1 cm and 3.5 cm between 1997 and 2007 respectively.

The core WF1 was surrounded by the encircling breakwater which was completed in 2007, and the sediment was deposited continually mainly because that the hydrodynamic effect within the encircling breakwater was significantly reduced (0-22 cm). The deposition rate of the core WF2 increased to 10.2 cm/a after 2007 due to the different position and protection of the encircling breakwater.

Formation of coastal landforms and hydrodynamic environment evolution were complex under the interaction between waves, tides, currents and human activities. Increasing human activities in coastal area, such as land reclamation, dams construction, sand excavation, nutrient and heavy metal element input played important roles in the evolution of hydrodynamic, sedimentary condition, and ecological environment deterioration. Evolution of marine hydrodynamic and sedimentary environment near Weifang Port was mainly performed in the change of deposition rate,

and it was mainly caused by the following factors: (1) Tidal current in the study area turned clockwise with characteristics of reciprocating flow. Construction of the port led to regional hydrodynamic environment changed, such as reduced current velocity and wave height, and enhanced deposition of suspended sediment on both sides of the port. (2) Sediments of silt-sandy beach was sensitive to hydrodynamic variation. Sediment of the study area is easy to be re-suspended, transported, and deposited near the port. (3) Residual and circular current system of Laizhou Bay was influenced by the port engineering. Tide-induced residual current in Laizhou Bay flows in clockwise direction. Sediment transportation trend of the study area is from east to west under the influence of tide-induced residual current. Wind-driven current also accounts for a certain proportion in Bohai circulation, and the wind-driven current in Laizhou Bay is an unclosed anti-clockwise circulation in winter. Construction of the port blocks the sediment transportation caused by residual current in the southern Laizhou Bay, and sediments are deposited on the both sides of the port.

Sediments of the two cores were relatively coarser and mainly composed of silty sand. Sediments above 230 cm in core WF1 and 218 cm in core WF2 were deposited since 1855 when the Yellow River appeared to deposit its sediments within the modern active delta, and the average deposition rate was between 0.3 and 0.5 cm/a. The average annual deposition rates were 5.1 cm and 3.5 cm in WF1 and WF2 respectively between 1997 and 2007. Content of heavy metals in sediments showed no obvious change in vertical, indicating that the heavy metals were less affected by human activity.

REFERENCES:

1. Chen, G. Q., Yi, L., Chen, S. L., et al., 2013. Partitioning of grain-size components of estuarine sediments and implications for sediment transport in southwestern Laizhou Bay, China. *Chinese Journal of Oceanology and Limnology*, 31(4): 895-906.
2. Huang, D. J., Su, J. L., and Zhang, L. R., 1998. Numerical study of the winter and summer circulation in the Bohai Sea. *Acta Aerodynamica Sinica*, 16(1): 115-121.
3. Li, G. S., Wang, H. L., Li, B. L., 2005. Numerical simulation on the wind-driven and tide-induced Lagrangian residual circulation and its seasonal spatial-temporal variations in the Bohai Sea. *Geographical Research*, 24(3): 359-370.

DIAGENESIS OF MAGNETIC MINERALS IN THE SEDIMENTS OF THE JAPAN SEA (YAMATO RISE) FOR THE LAST 78 KA AND ITS EFFECT ON THE GEOMAGNETIC AND CLIMATIC SIGNALS

Galina Malakhova¹, Sergey Gorbarenko², Xuefa Shi^{3,4}, Yanguan Liu^{3,4}, Jianjun Zou^{3,4}

¹ North-East Interdisciplinary Science Research Institute, FEB RAS, Magadan, Russia

² V.I. Il'ichev Pacific Oceanological Institute, FEB RAS, Vladivostok, Russia

³ Key Laboratory of Marine Sedimentology and Environmental Geology, First Institute of Oceanography, SOA, Qingdao, China

⁴ Laboratory for Marine Geology, Qingdao National Laboratory for Marine Science and Technology, Qingdao, China
galina.malakhova@mail.ru

The petromagnetic and magnetic properties of sediment of the earlier studied and dated core LV53-23 recovered from the Yamato Rise [1] were investigated with high resolution during last 78 calendar ka. The changes in the magnetic susceptibility (MS), characteristic magnetization (ChRM, paleomagnetically informative characteristic), anhysteretic remanent magnetization (ARM), all characterizing the concentration of the magnetic substance; parameters of the domain structure of ferromagnetic – the ratio of saturation remanence magnetization /saturation magnetization] (J_{rs}/J_s) and ratio of coercive force of saturation remanent magnetization/coercive force of saturation magnetization] (B_{cr}/B_c); calculated derivatives of the saturation isothermal remanent magnetization (HIRM and S_{ratio}), which show the ratio of the high-coercivity/low-coercivity particles and content of the secondary paramagnetic magnetization (PM) in the sediments, allowed us to identify three zones of diagenesis in the core (Fig.). Changes of sea level and accompanying changes in exchange between the waters of the Japan Sea and salt waters of the Pacific Ocean in the past had a profound effect on the salinity and density of the surface waters, ventilation of intermediate and deep waters and oxygen content in the bottom waters [2, 3] determining a diagenesis of sediments.

The sediments of the zone 1 (Z1), accumulated during the last 6 kyr (0-6 kyr), was formed during a high standing in sea-level with active water exchange between the Japan sea and the Pacific and high ventilation of deep waters. The strong concentration of magnetite and hematite of detrital origin, as high values of MS and ChRM show, points to the fact that a diagenesis has practically no action upon the primary magnetic particles (Fig.). The sediments of the Z1 zone are characterized by a typical set of the ferromagnetic, pseudo-single domain (PSD) grains with parameters of domain structure of $0.2 < J_{rs}/J_s < 0.3$ and $2 < B_{cr}/B_c < 3$ (Fig.).

The sediments of the Z2a and Z2b zones accumulated during 6.4-18.4 kyr and 18.4-27.4 kyr, respectively, have formed during the lowest standing of sea-level (up to 90-120 m below the present one). The Z2a zone is characterized by beginning of the paramagnetic pyrite (PM) formation and reduction in concentration of the finely-dispersed pseudo-single-domain magnetite particles as specified by lowering in values of ChRM, MS, ARM (Fig.).

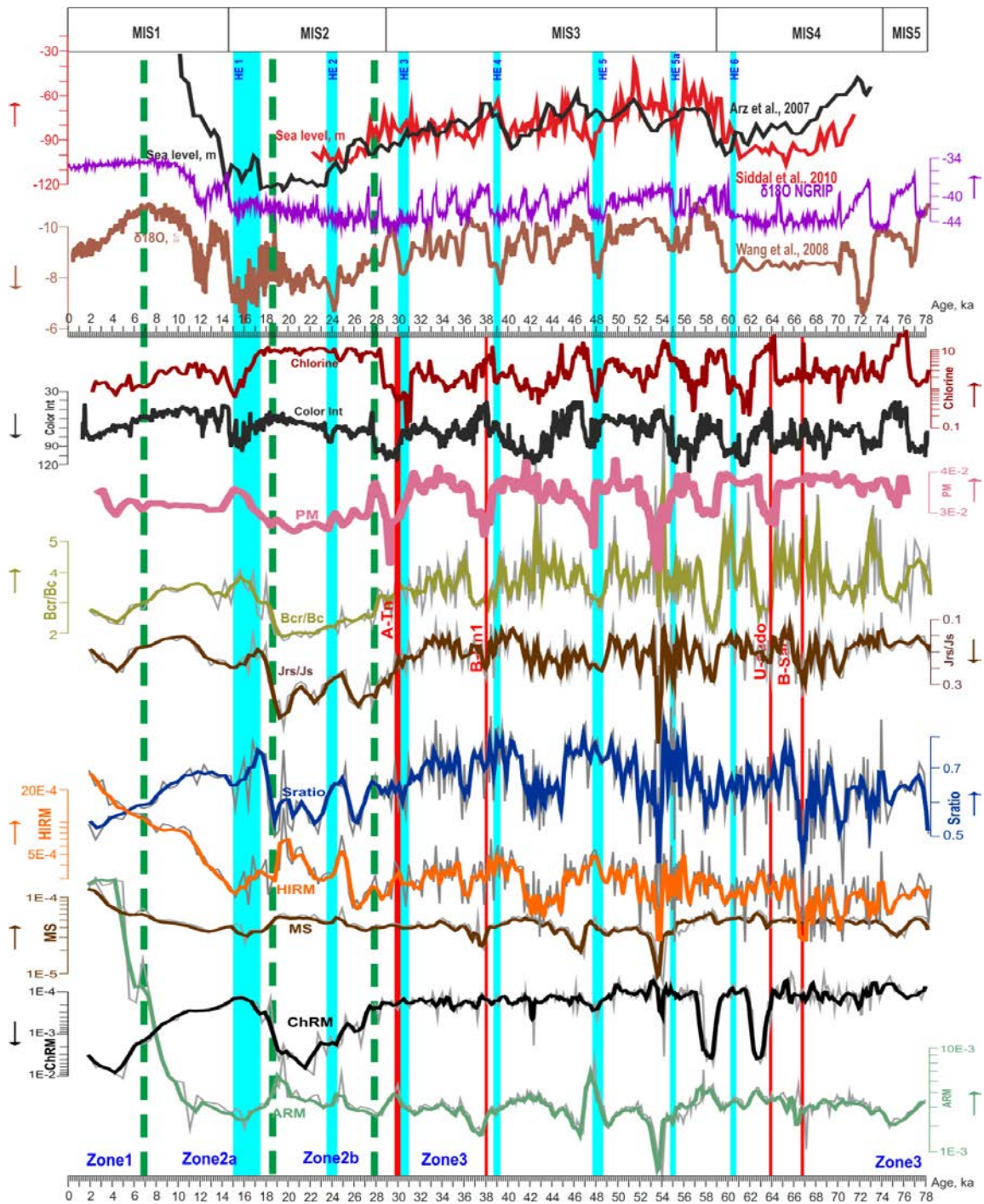


Fig. Correlations of the petro-magnetic characteristics of the core LV53-23-1 over the last 75 ka with changes in sea level [4] and $\delta^{18}O$ record of China cave stalagmite reflecting the changes in the summer monsoons in the East Asia [5], record of $\delta^{18}O$ values for Greenland ice [6] ARM, mA/m is the anhysteretic remanent magnetization; ChRM, mA/m is the characteristic magnetization strength; PM, Am²/kg is the paramagnetic magnetization strength; MS, un.SI is the volume magnetic susceptibility; A-Tn, B-Un1, U-sado, B-sado are the tephra layers, HIRM is the relative share of the high-coercivity magnetic component, S_{ratio} is the relative share of the low-coercivity particles. J_{rs}/J_s and B_{cr}/B_c are indices of the domain structure of particles [Day et al., 1987], Chlorin, ng/g is concentration of chlorophyll-a, Color Int is the color parameter. Boundaries of the diagenesis zones are shown by green dashed lines, the blue vertical stripes are cold Heinrich events HE1-HE6; the MIS 1-5 boundaries are shown according to [1] at the top.

Down the zone, the quantity of fine PSD-magnetite decreases slowly (reduction in HIRM values) but a content of coarse magnetic particles changes scarcely. A slight increase in S_{ratio} was registered and J_{rs}/J_s and B_{cr}/B_c ratios was equaled to 0.3 and 3 respectively (Fig.). Such variations of magnetic parameters of sediments imply the beginning of sediment diagenesis, especially at the bottom of the Z2a zone, owing to a low content of the dissolved oxygen in the near-bottom waters which resulted in dissolution of the fine PSD-magnetite and formation of the paramagnetic pyrite.

The Z2b zone, as parameters PM, ChRM and S_{ratio} demonstrate, is presented by paramagnetic iron sulfides, clastic magnetite and small amount of intermediate unstable phases of magnetic sulfide. The ranges of the domain structure parameters values ($0.3 < J_{rs}/J_s < 0.4$; $2 < B_{cr}/B_c < 3$) allow for the conclusion that the sizes of magnetic particles correspond to a mixture of fine pseudo-single-domain grains of magnetite and certain share of remaining single-domain greigite (Fig.). The obtained values of magnetic parameters of the Z2b zone sediments suggest the strong diagenesis of the Japan Sea sediments during 18.4-27.4 kyr BP due to the low standing of sea-level, very weak of deep water ventilation and practically anoxic conditions of the surface sediments (Fig.).

In sediment of the zone 3 (Z3, 27.6-78 kyr) the intensity of magnetic signal ChRM, MS is two orders of magnitude lower than in sediments of the Z1 (Fig.) which suggests the dissolution of the greater part of terrigenous magnetite and its transformation into the paramagnetic pyrite (PM). The indices of domain structure for samples of Z3 zone vary within the ranges of $0.15 < J_{rs}/J_s < 0.25$; $3 < B_{cr}/B_c < 5$ (Fig.) and correspond to the mixture of predominantly coarse pseudo-single-domain (PSD) – multi-domain (MD) grains which confirm strong sediment diagenesis. During decomposing of the organic matter in sediment with low content of dissolved oxygen, the fine magnetic fraction in sediments decays more intensively. The reduction in HIRM values suggests also the dissolution of the high-coercivity terrigenous ferromagnetic and formation of the bigger low-coercivity magnetic grains. At that time, the sea level has changed roughly from -90 m to -60 m, which resulted in weak ventilation of the near-bottom waters and low content of the dissolved oxygen in the surface sediment resulting to significant sediment diagenesis, consistently with demonstrated magnetic properties. The subsequent decrease in the sea level up to -120 m during marine isotopic stage (MIS) 2 and accompanying anoxic conditions of the near-bottom waters have aggravated the diagenesis of the Z3 zone sediments.

Despite the diagenesis of the Japan Sea sediments, such magnetic parameters of sediments as the B_{cr}/B_c , J_{rs}/J_s ratios, HIRM and S_{ratio} , reflecting the diagenesis extent (dissolution of the high-coercivity PSD and formation of the low-coercivity MD of magnetic fraction) as well as the content of paramagnetic substance (PM), change synchronously with variations of the basin productivity (chlorin, color intensity) and reflect the millennial scale changes of climate variability

in the middle-high latitudes of the northern hemisphere, recorded $\delta^{18}\text{O}$ values for the Greenland ice [6] and $\delta^{18}\text{O}$ of stalagmites of Chinese caves characterizing the activity of summer monsoon of the East Asia [5]. The most identifiable variations of magnetic signals in the Japan Sea sediments were demonstrated during coldest interstadials equivalent to the cold Heinrich events 6, 5a, 5 and 4 of the North Atlantic [7] due to decrease in productivity and diagenesis extent (Fig.). Normalization of the characteristic magnetization ChRM to ARM recorded in the Japan sea sediment do not correlate with the standard records of paleo-intensity of the Earth magnetic field, probably due to the strong sediment diagenesis.

This work was supported by the Russian Fund of Basic Research projects (№16-55-53048, 16-05-00127), Russian Federation budget (01201363042), the International Cooperation 40, Project of Global Change and Ocean-Atmosphere Interaction (GASIGEOGE-04), the National Natural Science Foundation of NNSF of China (41476056, 41611130042 and U1606401), international cooperative projects in polar regions (201613) and by Russia-Taiwan project (17-MHT-003).

REFERENCES:

1. Gorbarenko, S. X. Shi, et al., 2015. Fine structure of dark layers in the central Japan Sea and their relationship with the abrupt climate and sea level changes over the last 75 ka inferred from lithophysical, geochemical and pollen results. *Journal of Asian Earth Sciences*.
2. Tada, R., Irino, T., Koizumi, I., 1999. Land-ocean linkages over orbital and millennial timescales cycles recorded in late Quaternary sediments of the Japan Sea. *Paleoceanography*. 14, 236-247.
3. Gorbarenko, S.A., Southon, J.R., 2000. Detailed Japan Sea paleoceanography during the last 25 kyr: constraints from AMS dating and $\delta^{18}\text{O}$ of planktonic foraminifera. *Palaeogeogr. Palaeoclim. Palaeoecol.* 156, 177–193.
4. Arz, H.W., Lamy, F., Ganopolski, A., et al., 2007. Dominant Northern Hemisphere climate control over millennial-scale glacial sea-level variability. *Quatern. Sci. Rev.* 26, 312–321.
5. Wang, Y.J., Cheng, H., Edwards, R.L., 2008. Millennial- and orbital-scale changes in the East Asian monsoon over the past 224,000 years. *Nature* 451, 1090-1093.
6. North GRIP (Greenland Ice Core Project Members), 2004. High resolution climate record of the Northern Hemisphere reaching into the last interglacial period. *Nature* 431, 147–151.
7. Heinrich, H., 1988. Origin and consequences of cyclic ice rafted in the Northeast Atlantic Ocean during the past 130,000 years. *Q. Res.* 29, 142–152.

PASSIVE MICROWAVE SENSING OF THE NORTHWEST PACIFIC TROPICAL ZONE FROM THE CURRENT AND NEXT GENERATION SATELLITES

Leonid Mitnik, Maia Mitnik, Vladimir Kuleshov

V.I. Il'ichev Pacific Oceanological Institute, FEB RAS, Vladivostok, Russia

mitnik@poi.dvo.ru

Significant part of the Northwest Pacific Ocean is located in the tropical zone. This zone is characterized by the increased Sea Surface Temperature $SST > 20^{\circ} C$, higher values of the total water vapor content $V = 20-70 \text{ kg/m}^2$, power convective clouds with the total liquid water content $Q > 1 \text{ kg/m}^2$, heavy rains with rain rate R exceeding sometimes 50 mm/h and sea surface wind speed W reaching in the tropical cyclone areas 50-70 m/s. The various and changing oceanic phenomena are also observed in the tropical zone: periodic (tidal) and nonperiodic currents, warm and cold eddies and mushroom-like formations, upwellings, internal waves, coastal fronts etc.

Satellite observations in visible, infrared and microwave ranges enable to monitor both the atmospheric and oceanic phenomena and estimate their quantitative parameters. The data acquired by microwave (MW) sensors both by passive (radiometers) and active (scatterometers, altimeters, DPR, SARs) have a special interest for the tropical zone study since the observations are performed independently on sun illumination and cloudiness.

In a report, the main attention is given to the data obtained over the tropics by the multichannel scanning MW radiometers GCOM-W1 AMSR2, GPM GMI, SNPP ATMS and Meteor-M No. 2 MTVZA-GY which were launched on polar orbits during several last years. Performances of the MW instruments (frequencies, sensitivities, spatial resolution, etc.) as well as the incidence angles, scanning geometry and satellite orbits are different [1]. The algorithms for the retrieval of the key oceanic (SST , and W) and atmospheric (V , Q , and R) parameters were developed for each radiometer [1-5].

Fields of the brightness temperatures $T_B^{V,H}(\nu)$ with vertical (V) and horizontal (H) polarizations at frequencies ν and the retrieved parameters revealed the changes of spatial structure of the atmospheric and oceanic phenomena. The usage of the multisatellite data increases significantly the temporal resolution that is especially important for the study of the fast developing, changing and fast moving weather systems such as tropical cyclones, Intertropical Convergence Zone, fronts, atmospheric rivers, etc. The quantitative spatial data on the retrieved parameters (SST , W , V , Q , and R), the relevant satellite and ground truth data and the results of modeling serve as the main source of information for operational analysis and forecast of life cycle of the marine weather systems.

The advantages and features of the various multichannel and multisatellite microwave data are demonstrated by consideration of development and evolution of the Western Pacific tropical

cyclones Lionrock (19-31 August 2016) and Malakas (11-21 September 2016). The $T_B^{V,H(v)}$ at several frequencies and polarizations and the retrieved parameters are shown in Fig. 1.

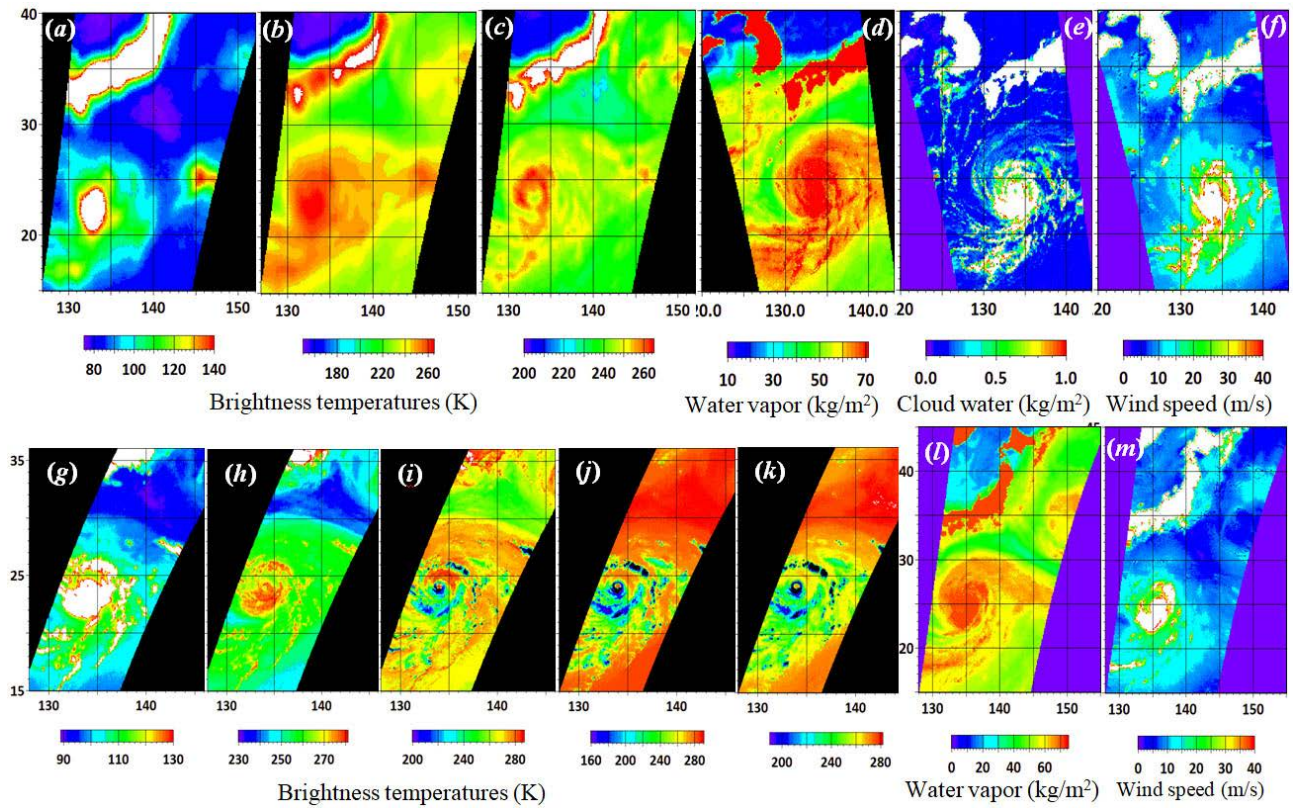


Fig.1. Typhoon Lionrock on 27 August 2016. Brightness temperatures acquired by MTVZA-GY at 02:51 UTC at frequencies 10.65 (a), 23.8 (b) and 48.0 GHz (c) with H-pol and by GMI at 06:06 UTC at 10.65 with H-pol. (g), 23.8 (h) and 89.0 (i) with V-pol., 166.0 with H-pol. (j) and 183.31 \pm 7 GHz with V-pol. (k) and total atmospheric water vapor content (d) and (l), total cloud liquid water content (e) and sea surface wind speed (f) and (m) retrieved from AMSR2 data at 04:23 UTC (d) - (f) and at 16:30 UTC (l) and (m).

Warm core in typhoons was detected in the brightness temperatures measured by the Suomi ATMS and Meteor-M No. 2 MTVZA-GY radiometers at several frequencies between 52.3 and 55.5 GHz.

The typhoon Lionrock central zone and rain bands (Fig. 2) are characterized by the high variations of the Normalized Radar Cross Section caused by the changes of the sea surface wind speed and direction and rain rate. Sentinel-1A SAR images were acquired at 20:54 UTC approximately 4.5 hours after AMSR2 measurements (Figure 1 l and m). Radar sensing was carried out with V-polarization and the backscattering signals were received both at V-pol (VV) and H-pol (VH). The swath width is equal to 405 km at the spatial resolution of 100 x 100 m.

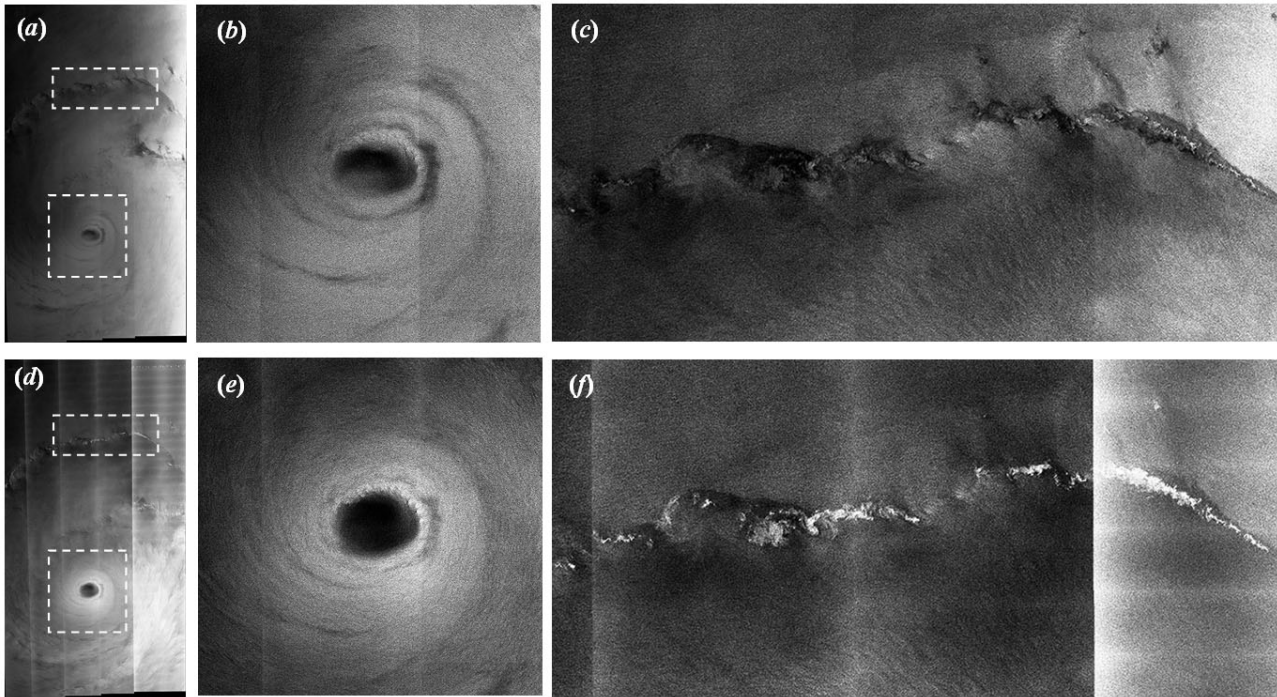


Fig. 2. Typhoon Lionrock on Sentinel-1A ASAR images with (a) VV- and (d) VH- polarization taken on 27 August 2016 at 20:54 UTC. The size of the images is 405 km x 750 km. The dotted rectangles mark the central zone (b) and (e) and rain band (c) and (f).

The possibilities of the tropical zone study using the next generation satellites with the passive and active microwave sensors are discussed in [5-9].

REFERENCES:

1. Katsaros K.B., Mitnik L.M., Black P.G. Microwave instruments for observing tropical cyclones / In: Typhoon Impacts and Crisis Management. Eds: DanLing) Tang, GuangJun Sui. 2014. Springer. P. 5-61.
2. Mitnik L.M., Mitnik M.L., Zabolotskikh E.V. Microwave sensing of the atmosphere-ocean system with ADEOS-II AMSR and Aqua AMSR-E // J. Remote Sensing Society of Japan, 2009. Vol. 29. No. 1. P. 156-165.
3. Mitnik M.L., Mitnik L.M. Algorithm for sea surface wind retrieval in tropics from AMSR-E data and its application to analysis of weather system // Current problems in the Earth Remote Sensing, 2011. Vol. 8. No. 3. P. 297-303 (in Russian).
4. Surussavadee C., Blackwell W.J., Entekhabi D., Leslie R.V. A global precipitation retrieval algorithm for Suomi NPP ATMS / The IEEE International Geoscience and Remote Sensing Symposium (IGARSS 2012), Munich, Germany. Proc. IGARSS 2012. P. 1924–1927, doi:10.1109/IGARSS.2012.6351128.
5. Zabolotskikh E.V., Mitnik L.M., Reul N., Chapron B. New possibilities for geophysical parameter retrievals opened by GCOM-W1 AMSR2 // IEEE Journal of Selected Topics in Applied Earth Observations and Remote Sensing. 2015. Vol. 8. No. 9. P. 4248-4261, doi: 10.1109/JSTARS.2015.2416514.
6. Barsukov I., Cherniavsky G., Cherny I., Mitnik L., Kuleshov V., Mitnik M. New Russian meteorological satellite Meteor-M N 2: Sensing of the subsurface, surface and atmospheric characteristics by MTVZA-GY microwave imager/sounder // The IEEE International Geoscience and Remote Sensing Symposium (IGARSS 2016), Beijing, China. Proc. IGARSS 2016. P. 5528-5531.
7. Mitnik L., Kuleshov V., Mitnik M., Streltsov A.M., Cherniavsky G., Cherny I. Microwave scanner sounder MTVZA-GY on new Russian meteorological satellite Meteor-M N 2: modeling, calibration and measurements // IEEE Journal of

Selected Topics in Applied Earth Observations and Remote Sensing. 2017. Vol. 10. No. 7. P. 3036-3045,, doi: 10.1109/JSTARS.2017.2695224.

8. Cherny I.V., Chernyavsky G.M., Mitnik L.M., Kuleshov V.P., Mitnik M.L., Uspensky A.B. Advanced Microwave Imager/Sounder MTVZA-GY-MP for New Russian Meteorological Satellite // The IEEE International Geoscience and Remote Sensing Symposium (IGARSS 2017), Fort Worth, Texas, USA. Proc. IGARSS 2017, P. 1220-1223.

9. Zavorotny V.U., Gleason S., Cardellach E., Camps A. Tutorial on Remote Sensing Using GNSS Bistatic Radar of Opportunity // IEEE Geoscience and Remote Sensing Magazine. 2014. Vol. 2. No. 4. P. 8–45. [doi:10.1109/MGRS.2014.2374220](https://doi.org/10.1109/MGRS.2014.2374220)

THE WORLD OCEAN AS THE MAIN DRIVER OF CLIMATE CHANGE

Vadim Navrotsky

V.I. Il'ichev Pacific Oceanological Institute, FEB RAS, Vladivostok, Russia

vnavr@poi.dvo.ru

The Earth Climate is space-time distribution over the Globe of *an ensemble of processes* that can be described by such parameters as temperature, pressure, wind velocity, cloudiness, humidity, precipitations etc. *averaged over some conditional spatial and temporal scales*. These highly nonlinear *climatic* processes carry out energy and mass exchanges in the Earth Climate System (CS) that includes oceans, atmosphere, land, biota and human civilization. With the ever changing components of CS, Climate by definition must change. The notion of “Climate Change” was introduced to bring out that something disturbing for humanity is going on in the CS. Climate Change (CC) is a result of fluctuations of energy content and redistribution in the Climate System, The main natural source of energy in the Earth system is the Sun emanation, and the World Ocean is the main recipient, transformer, **accumulator**, and redistributor of solar energy and, consequently, the main supplier of energy for CC. Therefore, to understand Climate Change and its effects, we should study, first and foremost, external and internal processes leading to changes in energy income, assimilation, transformation, and redistribution in the ocean, and space-time structure of the energy and mass interchange between the ocean and atmosphere that creates the main features of Global Climate. During the last 50-60 years the ocean heat content gain has been 30-40 times more than on land and in atmosphere, and the unknown equilibrium balance between CS components can be shifted in favor of oceans. The main problems stemming from the ocean overheating are rise of sea level, infringement of water balance between land and ocean, amplification of intensity and frequency of hurricanes, and changes in biosphere. In the presentation the main aspects of climate problem are proposed for discussion with special attention given to role of oceanic ecosystems and external factors in Climate Change.

FEATURES OF THE PHYTOPLANKTON COMMUNITIES IN THE SAKHALIN ISLAND COASTAL ZONE AND CHARACTERISTIC OF POTENTIAL TOXIC ALGAL SPECIES IN THE SUMMER-AUTUMN PERIOD 2015

Tatiana V. Nikulina¹, Tatiana A. Mogilnikova²

1. Federal Scientific Center of the East Asia Terrestrial Biodiversity FEB RAS, Vladivostok, Russia

2. Sakhalin Research Institute of Fisheries and Oceanography, Yuzhno-Sakhalinsk, Russia

nikulina@ibss.dvo.ru

Investigations to identify the species composition and quantitative characteristics of phytoplankton in the coastal waters of southwestern and southern Sakhalin in the summer-autumn period of 2015 were carried out.

A species composition of the coastal flora of the Sakhalin Island since was represented by 465 species, varieties and forms from nine divisions: Cyanobacteria, Bacillariophyta, Chlorophyta, Euglenophyta, Chrysophyta, Cryptophyta, Dinophyta, Haptophyta и Ochrophyta. Species *Cocconeis scutellum* Ehrenberg, *Skeletonema costatum* (Greville) Cleve, *Teleaulax acuta* (Butcher) Hill, *Melosira lineata* (Dillwyn) Agardh, *Pleurosigma formosum* W. Smith, *Leptocylindrus minimus* Cleve are noted among the dominant species most often [1].

Mass growth of diatom, cryptophytes and dinoflagellate algae was recorded in the coastal zone of the southwestern (Tatar Strait) and southern (Aniva Bay) Sakhalin in the summer-autumn period of 2015. At the south-west coast, the total phytoplankton abundance varied from $1,147 \times 10^3$ cell/L (August) to $1683,318 \times 10^3$ cell/L (July); the maximum biomass of algae was formed in July – $2174,9 \text{ mg/m}^3$, the minimum was recorded in August – $6,5 \text{ mg/m}^3$. In the coastal zone of the Aniva Bay, algae abundance varied from $15,061 \times 10^3$ (October) to $512,957 \times 10^3$ cell/L (September), biomass from 13,64 (June) to $908,20 \text{ mg/m}^3$ (August). Diatoms prevailed by abundance, and cryptophytes prevailed more rarely. The highest quantitative indices of planktonic algae were observed in the mouth of Taranai River [1].

Potentially toxic and harmful algae are registered in the coastal zone of Sakhalin Island. Algae were recorded on the south-western coast: species of the genus *Pseudo-nitzschia*, *Dinophysis* cf. *rapa*, *Prorocentrum micans*, *P. cordatum*, *Alexandrium monilatum* (they had temperate or low numbers) and *Ostreopsis siamensis* (the species had a mass vegetation). On the southern coast of the Sakhalin Island there was a mass growth of species from the genus *Pseudo-nitzschia*, species *Prorocentrum cordatum*, *P. balticum*, *P. micans*, *Dinophysis* aff. *arctica*, *D. acuminata*, *D. acuta*, *Ostreopsis siamensis*, *Alexandrium ostenfeldii* were of temperate or low numbers.

REFERENCE:

1. Mogilnikova, T.A. Nikulina, T.V., Koreneva, T.G., Latkovskaya, E.M., Vedernikova, A.A. // Vladimir Ya. Levanidov's Biennial Memorial Meetings. Vol. 7. Vladivostok : Dalnauka, 2017. P. 159–177.

GASGEOCHEMICAL INDICATORS GEOLOGICAL PROCESSES ON THE COSTAL AND SEA

Anatoly Obzhirov

V.I. Il'ichev Pacific Oceanological Institute, FEB RAS, Vladivostok, Russia

obzhirov@poi.dvo.ru

All geological, geophysical, gas geochemical, hydroacoustic, morphostructure complex are very important to use like indicators to search gas hydrate and to understand regularity to form and to destroy of it. Thus, complex investigations allow us to discover methane fluxes, gas hydrate and to find much geological regularity around gas hydrate in the Japan and Okhotsk Seas as well as to examine relationship between methane fluxes, gas hydrate, oil-gas and coal deposit. It is knowledge help to work out of mining hydrocarbon from gas hydrate to use it like source of unconventional energy.

The large scale gas emission installed in the Laptev, Okhotsk, Japan, Philippine and the South China seas. Mud volcanic nature the giant gas flare (>2000 m high, the highest in the World Ocean, Fig. 1) in the west of Kurile Basin and geochemical fields of seas, including hydrogen anomalies up to 200 ppm in the area, related to geotectonic lineaments. Co-seismic, short post-seismic, long post-seismic, and pre-seismic types of the gas emission are suggested. The gas emission origin in the seas is discussed. The authors suggest their possible connection with vertical movement of the mantle mass and the torsion of the separate crustal blocks. The formation of lithosphere vortex structures and the allocation of the particular type of geomorphologic objects (Yin-Yang systems) Asia - Pacific margin is the result arising from these shifts movements.

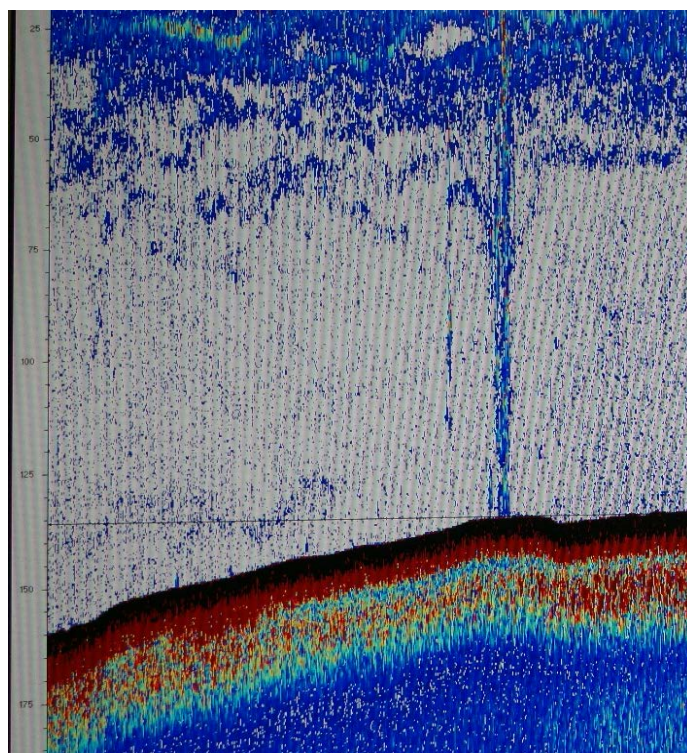


Fig. 1 Change surface of sediment in the area with flux methane and gas hydrate.

These processes generate vortex turning of tectonic masses under the dominance of the Earth's axial rotation and pulsation electromagnetic field. The resulting horizontal dynamic stresses lead to lateral displacement of the lithosphere masses on the periphery of the vortex tectonic system. It is the result of shear interactions of continental and oceanic plates. Regions of their intersection are the most tectonically active zones of marine basins [1]. Gas hydrate is forming in the seismic active areas with zones fault and methane fluxes in the big pressure and low temperature (Fig. 1 and Fig. 2).



Fig. 2 White layers are gas hydrate in the bottom sediment Okhotsk Sea.

REFERENCE:

1. Operation Report of Sakhalin Slope Gas Hydrate (SAKHALIN) Project II, 2015, R/V Akademik M.A. Lavrentyev Cruise 70 (2016) Kitami Institute of Technology. Edited by N. Minami, Y.K. Jin, B. Baranov, N. Nikolaeva and A. Obzhirov. 119 p.

LOCAL WINTERTIME VENTILATION IN THE CENTRAL NORTH PACIFIC

Aijun Pan

Third Institute of Oceanography, SOA, Xiamen, China

aijunpan@tio.org.cn

Using ARGO observations provided by the French Coriolis Data Centre (IFREMER), in conjunction with the geostrophic current data from AVISO, the interannual variations of the Kuroshio Extension (KE) and its impacts on the local wintertime ventilation in the central North Pacific is explored. By studying the “formation locality” of the North Pacific Central Mode Water (CMW), the locally vertical mixing regime in the central North Pacific is identified and moreover, impacts of the northward branch of the KE on the local ventilation of the thermocline are confirmed. It reveals that significant changes of the KE, especially its northward branch (warm advection) between the Shatesky Rise (159°E) and the Emperor Seamount (171°E) serves as the key factor for inducing the locally deep wintertime mixing in the central North Pacific. Eventually, it counteracts the cooling trend of the mixed layer along the KE triggered by surface heat losses, vertical entrainment and southward Ekman advection. As a result, the northward KE branch acts to quantify well the west bound of the “stability gap” of the stratification and therefore, contribute to the emergence of the “formation locality” of the CMW in the following spring and the local ventilation of the thermocline. Our results suggest that both of the real-time ARGO observations and Altimeter data, once assimilated into predictive systems, have a strong potential to enhance the tropical Pacific’s interannual and decadal changes forecasting skills.

DISTRIBUTION AND AIR-SEA FLUXES OF CARBON DIOXIDE ON THE CHUKCHI SEA SHELF

**Irina Pipko^{1,2}, Svetlana Pugach^{1,2}, Irina Repina³, Oleg Dudarev^{1,2}, Alexander Charkin^{1,2},
Igor Semiletov^{1,2}**

¹ V.I. Il'ichev Pacific Oceanological Institute, FEB RAS, Vladivostok, Russia

² National Research Tomsk Polytechnic University, Tomsk, Russia

³ A.M. Obukhov Institute of Atmospheric Physics, Moscow, Russia

irina@poi.dvo.ru

The Arctic now is undergoing dramatic changes, which cover the entire range of natural processes; from extreme increases in the temperatures of air, soil, and water, to changes in the cryosphere, the biodiversity of Arctic waters, and land vegetation. Small changes in the largest marine carbon pool, the dissolved inorganic carbon pool, can have profound impact on the carbon dioxide (CO₂) flux between the ocean and the atmosphere, and the feedback of this flux to climate. Knowledge of relevant processes in the Arctic seas improves the evaluation and projection of the carbon cycle dynamics under conditions of rapid climate change.

The report presents the results of long-term investigations of the carbonate system's dynamics and air-sea carbon dioxide fluxes on the Chukchi Sea shelf during the summer seasons of 1996, 2000, 2002, 2008 and 2011. Our investigation showed that surface waters of ice-free highly productive Chukchi Sea shelf during summer and early autumn are undersaturated in CO₂ and therefore serve as a significant regional sink for atmospheric CO₂. Because of the complex effect of physical and biological factors, the surface waters pCO₂ varied in the range from 134 to 359 μatm. Mean CO₂ fluxes from atmosphere to surface water were estimated in the range from -4 to -22.0 mmol/(m² day) in different years. It is significantly higher than the average value of the air-sea CO₂ flux in the World Ocean. According to our estimation, the minimal value of carbon absorbed by the Chukchi Sea shelf water from the atmosphere during the ice-free period is approximately 13×10^{12} g; a significant part of this carbon is then transported to lower water layers and isolated from the atmosphere for a long time.

The data obtained during our investigation add information about the CO₂ fluxes over the Chukchi Sea shelf, enabling a more accurate estimation of the absorption capacity of the whole Chukchi Sea in the summer/fall season. Our investigation shows the importance of processes that vary on small scales, both in time and space, for estimating the air-sea exchange of CO₂. It stresses the need for high-resolution coverage of ocean observations as well as time series. Furthermore, time series must include multi-year studies in the dynamic shelf regions of the Arctic Ocean during these times of environmental change.

A HISTORY OF METHANE RELEASE IN SOUTHWESTERN PART OF THE OKHOTSK SEA DURING THE LAST 10 000 YEARS (FORAMINIFERA, $\delta^{13}\text{C}$, $\delta^{18}\text{O}$, ^{14}C)

Sergei Pletnev¹, Yonghua Wu², Alexandra Romanova³, Vladimir Annin¹, Olga Vereshchagina¹, Igor Utkin¹

¹ V.I. Il'ichev Pacific Oceanological Institute, FEB RAS, Vladivostok, Russia

² Key Laboratory of Marine Sedimentology and Environment Geology, First Institute of Oceanography, SOA, Qingdao, China.

³ Far Eastern Geological Institute, Vladivostok, Russia

pletnev@poi.dvo.ru

The Okhotsk Sea is one of the largest reservoirs of gas worldwide [3]. Methane releases were first discovered near the Paramushir Island [8]. Next expeditions revealed more than 500 methane seeps and 17 gas hydrate fields on the sea bottom within depths between 150 and 1440 m [6]. We report several negative carbon stable isotope excursions in benthic foraminifera in a gas-bearing core LV50-05, collected from an area of active methane venting on the Eastern Slope of Sakhalin Island, the Okhotsk Sea. These negative peaks reflect regional history methane releases over the past 10 000 yr BP. The chronostratigraphic framework of the core has been derived from AMS ^{14}C dates and biostratigraphic analyses. While benthic foraminifera (*Nonionellina labradorica* and *Uvigerina parvocostata*) from some intervals have $\delta^{13}\text{C}$ within the normal marine range (about -1‰), some intervals are characterized by strongly depleted $\delta^{13}\text{C}$ (as low as -34.5‰ VPDB). These negative $\delta^{13}\text{C}$ peaks are interpreted to record methane events (ME) at the seafloor during primary (lifetime) biomineralization and postsedimentary calcification in foraminifera tests.

The radiometric dating was performed at the National Ocean Sciences Accelerator Mass Spectrometry (NOSAMS) Facility at Woods Hole Oceanographic Institution. All ^{14}C ages were converted into calendar ages according to Fairbanks et al. [2] with the regional sea surface water reservoir ages of 950 yr BP [4]. The isotopic composition determinations were conducted with the use of the Finnigan-Mat 253 mass spectrometer in the State Key Laboratory of Marine Geology at the Tonji University. The standard deviation was 0.05‰ for $\delta^{13}\text{C}$ and 0.07‰ for $\delta^{18}\text{O}$, and all received measurements were related to the international scale (V-PDB) with the NBS19 Standard [1]. Combining sedimentation rates with AMS ^{14}C and biostratigraphical data we estimate the beginning of accumulation in the core LV50-5. It starts in Preboreal, about 10,000 yr B.P.

The most valuable record of $\delta^{13}\text{C}$ for *N. labradorica* fixes four methane events (ME): ME-1 (nearly 700 yr BP), ME-2 (from 1000 to 1400 yr BP), ME-3 (2500 -5400 yr BP) and ME-4 (7400-10000 yr BP). These events can be correlated with methane releases in studied area.

Most depleted $\delta^{13}\text{C}$ for *N. labradorica* mostly present isotope signal of authigenic carbonate (MDAC) on dead tests of foraminifera. Depleted $\delta^{13}\text{C}$ for *Uvigerina parvocostata* fixes vital isotope signal during ME-1, ME-2 and ME-3. The most ^{13}C -depleted value for *Uvigerina parvocostata* (-

3.8 ‰) in ME-3 (at 180 cm bsf) reflect a combination signal of vital and precipitation of the MDAC. Such mixed signals mark for *labradorica* and *U. parvocostata* in ME-4. Secondary calcification of the shells changed the original age of AMS¹⁴C data. Only four AMS ¹⁴C dates from of 8 were recognized as valid. Processes of sulfate reduction and anaerobic oxidation of methane had a large influence on negative $\delta^{13}\text{C}$ excursions for ME-3 – ME-1. During ME-3 primary production (diatoms) increased due to surface water warming, ice retreatment, an increase supply of biogenic elements from land and the Amur River. Sedimentation regime changes intensified biogeochemical processes. Role of microbial methane in near-surface sediments sharply increased. The negative values of $\delta^{13}\text{C}$ for the foraminifera are mainly caused by calcification in the presence of depleted ¹³C DIC and consumption (food) of ¹³C-depleted methanotrophic microbes. The border of the modern SMI is located at 300 cm bsf in core LV50-05. In ME-4 sediments, a relict SMI level has been found out at 430-450 cm. This interval is enriched by the solid carbonate concretions (Fig.). Negative excursions of $\delta^{13}\text{C}$ for ME-1 and ME-2 fixed traces of two short-term events that interrupted the normal marine regime during the last 2300 years. ME-2 synchronizes with catastrophic eruption of the Baitoushan Volcano on the boundary between China and Korea. The reason for the ME-1 are still being debated.

LV50 Site is located in the zone of active seismic and tectonic processes, near the fault Lavrentyev Fault Zone. The seepages during ME-3 and ME-4 were most likely associated with regional stress-related faulting. The beginning of Early ME-4 corresponds to Preboreal. Planetary increase of atmospheric methane concentration is noted during this period [5].

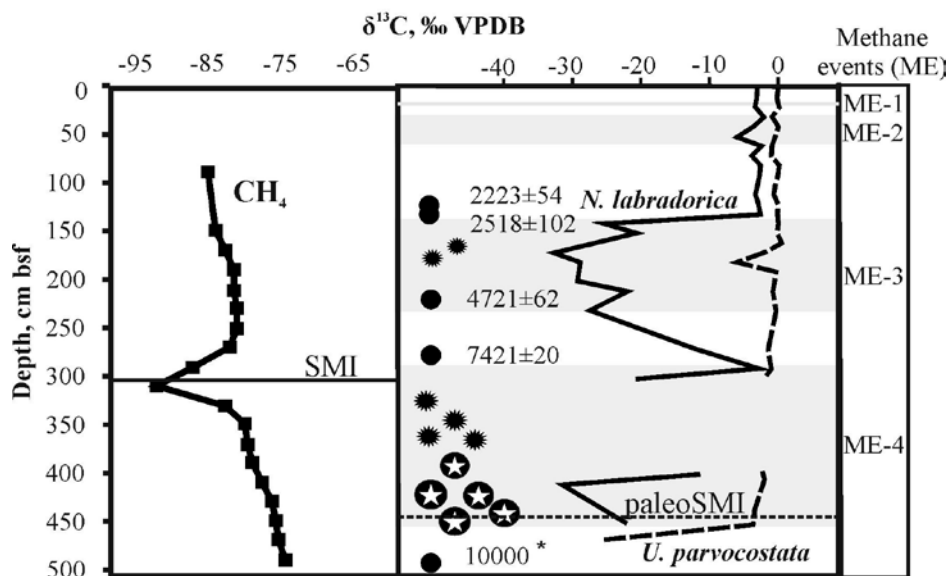


Fig. $\delta^{13}\text{C}$ variations in the core LV50-05. The left part shows $\delta^{13}\text{C}$ variation of methane in the pore waters [9] and the position of the modern SMI boundary. Right - $\delta^{13}\text{C}$ changes in calcite shells of two benthic foraminifera species, relict border of SMI and AMS ¹⁴C dates. Dark circle with an asterisk - solid carbonate concretions; an asterisk - "soft" carbonate concretions.

REFERENCES:

1. Cheng, X., Huang, B., Jian, Z. et al. Foraminiferal isotopic evidence for monsoonal activity in the South China Sea: a present-LGM comparison // *Marine Micropaleontology*. 2005. V. 34. P. 25–139.
2. Fairbanks, R.G., Mortlock, R.A., Chiu, T.C. et al. Marine radiocarbon calibration curve spanning 10,000 to 50,000 years BP based on paired $^{230}\text{Th}/^{234}\text{U}/^{238}\text{U}$ and ^{14}C dates on pristine corals // *Quat. Sci. Rev.* 2005. V. 24. P. 1781–1796.
3. Ginsburg G.D., Soloviev V.A. Submarine gas hydrates // Saint-Peterburg: VNIIOkeanologia. 1994. 216 p. (in Russian).
4. Keigwin L.D. Glacial-age hydrography of the far northwest Pacific Ocean // *Paleoceanography*. 1998. V. 13. P. 323–339.
5. Maslin, M., Owen, M., Day, S. et al. Linking continental-slope failures and climate change: testing the clathrate gun hypothesis. // *Geology*. 2004. V. 32. P. 53–56.
6. Obzhirov A.I., Telegin Yu. A., Boloban A.V. Methane fluxes and Gas Hydrate in the Okhotsk Sea. // *Underwater Investigations and Robotics*. 2015. V. 1 (19). P. 56-63.
7. Utkin I.V. Reconstructing the Setting for Deposition of Distal Tephra in the Sea of Japan Basin: A Catastrophic Eruption of Baitoushan Volcano // *Journal of Volcanology and Seismology*. 2014. V. 8(4). P. 228–238.
8. Zonenshine L.P., Murdmaa I.O., Baranov B.V. et al. The submarine gas source in the Okhotsk Sea to the west from Paramushir Island // *Okeanologiya (Oceanology)*. 1987. V. 5. P. 598–602 (in Russian).
9. Hachikubo A., Tatsumi K., Sakagami H. et al. Molecular and isotopic compositions of hydrate-bound hydrocarbons in subsurface sediments from offshore Sakhalin Island, Sea of Okhotsk // *Proceedings of the 7th International Conference on Gas Hydrates (ICGH 2011)*, Edinburgh, Scotland, United Kingdom, July 17–21, 2011. Edinburgh, 2011. <http://www.researchgate.net/publication/259493672>

CLIMATE REGIME CHANGE IN THE LAND-OCEAN-ATMOSPHERE SYSTEM AT THE TURN OF 20-21 CENTURIES

Vladimir Ponomarev, Elena Dmitrieva, Svetlana Shkorba, Aleksandr Karnaukhov

V.I. Il'ichev Pacific Oceanological Institute, FEB RAS, Vladivostok, Russia

pvi711@yandex.ru

The regional climate regime shift in late 90s - 2000 is shown in the state of North Atlantic [1], North Pacific [2-6]. In the North Atlantic it is shown in terms of phase trajectory of Sea Level Pressure (SLP), Sea Surface Temperature (SST) differences between its values in the Azores High area and Icelandic Low region [1]. Recent change in climate regime of planetary scale at the turn of 20-21 centuries was revealed by using monthly mean oceanographic and meteorological observation data. Time series (from 1900/1946 to 2016) of global fields of Hadley, Reynolds SST, surface net heat flux (Q), latent and sensible heat fluxes, atmospheric pressure (SLP), air temperature (SAT), precipitation, Precipitable Water Content (PWC) from NCEP NCAR reanalyses (1948-2016) and other data sets are involved into statistical analyses. We use different statistical methods, including correlation analyses, Principal Component Analyses (PCA) and cluster analysis via PCA. Based on Correlation and Cluster analyses via PCA we select large scale areas, at first, in Asia Pacific, Indo Pacific and Southern Ocean to use monthly mean time series of meteorological and oceanographic characteristics averaged within the areas shown in Fig.1 [5, 6].

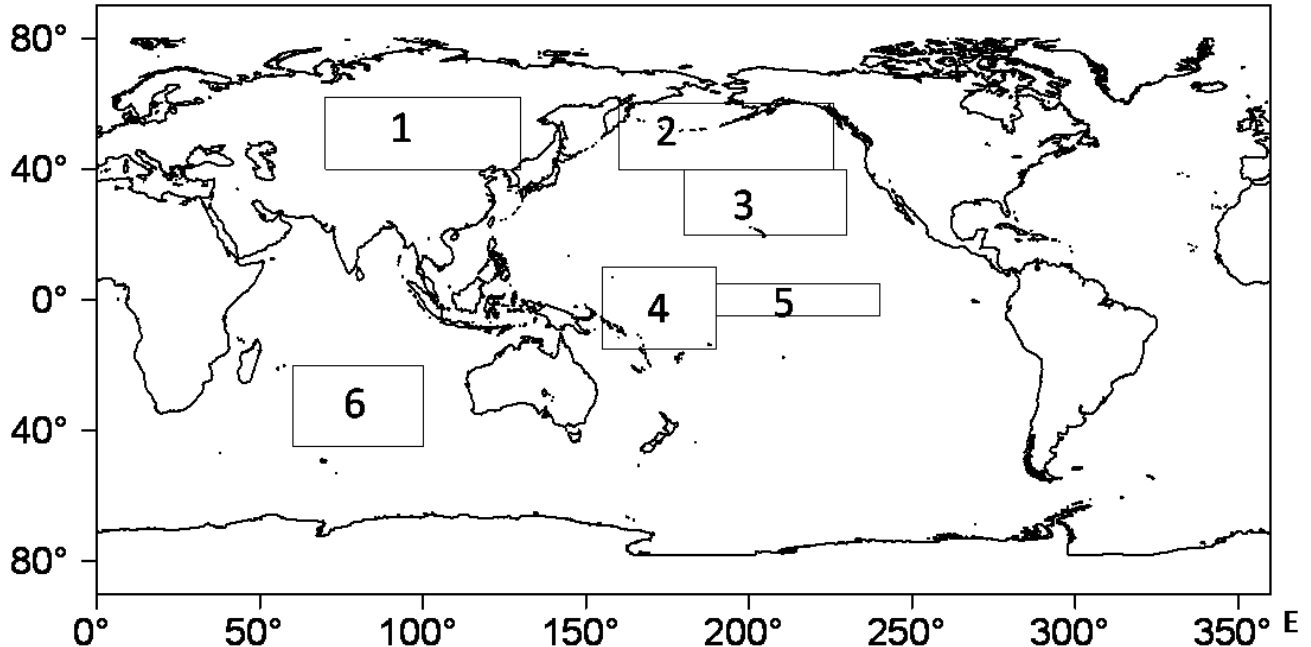


Fig.1. Regions of Q, SLP, Pr, TWC , SST averaging in Asia, Pacific and Indian Oceans : 1 – the zone of temperate latitudes of Asia; 2 – Subarctic Pacific; 3 – Eastern Subtropical Pacific; 4 – Western Equatorial Pacific; 5 – Central Equatorial Pacific 6 – South Indian Ocean

The climate regime change is estimated, at first, in terms of phase trajectory of certain characteristics in two selected regions. Fig. 2 shows climate shift both in mid 70s and late 90s in phase trajectory of two net heat fluxes (Q, W/m²) time series of Q₂ in Subarctic Pacific (axes Y

region 2), and Q6 in South Indian Ocean (axes Y region 6) from 1948 to 2015 in boreal hydrological winter (JFM).

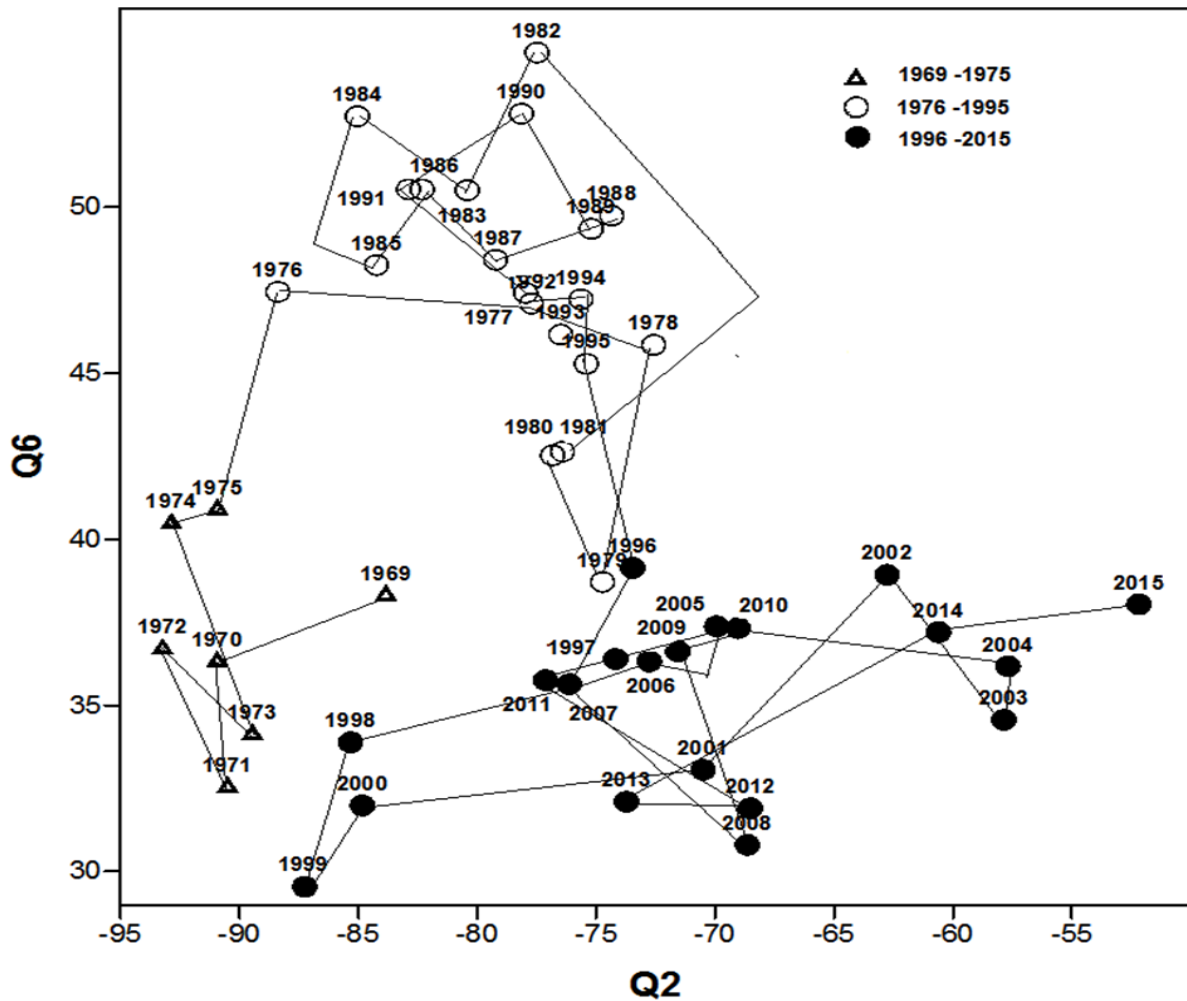


Fig. 2. Phase trajectory of the surface net heat fluxes (Q , W/m^2) of 3-years running mean time series (1969 - 2015) averaged in Subarctic Pacific (Q_2) and South Indian Ocean (Q_6) in boreal winter (JFM). Regions 2 and 6 are shown in Fig. 1.

Similar two climate regime shifts in the phase trajectory of the net heat flux at the ocean surface in Subarctic Pacific and South Indian Ocean is also found in summer (JJA) time series of Q_2 and Q_6 . The winter and summer time series of Q_2 and Q_6 are shown in Fig. 3, 4 correspondently.

Recent climate shift the net heat flux in 90s in both Subarctic Pacific (Q_2) and South Indian Ocean (Q_1) is most prevailed in boreal winter. Rapid reduction of Q directed to the ocean in South Indian (summer in Southern Hemisphere) accompany rapid reduction of Q directed from the ocean to the atmosphere in the Subarctic Pacific (Northern Hemisphere).

Two shifts of the climate regime both in mid 70s and late 90s are also revealed in terms of phase trajectory of PC1, PC2 of set included 18 time series of differences between values of both Q and SLP in boreal winter in all of 6 selected areas. Two similar climate regime shifts are also found in terms of phase trajectory of 3-years running mean annual SAT differences, particularly between

regions T2-T4, T1-T2, as well as in phase trajectory of PC1 and PC2 of set, which includes 12 time series (1948 - 2015) of annual Q and PWC in all of 6 selected areas (Fig.3).

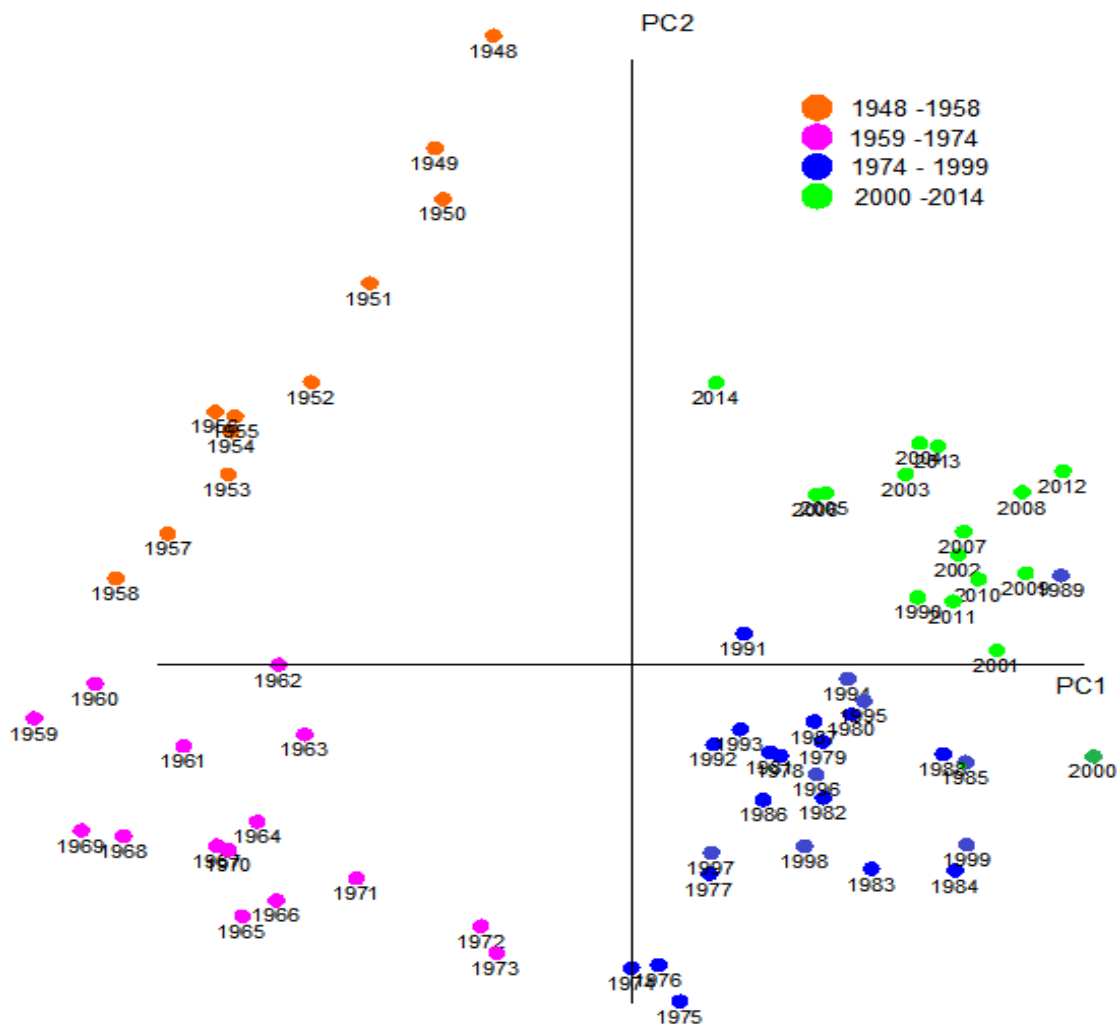


Fig. 3. Phase trajectory of 3-years running mean PC1 and PC2 of set, which includes 12 time series (1948 - 2015) of annual surface net heat flux Q and Precipitable Water Content (PWC) in all of 6 selected areas (Fig. 1). Four major classes of PC1 and PC2 determined by cluster analyses are marked by color symbols.

It is also shown that the climate regime is significantly changed in all of the Eurasia, Southern and Atlantic Ocean at the end of the 20th century in terms of Q, SLP, SST, SAT, PWC. After the recent climate regime shift in late 90s the SLP increases mainly in central extratropical areas of both North and South Pacific, in South Indian Ocean with maximal changed in winter. The SLP also increases in central continental Asia of temperate latitudes, particularly in Mongolia and South Siberia, Baikal Lake Basin, where maximal SLP change occurs in summer. The SLP decrease and intensification of cyclonic activity occur in the marginal ocean-land areas of the North and South Pacific, Indian, Southern and Arctic oceans including their marginal seas. Total water content in the atmosphere and precipitation significantly increase in this zone. Surface air temperature in most of marginal areas rises in fall and winter while decrease in spring and early summer. Repeatability of number of strong storms, tropical and extratropical cyclones has increased in the Western Pacific and its marginal Seas, Western and Eastern Atlantic Ocean. Recent climate regime

in comparison with previous one is characterized by reduce of Q amplitude in annual cycle and meridional gradients of annual and seasonal Q, PWC, SST. Absolute values of Q directed to the ocean in summer and to the atmosphere in winter are usually reduced after late 90s of the 20th century.

It accompanies change in the ocean vertical structure, circulation and meridional heat transport in both global atmosphere and World Ocean. The meridional heat transport both in the atmosphere and ocean is increasing from the tropics and subtropics to subarctic and arctic regions, being prevailed in western ocean-land marginal areas. It results in warming in subarctic and Arctic regions being prevailing in summer, decrease of meridional temperature gradient and increase of zonal temperature contracts in the ocean and continental areas. Intensification of tropical and extratropical cyclones in the marginal land-ocean zones results in unusual extreme storms, hurricanes and floods in the East Asia, North America and North Europe, while extreme drying occurs in Asian deserts and adjacent regions including South Siberia, Lake Baikal catchment area.

Our study was supported by the Program "Dalniy Vostok" of the Russian Branch of the Russian Academy of Sciences (Project 15-I-1-047).

REFERENCES:

1. Byshev V.I., Neiman V.G., Romanov Yu.A. et al. Phase variability of some characteristics of the present-day climate in the Northern Atlantic region // *Doklady Earth Sciences*. 2011. V. 438. P. 887-892. Original Russian Text published in *Doklady Akademii Nauk*, V. 438, P. 92–96.
2. Bond N., Overland J., Spillane M. et al. Recent shifts in the state of the North Pacific // *Geophys. Res. Lett.* 2003. V. 30 (23). P. 2183-2186.
3. Yeh S.-W., Kang Y.-J., Noh Y., and Miller A. J. The North Pacific climate transitions of the winters of 1976/77 and 1988/89 // *J. Climate*,. 2011. V. 24(4). P. 1170–1183.
4. Jo H.-S., Yeh S.-W., Kim C.-H. A possible mechanism for the North Pacific regime shift in winter of 1998/1999 // *Geophys. Res. Lett.* 2013. V. 40. P.4380–4385.
5. Ponomarev V.I., Dmitrieva E.V., Shkorba S.P. Features of climatic regimes in the North Asia Pacific. // *Sistemy kontrolya okruzhayuschei sredy*, (J. Systems of environment control published in Russian). Sevastopol. 2015. V. 1 (21). P. 67-72 (in Russian).
6. Ponomarev V., Dmitrieva E., Shkorba S., Mashkina I., Karnaukhov A. Climatic regime change in the Asian Pacific Region, Indian and Southern Oceans at the end of the 20th century// *Proceedings of International Conference "Managing risks to coastal regions and communities in a changing world" (EMECS'11 - SeaCoasts XXVI)*. St. Petersburg, 22-27.08.2016). Moscow, RIOR Publ., 2016. N 156 P.1-14.

HOW EDDIES GAIN, RETAIN AND RELEASE WATER: THE LAGRANGIAN APPROACH

Sergey Prants

V.I. Il'ichev Pacific Oceanological Institute, FEB RAS, Vladivostok, Russia

prants@poi.dvo.ru

A special Lagrangian methodology is developed to simulate and analyze the processes of entrainment and detrainment of waters to and from oceanic eddies. It includes computer integration of equations of motion for passive particles advected by altimetry- or numerically-derived velocity fields, computation of different Lagrangian indicators and representing the information obtained as geographical maps. A number of examples with mesoscale eddies in the Northwestern Pacific demonstrates the effectiveness of that methodology to study how eddies gain, retain and release water and document their life history from the birth to a decay. An extensive review of these methods with applications can be found in the new coming book “Lagrangian oceanography: large-scale transport and mixing in the ocean. Berlin, New York. Springer Verlag. 2017” by S.V. Prants, M.Yu. Uleysky and M.V. Budyansky.

BOTTOM WATER CONDITION CHANGES IN THE NW PACIFIC DURING THE LAST GLACIAL MAXIMUM- HOLOCENE ACCORDING TO BENTHIC FORAMINIFERA

**Olga Psheneva¹, Tiegang Li^{2,3}, Sergey Gorbarenko¹, Xuefa Shi^{2,3}, Yanguang Liu^{2,3},
Jianjun Zou^{2,3}**

¹V.I. Il'ichev Pacific Oceanological Institute, FEB RAS, Vladivostok, Russia

²First Institute of Oceanography, SOA, Qingdao, China

³Qingdao National Laboratory for Marine Science and Technology, Qingdao, China

psheneva@poi.dvo.ru

We reconstructed changes in the condition of the sedimentary environments of the northwestern (NW) Pacific during the Last Glacial Maximum (LGM) - Holocene on the basis of variation in species composition of the benthic foraminiferal assemblages, fossil abundance, and species richness in core LV 63-41-2 recovered during the Joint Russian-Chinese Expedition in 2013.

Benthic foraminifera (BF) were examined in 236 sediment samples with a interval of 1-2 or 4 cm. BF were studied in sediment size fraction of more than 63 μm . The taxonomic composition of the assemblages, benthic foraminifera abundance (BFA, # individual/1gram of dry sediment), species richness (SR, # species/sample), absolute abundance (# ind./1gds) and relative abundance (%) for each species were calculated. The age model of studied core was constructed using AMS ¹⁴C data (Fig. 1) and correlation of the productivity events and Relative Paleointensity curve with ones of well dated nearby core SO02-12KL [1].

BFA varies strongly through the core depth from very low value of several units up to several hundred ones with sharp strong peaks (Fig.1). The SR changes from 12 to 23 species in the lower part of core (466-250 cm), then decreases to 18-7 species in the middle part and to less than 7-8 species in the upper layer of 100 cm. The general pattern of dominant and ecologically significant species varies significantly through the core depth. Phytodetritus species *Alabaminella (A.) weddellensis* and *Islandiella (I.) norcrossi* prevailed in assemblages in the lower part of core below 340 cm and showed a peak nearly at the level of 270-280 cm. *Bulimina (B.) tenuata* is most abundant (75%) in the intervals of 330-280 cm and 186-170 cm. The largest number of the *Epistominella (E.) pacifica* in assemblages was observed at the top of core and at the interval of 220-190 cm. *Nonionellina labradorica* had a high percent at the intervals of 380-280 cm, 180-150 cm and upper 20 cm. The species *Uvigerina (U.) akitaensis* was detected in all intervals, but was not dominant, except the middle (288-150 cm) and upper (110-50 cm) parts of the core. The species *Globobulimina (G.) auriculata* was dominated in the intervals 330-290 cm and above 190 cm and shows the largest relative abundance above 100 cm (up to 30%). The taxa *Elphidium (E.) batialis*

was abundant (up to 40%) in the middle (270-230 cm) and upper (above 100 cm) parts.

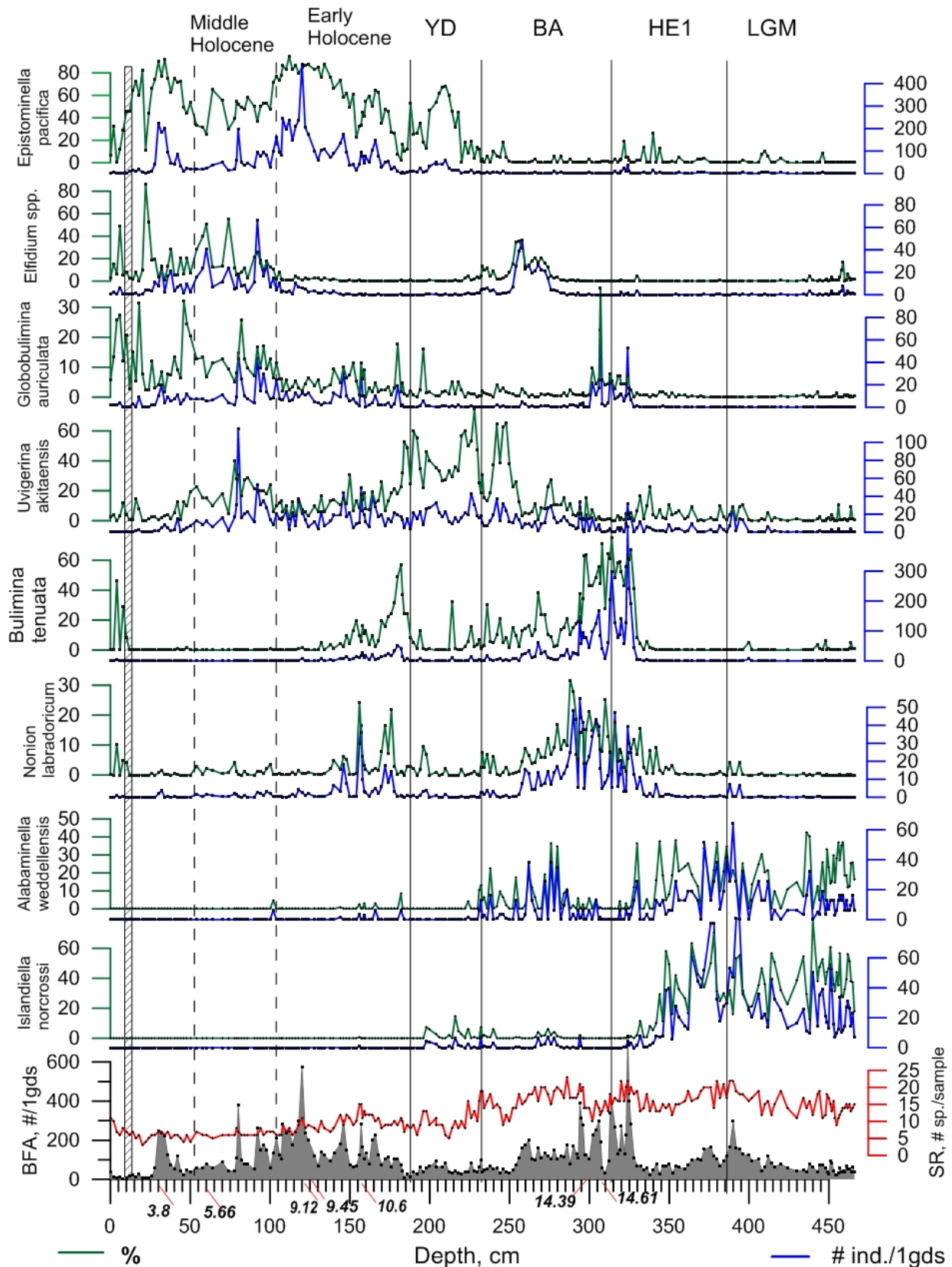


Fig. 1. Records of the total BFA (#ind./1gds), species richness (SR, # species/sample) and relative abundances (%) of ecologically significant species of BF versus core LV63-41-2 depth. The solid lines show the boundaries of Last Glacial Maximum (LGM), cold Heinrich Event 1 (HE1), Bølling-Allerød warming (BA), Younger Drays cooling (YD) and Holocene, according to [1]. The dashed line shows the Early Holocene and the Middle Holocene boundaries. AMS ¹⁴C data at the base.

BFA, SR and species composition in the assemblages changed significantly during the LGM, Heinrich Event 1 (HE1), Bølling-Allerød warming (BA), Younger Drays cooling (YD) and Holocene (Fig. 2). BFA was small during the LGM and HE1 with sharp increase since 15.4 ka BP. The phytodetritus-consuming benthic species *A. weddellensis* and *I. norcrossi*, typical of the conditions of seasonal organic flux to the bottom, dominate in the assemblages during LGM and HE1, likely, due to enhanced winter sea ice cover, accompanied by high terrigenous matter delivery through sea ice according to magnetic susceptibility (MS) record. Low productivity during this period according to the chlorin and total organic content (TOC) records contributes to low BF production.

The sharp decrease in the winter sea ice cover since 15.4 ka BP, according to the MS record, led to strong increase in BFA and species distribution in assemblages, which continue during the BA. The “high productivity” taxa *B. tenuata* sharply dominated since 15.4 ka BP indicating the dysoxic bottom condition, consistently with high content of productivity proxies (chlorin, TOC and Si-bio). The suboxic species *U. akitaensis* dominated in the assemblages at the end of BA and displaced *B. tenuata*.

The YD period was characterized by a return to environmental condition typical of glacial with low productivity and BFA (up to 30-40# ind./1gds) (Fig. 2). *E. pacifica*, as an indicator of suboxic - oxic condition, reappeared since middle of YD (12.4 ka BP) and prevailed in the assemblages further during the Holocene. The sharp increase in production of silica and carbonated phytoplankton since onset of Holocene, as show records of Si-bio and chlorin content, leads to a dominance of species *B. tenuata* and *U. akitaensis*, indicators of dysoxic surface sediment condition (Fig. 2). *E. pacifica* remain as dominated species in assemblages during Early Holocene up to 8 ka BP consistently with continuous increase of productivity proxies. In the middle of Holocene (8-5 kyr), the decrease in abundance of *E. pacifica* was accompanied by rises in abundances of dysoxic and suboxic species *G. auriculata*, *U. akitaensis* and *E. batialis*. From 5 to 1.2 kyr *E. pacifica* dominated again, consistent with a significant increase in primary production according to TOC and chlorin records (Fig. 2).

This research work was supported by the RFBR projects (No. 16-55-53048 and 16-05-00127), Russian Federation budget (01201363042), International Cooperation 40, Project of Global Change and Ocean-Atmosphere Interaction (GASIGEOGE-04), National Natural Science Foundation of NNSF of China (41476056, 41611130042 and U1606401), international cooperative projects in polar regions (201613) and by Russia-Taiwan project (17-MHT-003).

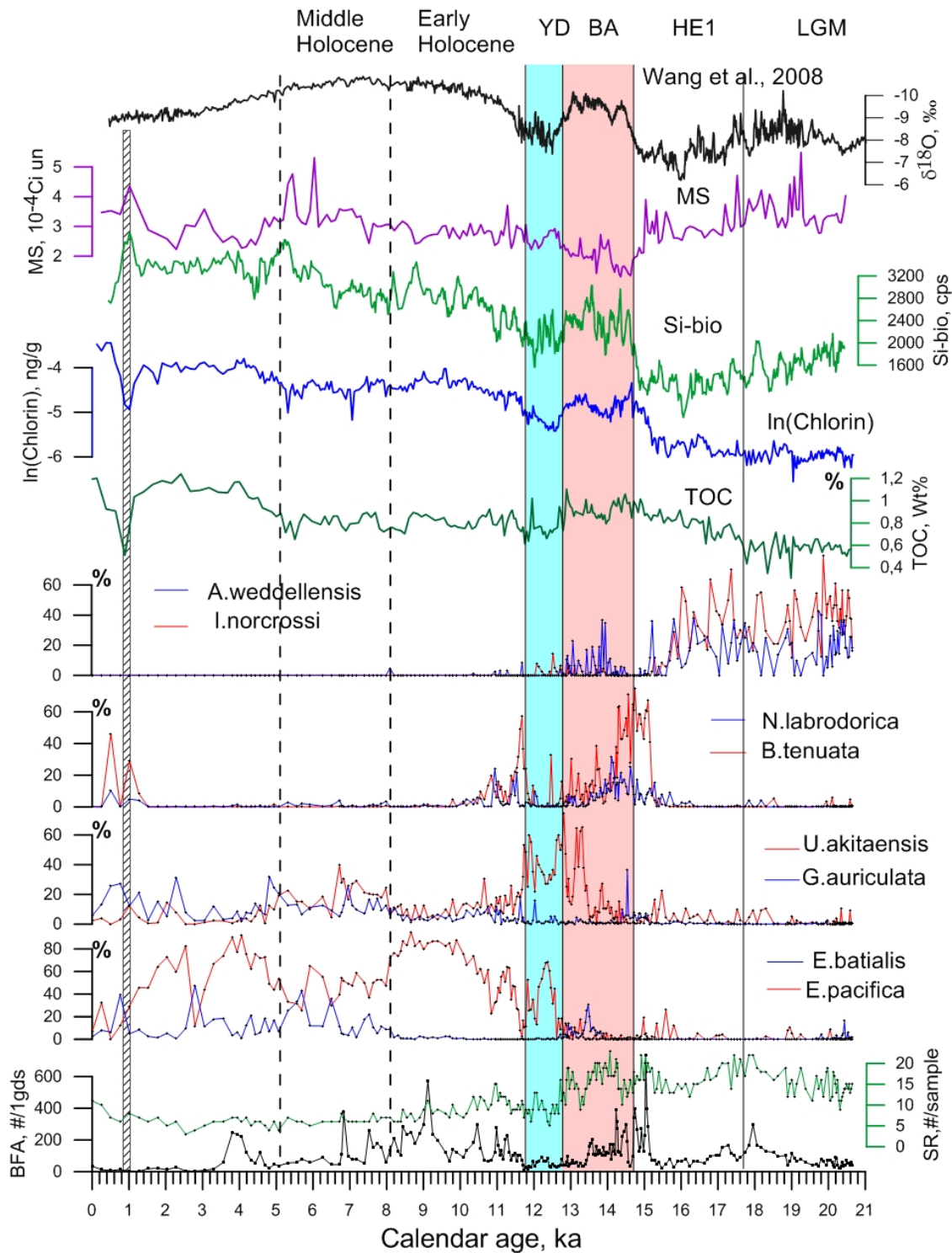


Fig. 2. Time-series comparison of the BFA, SR and relative abundances (%) of the BF dominant species changes with variations of the surface water productivity (chlorine (ng/g), TOC (wt %), Si-bio (cps), and MS (10^{-4} Si un). $\delta^{18}\text{O}$ records of stalagmites in Chinese caves [2] are shown at the top for correlation.

REFERENCES:

- Gorbarenko S.A., Shi X., Malakhova G.Y., Bosin A.A., Zou J., Liu J., Chen M-T. Centennial to millennial climate variability in the far northwestern Pacific (off Kamchatka) and its linkage to the East Asian monsoon and North Atlantic from the Last Glacial Maximum to the Early Holocene // *Clim. Past.* 2017. 13. P. 1063-1080. <https://doi.org/10.5194/cp-13-1063-2017>
- Wang Y.J., Cheng H., Edwards R.L. et al. Millennial- and orbital-scale changes in the East Asian monsoon over the past 224,000 years // *Nature.* 2008. Vol. 451. P. 1090-1093.

SEDIMENT ACCUMULATION AND BUDGET IN THE BOHAI SEA, YELLOW SEA AND EAST CHINA SEA

**Shuqing Qiao^{1,2}, Xuefa Shi^{1,2}, Lin Zhou³, Limin Hu^{1,2}, Gang Yang^{1,2}, Yanguang Liu^{1,2},
Zhengquan Yao^{1,2}**

¹ Key Laboratory of Marine Sedimentology and Environmental Geology, First Institute of Oceanography, SOA, Qingdao, China

² Laboratory for Marine Geology, Qingdao National Laboratory for Marine Science and Technology, Qingdao, China

³ Marine Information and Computer Center, First Institute of Oceanography, SOA, Qingdao, China

Qiaoshuqing@fio.org.cn

Sediment accumulation and budget in the continental margins provides abundant information of source-sink processes from the land to the sea, including weathering, human activities and sedimentary environment. Here we show the distribution of mud areas, modern sedimentation rates and sediment budget in the Bohai Sea, Yellow Sea and East China Sea. Using grain size data of more than 18 000 surface sediment samples and ²¹⁰Pb data from 413 sites, we identify five areas with sediments mainly composed of fine-grained fractions (mean grain size more than 6 φ) and find a relatively high sedimentation rates of >1.5 mm/yr in the mud areas. Near the Yellow and Yangtze River deltas sedimentation reaches >95 mm/yr. Approximately 1185×10⁶ tons of fine-grained sediment accumulate annually in the mud areas of the east China seas. Atmospheric deposition contributes <2% (18.37 ×10⁶ tons/yr), while the riverine sediment inputs account for >75% (917×10⁶ tons/yr). The remainder comes from all other sources including coastal erosion and resuspension of bottom sediments. In addition, ~45% of the fluvial sediment supply deposits on the subaerial delta, ~40–50% is trapped on the subaqueous delta and shelf, and the remainder less than 5% escapes the shelf edge. The results will be a strong foundation for understanding of the transport, deposit and preservation of sediment and other relevant material (e.g. carbon and nutrient etc.) of terrestrial materials in the sea.

CONTROLS ON THE CONCENTRATION OF CO IN FERROMANGANESE CRUSTS FROM THE MAGELLAN SEAMOUNTS, WEST PACIFIC

Xiangwen Ren¹, James R. Hein², Li Li¹, Zanzhong Yang³, Na Xing⁴, Aimei Zhu¹, Xuefa Shi¹

¹ First Institute of Oceanography, SOA, Qingdao, China

² Pacific Coastal and Marine Science Center, U.S. Geological Survey, Santa Cruz, USA

³ Shandong University of Technology, Shandong, China

⁴ Xiamen University, Fujian, China

renxiangwen@fio.org.cn

Ferromanganese crusts are known as a potential cobalt resource in the deep ocean, and mainly occur on the seamounts of the northwest Pacific, such as the Magellan seamounts. In order to clarify the controls on Co concentration of hydrogenetic unphosphatized ferromanganese crusts, an conceptual model was established (Fig.) and then an equation was deduced based on Fick's Second Law: $\overline{C}_{cr} = D_{sw} \cdot \frac{\overline{C}_{sw}}{\delta} \cdot S_{sp} \cdot \frac{z}{GR}$, and eight potential controls are gleaned from this equation, including dilution, diffusivity of Co ions in seawater (D_{sw}), temperature which controls the D_{sw} , Co ion concentration in seawater (\overline{C}_{sw}), the diffusion distance of Co ions near the interface of seawater and Fe-Mn crusts (δ), thickness of one molecular layer (z), growth rate (GR), and specific surface area of Fe-Mn crusts (S_{sp}). In order to estimate the value of δ , we determined the Co concentrations, growth rates, and specific surface area of the outermost layer of Fe-Mn crusts from the Caiwei seamount of the Magellan seamounts, calculated diffusivity of Co^{2+} , and analyzed Co concentration in the ambient seawater. The δ for the Fe-Mn crusts from Caiwei seamount was determined to be 69-279 μm . According to the equation established in this study, the trend of decreasing Co concentration in Fe-Mn crusts with increasing water depth is controlled mainly by dilution effects and to a lesser extent by seawater Co ion concentration, temperature of seawater, and consequently the diffusivity of Co ions in seawater.

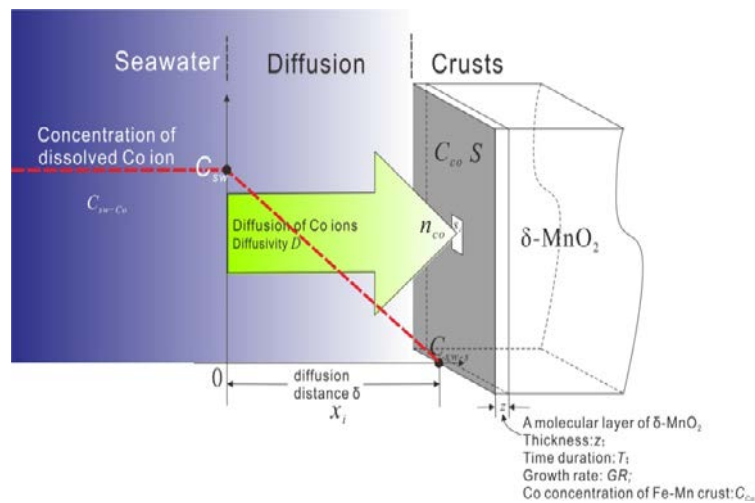


Fig. Conceptual model of Co in seawater enriching onto the surface of ferromanganese crusts

FEATURES OF THE GEOLOGICAL STRUCTURE OF MARGINAL SEAS OF THE EAST ASIA

Vladimir S'edin, Yury Mel'nichenko, Evgeny Terekhov

V.I. Il'ichev Pacific Oceanological Institute, FEB RAS, Vladivostok, Russia

sedin@poi.dvo.ru

Marginal seas (MS) are one of main types of geostructures of the Earth. They mainly are located in the west part of the Pacific Ocean. Marginal seas of the west part of the Pacific Ocean are divided on two groups: 1 - marginal seas of the north-west part of the Pacific Ocean, which are located near of the East Asia; 2 - marginal seas of the south-west part of the Pacific Ocean, which are located near of the Austral. Marginal seas of the north-west part of the Pacific Ocean (marginal seas of the East Asia) form the long chain from the Bering Sea (the north part) to South-China Sea and Philippine Sea (the south part). Marginal seas, island arcs and trenches form the transitional zone of the West-Pacific type. Marginal seas are by main unit (element) of the transitional zone of the West-Pacific type. Origin of the MS are discussed. The purpose of this work to consider features of the geological structure of MS marginal seas of the north-west part of the Pacific Ocean (of the East Asia).

Marginal Seas of the north-west part of the Pacific Ocean significantly are distinguished one from the other, although they are by geostructures of the one type. Scientists for long time turned one's mind to that fact. There are two classifications of marginal seas of the East Asia. The First classification basis to study of features of the relief of marginal seas of the East Asia [1]. These authors distinguished 3 types MS: 1 – the type of the Okhotsk Sea; 2 – the type of the Japan Sea; 3 - the type of the Bering Sea. The Second classification basis to study of features of transformation (the level transformation) of the Earth Crust of marginal seas of the East Asia [2]. These authors also distinguished 3 types MS: 1 – the type of the Okhotsk Sea; 2 – the type of the Japan Sea; 3 - the type of the Philippine Sea. These authors used only the one factor for classification of marginal seas of the East Asia – the study of features of the relief marginal seas [1], or - the study of the level transformation of the Earth Crust of marginal seas [2]. We consider that to use insufficiently only the one factor for classification of marginal seas of the East Asia.

Today there are many data for features of the relief marginal seas also for features of the geological and geophysical structure of the major morfostructures of marginal seas of the East Asia. We consider that necessary for classification of marginal seas of the East Asia is to use complex of factors. We propose to distinguish 4 types of Marginal Seas of the East Asia: 1 – the type of the Okhotsk Sea (Okhotsk Sea, East-China Sea and Yellow Sea); 2 – the type of the Japan Sea (Japan Sea, South-China Sea); 3 - the type of the Bering Sea (Bering Sea); 4 - the type of the Philippine

Sea (Philippine Sea). This classification of marginal seas of the East Asia are used complex of data, which are for of MS of the north-west part of the Pacific Ocean.

REFERENCES:

1. Kazansky B.A., Mel'nichenko Yu.I., Sigova K.I. Evolutional rows of Marginal Seas of the West-Pacific transitional zone // Geophysics and Tectonics of the transitional zone of the West-Pacific type. Vladivostok: Far East Centre of the USSR Academy of Sciences. 1985. P. 36-44. (in Russian).
2. Frolova T.I., Perchuk L.L., Burikova I.A. Magmatism and transformation of the Earth Crust of active margins. M: Nedra, 1989. 261 p. (in Russian).

INITIAL RESULTS ON METHANE ISOTOPIC COMPOSITION IN THE EAST SIBERIAN SEAS AND OB RIVER

Kseniia Shcherbakova^{1,2}, Denis Kosmach¹, Elena Panova², Igor Semiletov^{1,2,4}, Natalia Shakhova^{2,4}, Örjan Gustafsson³

¹ V.I. Il'ichev Pacific Oceanological Institute, FEB RAS, Vladivostok, Russia

² National Tomsk Research Polytechnical University, Tomsk, Russia

³ Department of Environmental Science and Analytical Chemistry, Bolin Centre for Climate Research, Stockholm University, Stockholm, Sweden

⁴ International Arctic Research Center, University of Alaska Fairbanks, USA

Kseniya.Shcherbakova@poi.dvo.ru

Large amounts of methane (CH₄) are stored beneath the East Siberian Arctic Shelf (ESAS) within subsea permafrost, as gas hydrates or free gas underneath. With the ongoing climate warming in that region, there is potential for significant release of CH₄ to the water column and eventually to the atmosphere. Over a decade of shipboard expeditions has shown enhanced CH₄ levels in large parts of the ESAS waters, but we still lack knowledge on which pools are responsible for the releases, as well release mechanisms and removal processes in the water column.

Here we show dissolved methane concentration and $\delta^{13}\text{C-CH}_4$ data from water column profiles along a transect across the outer East Siberian Sea, ranging from 140°E to 170°E, taken during the SWERUS-C3 expedition in summer 2014.

Elevated CH₄ levels were observed throughout the transect; reaching a maximum value of 716 nM and a median of 30 nM. Due to ice cover in large parts, concentration maxima were mainly located close to the surface or around the pycnocline, with the exception of bottom maximum close to a seep area around 160 °N. Initial results for $\delta^{13}\text{C-CH}_4$ range from -60 to -47 per mille vs VPDB.

Two expeditions were performed during summer-autumn period of 2016. In July there was the expedition on Ob River and Gulf of Ob where 113 samples for stable isotopes and 10 samples for ¹⁴C isotope analysis were obtained. During the September-October expedition in the East Siberian Seas there were collected samples from 12 stations for ¹⁴C radiocarbon analysis and from 33 stations for stable isotope analysis.

VARIATIONS IN SEDIMENTARY DEPOSITS AND ENVIRONMENT IN THE NW PACIFIC DURING THE LATE QUATERNARY

Xuefa Shi^{1,2}, Jianjun Zou^{1,2}, Sergey Gobarenko³

¹ Key Laboratory of Marine Sedimentology and Environmental Geology, First Institute of Oceanography, SOA, Qingdao, China

² Laboratory for Marine Geology, Qingdao National Laboratory for Marine Science and Technology, Qingdao, China

³ V.I. Il'ichev Pacific Oceanological Institute, FEB RAS, Vladivostok, Russia

xfshi@fio.org.cn

A suite of marginal seas that exist along the rim of NW Pacific, cross tropic, temperate and boreal three climatic zones. Amounts of terrestrial materials delivered by river, wind and sea ice deposit in the marginal seas and their dispersions in the sea are further constrained by regional oceanic circulation. As one of the main research themes, understanding the sedimentary processes and environmental sequences is particular of interest in the north Pacific during the late Quaternary. Preliminary studies show that detritus materials deposited at the rim of NW Pacific mainly derive from the weathering products on adjacent land, while regional geological agency is the main factor for affecting the accumulation and deposition of terrigenous materials. In the Okhotsk and the Bering Seas, the provenances of detritus materials are mainly sourced from the East Siberia and the Alaska, which are mainly delivered into the seas by river and sea ice. Sea ice is a major geological agency in shaping environment and climate in these marginal seas during the glacial period, while both river and sea ice occur during interglacial period. Due to the high sill of the Japan Sea, both eolian and Tsushima Warm Current are main ways in controlling the accumulation and deposition of terrestrial materials, among which, eolian dust are mainly derived from the desert, Gobi and Chinese Loess Plateau with variations in glacial cycles. In the China seas, summer Asian Monsoon exerts an important role in determining river's fluxes and subsequent depositions. Moreover, the Kuroshio and its branches can further redistribute the accumulation of terrestrial materials. Besides the contribution of terrigenous materials, a series of volcanic island arc, the sediment is also rich in amounts of volcanic debris. The provenance, distribution and accumulation of terrigenous materials in the marginal seas of the NW Pacific are closely related to regional climate and sea level.

This work is granted by the national program on global change and Air Sea Interaction (GASI-GEOGE-03, 04, by the National Natural Science Foundation of China (Grant No: U1606501, 41476056, 41420104005).

DERIVE CHLOROPHYLL DISTRIBUTIONAL PATTERN FROM ‘GAPPY’ SATELLITE DATA IN THE ARCTIC OCEAN: A STATISTICAL APPROACH

Hongjun Song¹, Rubao Ji², Yun Li², Andrew R. Solow²

¹First Institute of Oceanography, SOA, Qingdao, China

²Woods Hole Oceanographic Institution, USA

songhongjun@fio.org.cn

With the advantages of high temporal and spatial resolution, satellite-derived chlorophyll data have been widely used to view the large-scale ocean biological processes, even more important in the inaccessible locations and extreme waters, e.g. polar oceans. However, due to cloud cover and sensor sensitivity, the satellite data gaps still exist and often trouble the scientists in obtaining regional and temporal high-frequency data, especially in the high latitude. Both deterministic and statistical methods have been used to fill the oceanographic data gap, but there has been almost no study combining these two methods to test how about the interpolation improved. In this presentation, a new method combining generalized additive model (GAM) and spatio-temporal kriging is introduced to the interpolation of the satellite-derived chlorophyll data in the Arctic Ocean, to improve the quality of the gappy satellite data. First, we incorporate easily-obtainable environmental factors into generalized additive models (GAMs) to explain the variability of chlorophyll in the Arctic Ocean. Second, spatio-temporal kriging is performed on GAM residuals, and the combination of GAM and kriging method (named GK) is to improve the chlorophyll interpolation. In addition, the advantage of GK method is also compared with the existing methods.

DIATOMS AS INDICATORS OF THE LATE HOLOCENE ENVIRONMENTAL CHANGES IN THE EAST SIBERIAN AND CHUKCHI SEAS

Ira Tsoy¹, Mariia Obrezkova¹, Anatoly Astakhov¹, Xuefa Shi², Limin Hu²

¹ V.I. Il'ichev Pacific Oceanological Institute, FEB RAS, Vladivostok, Russia

² First Institute of Oceanography, SOA, Qingdao, China

tsoy@poi.dvo.ru

The Arctic shelf of Eurasia is a very important object for scientific investigations for many reasons. Its role in the formation of our planet's climate has been proven, and its resource potential has been estimated as virtually inexhaustible. Particularly, sedimentation in the Arctic seas has been studied to understand such fundamental processes as lithogenesis in the shelf cryolithozone, climatic zoning of sedimentation in the oceans, and trends in environmental changes in the past, the present and the future. Diatom algae, one of the main phytoplankton groups of the Arctic and Subarctic seas, are widely used in such paleogeographic studies. Their siliceous frustules are well preserved in sediments and serve as indicators of environmental conditions in the past. This allows using them to reconstruct paleo-conditions in northern latitudes, where calcareous nannoplankton and foraminiferans have lower contents in sediments and are commonly more destructed than diatoms. It is necessary to study diatoms in sea bottom sediments to make detailed and reliable reconstructions of sedimentation conditions in the geological past and to predict their changes in the future.

This investigation is mainly aimed at reconstructing the paleoenvironmental changes in the East Siberian and Chukchi seas based on diatom analysis. We distinguished the patterns of diatom distribution in the surface sediments of East Siberia and Chukchi seas depending on different environmental conditions as well as changes in the diatom content, the number of dominant species of diatoms, and the ecological structure of diatom assemblages in sedimentation cores.

The distribution features of diatoms in the Late Holocene sediments of the East-Siberian and Chukchi seas were studied. In the East Siberian Sea (ESS) the content of diatoms varied considerably, increasing from the west to the east, similarly to the distribution of diatoms in the tanatocenoses of surface sediments [5], as well as to the distribution of phytoplankton primary production, which was determined and modeled by the chlorophyll content data obtained from satellites [6]. The western and eastern regions of the ESS are different both in the spatial distribution and in the composition of suspension. There are two main sources of suspended material for this sea: the suspended phase of the river inflow runoff and the late Pleistocene ice sediments of the thermoabrasive coast. The latter are wider distributed in the western region of the sea, having the main stock of sedimentary material [2]. Therefore, great amount of terrigenous matter, arriving at the ESS sediments with the river runoff and with the thermal and wave abrasion, "dilutes" the biogenic component of the sediments. The diatom content in the sediments was lowest

north of the Indigirka River estuary and near the Novosibirsk Archipelago. The content of diatoms consecutively increased eastward of the Kolyma River and was highest for the ESS between the Chaunskaya Bay and the Long Strait [4].

In the Chukchi Sea, the diatom content was lowest in the Bering Strait, where the water flow is fastest and there is virtually no sedimentation. In the adjacent northwestern regions of the Chukchi Sea shelf the transferred suspended material is being heavily deposited, forming a large distinctive detrital cone [3]. The diatom content was highest in the center of the sea, where nutrient-rich waters from the Bering Sea shelf and the Gulf of Anadyr waters are transported to. This is consistent with the measurements of primary production in the Chukchi Sea conducted during expeditions [6]. The region mentioned is characterized by permanent high values of C_{org} , chlorine, and opal [1]. The content of diatoms decreased westward, in the center of the Long Strait, where the colder and denser waters of the ESS come to. The diatom abundance was lowest at the northern stations of the Chukchi Sea, located at much greater depths, in the sea areas with a permanent ice cover.

Cluster analysis revealed several diatom assemblages in the surface sediments of the studied region; their distribution depended on the hydrological conditions. A coldwater *Th. antarctica* assemblage was distinguished in the eastern part of the ESS and in the northern Chukchi Sea; a highly productive *Chaetoceros* assemblage was noted in the Herald Canyon area; a sublittoral *Odontella aurita* assemblage occurred in sandy sediments of the Herald Shoal; a *Paralia sulcata* assemblage, which is an indicator of low salinity waters, was found in the eastern Chukchi Sea near Alaska; and "sea-ice" *Th. nordenskiöldii* and *Fragillariopsis oceanica* assemblages occurred in the southern Chukchi Sea [1, 4].

The diatom study in the HC11 core obtained from the southwestern part of the Chukchi Sea, allowed us to establish that during the last 2300 years in the southern Chukchi Sea there were two warmings and one cooling, which corresponded to the global climate changes in the late Subatlantic. The most favorable conditions for diatoms occurred during the warming at the end of the early Subatlantic (~296 BC– 630 AD). The conditions were close to contemporary ones, but the influence of Bering Sea water was greater and a branch of the relatively warm Anadyr Current probably ran west of its present position. In the middle Subatlantic (~630-1300), the environmental conditions were unstable but generally favorable and close to the conditions at present characteristic of the southernmost region of the Chukchi Sea. The relatively short-term warming during ~680-860 AD led to reduced water productivity, as was reflected in the low concentration of diatoms in sediments of that period. At the end of the late Subatlantic (~1300-1860), the sediments formed under harsh conditions due to the global cooling (Little Ice Age), which led to the appearance of

almost permanent ice cover in the southern Chukchi Sea and to the reduced inflow of relatively warm Bering Sea waters. Modern sedimentation began approximately from 1860 [7].

The work was supported by the Russian Science Foundation (project No. 16-17-10109).

REFERENCES:

1. Astakhov A.S., Bosin A.A., Kolesnik A.N., Obrezkova M.S. Sediment geochemistry and diatom distribution in the Chukchi Sea: application for bioproductivity and paleocenography // *Ocenography*. 28(3):190-201. 2015. DOI: 10.5670/oceanog.2015.65
2. Dudarev O.V., Charkin A.N., Shakhova N.E. et al. Modern litho- and morphogenesis in the Russian East Arctic shelf. Tomsk: Publishing House of Tomsk Polytechnic University, 2016. 192 p.
3. *Geocologiya shel'fa i beregov morei Rossii (Geological Ecology of Shelf and Coasts of the Russian Seas)*, Aibulatov, N.A., Ed., Moscow: Noosfera, 2001.
4. Obrezkova M. S., Kolesnik A. N. and Semiletov I. P. 2014. The Diatom Distribution in the Surface Sediments of the Eastern Arctic Seas of Russia. *Russian Journal of Marine Biology*. Vol. 40, No. 6, pp. 465–472. DOI: 10.1134/S1063074014060170.
5. Polyakova, E.I., *Arkticheskie morya Evrazii v pozdnem kainozoe (Arctic Seas of Eurasia in the late Cainozoic)*, Moscow: Nauchny Mir, 1997.
6. Romankevich, E.A. and Vetrov, A.A., *Tsikl ugleroda v arkticheskikh moryakh Rossii (Carbon Cycle in the Arctic Seas of Russia)*, Moscow: Nauka, 2001.
7. Tsoy I.B., Obrezkova M.S., Aksentov K.I., Kolesnik A.N., Panov V.S. Late Holocene Environmental Changes in the Southwestern Chukchi Sea Inferred from Diatom Analysis. *Russian Journal of Marine Biology*, 2017, Vol. 43, No. 4, pp. 276–285. DOI:1134/S1063074017040113

THE SEA ICE CONDUCTION IN THE EASTERN SEA OF OKHOTSK DURING THE DEGLACIATION AND HOLOCENE

Yuriy Vasilenko¹, Sergey Gorbarenko¹, Aleksandr Bosin¹, Xuefa Shi^{2,3}, Tatyana Khusid⁴, Jianjun Zou^{2,3}, Yanguang Liu^{2,3}, Mikhail Savenko¹

¹ V.I. Il'ichev Pacific Oceanological Institute, Vladivostok, Russia

² Key Laboratory of Marine Sedimentology and Environmental Geology, First Institute of Oceanography, Qingdao, China

³ Laboratory for Marine Geology, Qingdao National Laboratory for Marine Science and Technology, Qingdao, China

⁴ P.P. Shirshov Institute of Oceanology, Moscow, Russia

vasilenko@poi.dvo.ru

We studied variation of ice-rafted debris (IRD) content and productivity proxies in sediment cores LV55-12-3, LV28-43-5 and LV28-44-4 from the eastern Sea of Okhotsk (Fig. 1). High-resolution age models for these cores were constructed on the base of AMS ¹⁴C datings, tephrochronology, magnetic susceptibility, productivity proxies (chlorin, TOC, opal and CaCO₃) (Fig. 2; Vasilenko et al., 2017 in press).

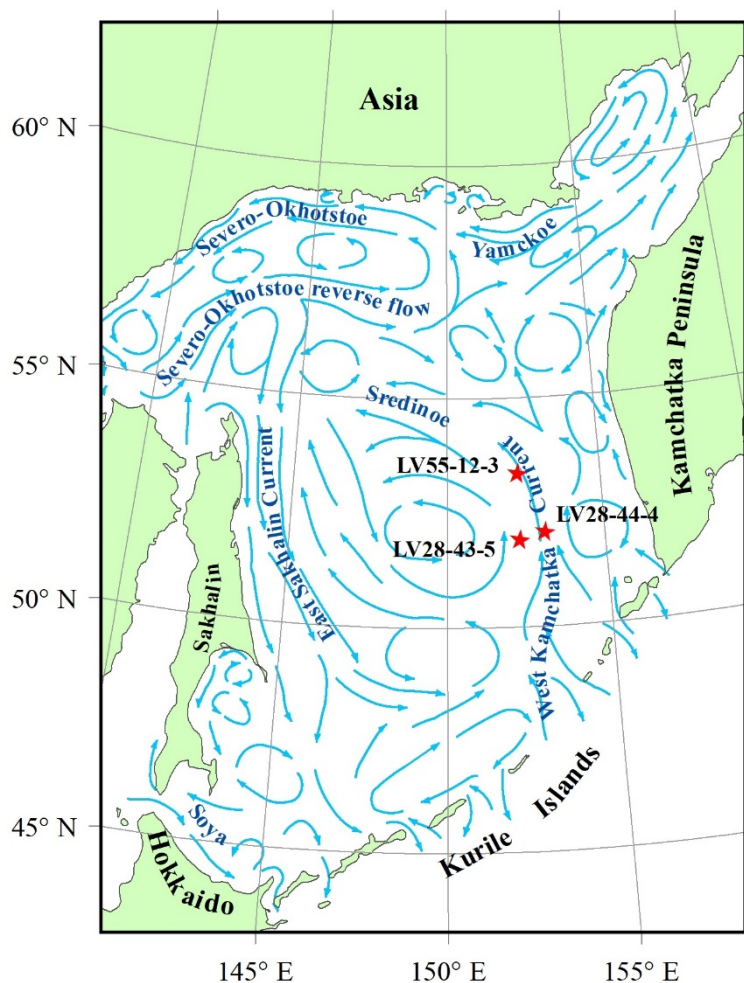


Fig. 1. Map of locations of the studied sediment cores. Scheme of surface currents after Chernyavsky (1987) shown with simplifications. The red stars denote the location of the cores.

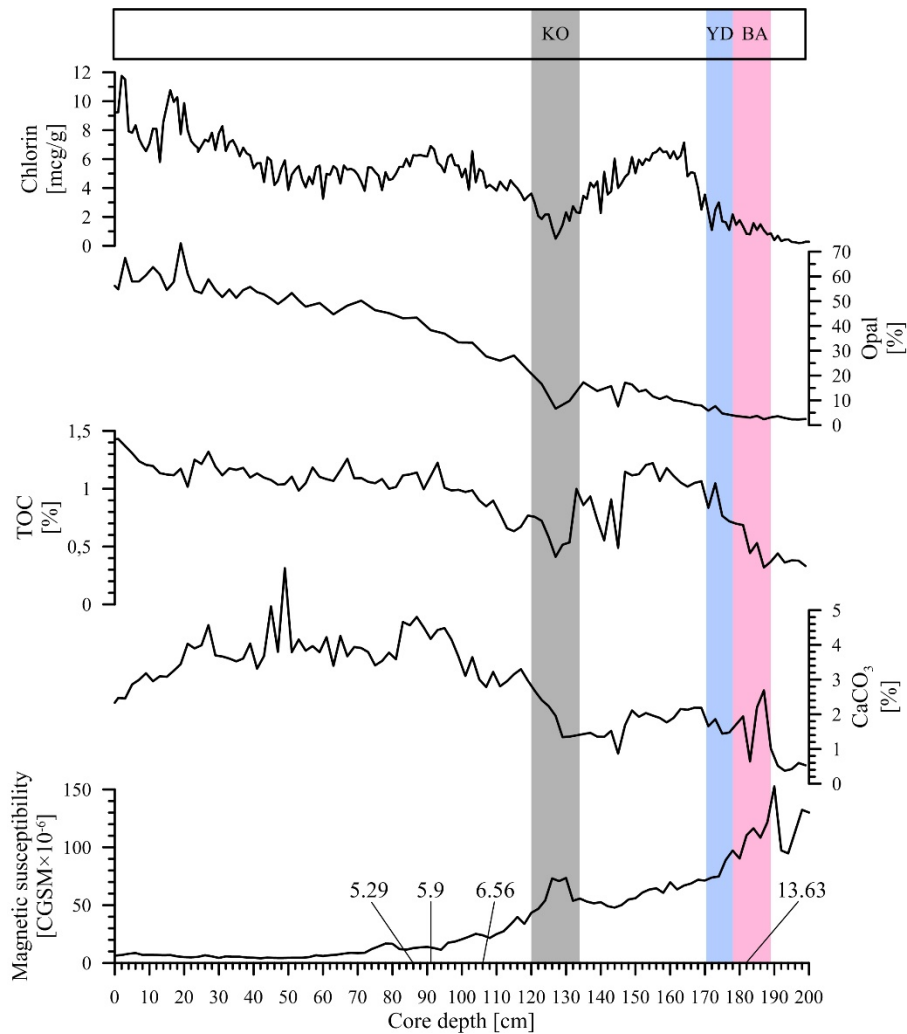


Fig. 2. The age model of core LV55-12-3 based on the magnetic susceptibility, productivity proxies (CaCO₃, TOC, opal and chlorin), tephrochronology and AMS¹⁴C data. The pink bar denote the positions of the Bølling–Allerød warming (BA). The blue bar denote the positions of the Younger Dryas (YD). The darkened bar denote the position of the layer of volcanic ash KO. AMS¹⁴C dating are shown at the base.

Since the Bølling–Allerød warming to present the general trend reflects the decreasing of IRD and increasing of productivity proxies (PP) in these cores (Fig. 3). However, the trend is complicated with significant oscillations at 14.7–9 kyr.

Bølling–Allerød. The variation of IRD at the cores LV28-44-4 and LV28-43-5 marked with sharp peaks in opposite of the northern core LV55-12-3. The most significant ones is observed at the eastern core LV28-44-4 (Fig. 3).

Younger Dryas. However, during the Younger Dryas cooling the increasing of IRD and PP is noted in core LV55-12-3 unlike the southern cores LV28-43-5 and LV28-44-4.

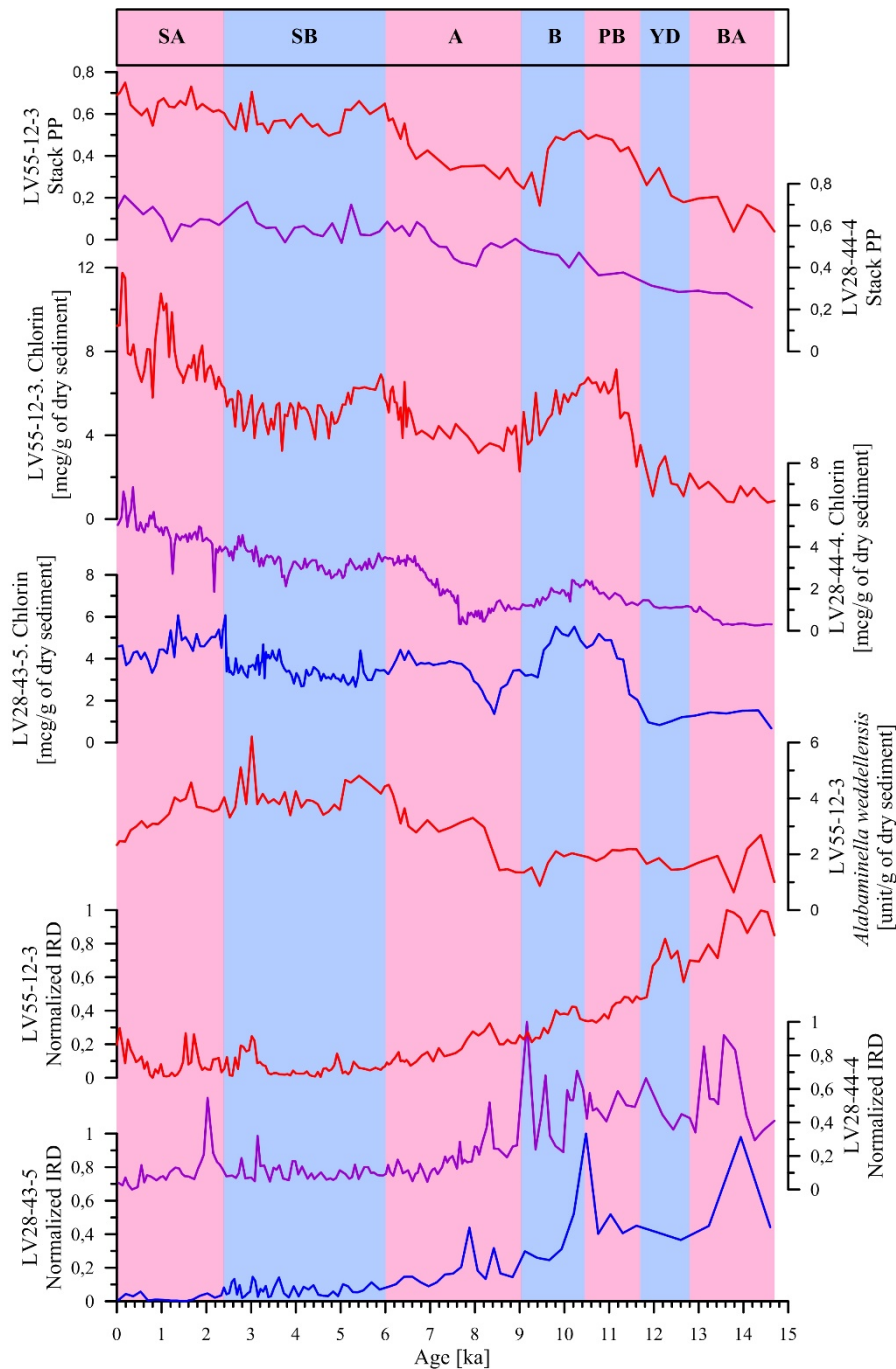


Fig. 3. Changes IRD content, chlorin, and productivity proxies for cores LV55-12-3, LV28-44-5 and LV28-43-5. The ‘BA’, ‘YD’, ‘PB’, ‘B’, ‘A’, ‘SB’ and ‘SA’ stand for Bølling–Allerød, Younger Dryas, Preboreal, Boreal, Atlantic, Subboreal and Subatlantic.

Preboreal. The sharp increasing of PP in all these cores during the Preboreal. The most expressed variation in northern core LV55-12-3 and western core LV28-43-5. While, the sharp decreasing is observed in northern core LV55-12-3 lasted until the Boreal. At opposite, the southern cores LV28-44-4 and LV28-43-5 are characterized by the sharp increasing of IRD.

We suggested that the variations of IRD and PP depend on hydrology of the Sea of Okhotsk and on atmospheric circulation above eastern Asia and northwestern Pacific. The atmospheric circulation led to enhancing of eastern winds during Bølling–Allerød, Boreal and Preboreal. But, during Younger Dryas it led to enhancing of northern winds.

Since the middle of Atlantic until present the variations of IRD and PP are rather smoothed in all cores that indicate to relative stabilization of climate processes, first of all, the atmospheric circulation above the Sea of Okhotsk followed by domination of southern and south-eastern winds during cold season.

This research is the result of the collaboration with the GEOMAR (German) Project undertaken in the framework of the KOMEX Program. This work was supported by the Russian Foundation for Basic Research (grant numbers 16-35-60019 mol_a_dk, 16-05-00127 A, and 16-55-53048 GFEN_a); the Russian state budget theme No. 5 of POI FEB RAS, the International Cooperation Project of Global Change and Ocean-Atmosphere Interaction (GASIGEOGE-04) and the National Natural Science Foundation of China (grant numbers 41476056, 41611130042, and U1606401) and International Cooperative Projects in polar regions (201613); international Taiwan-FEB RAS, and Project of Ministry of Science and Technology Taiwan (grant number 17-MHT-003).

REFERENCE:

1. Vasilenko Yu.P., Gorbarenko S.A., Bosin A.A., Shi X., Chen M.-T., Zou J., Liu Y., Artemova A.V., Yanchenko E.A., Savenko M.P. 2017. Millennial mode of variability of sea ice conditions in the Okhotsk Sea during the last glaciation (MIS 4–MIS 2). *Quaternary International* (in press).

SSTA AND CHL_A_ AS INDICATORS OF UPWELLING ALONG THE COAST OF VIETNAM

Galina Vlasova, Svetlana Marchenko, Natalya Rudykh

V.I. Il'ichev Pacific Oceanological Institute, FEB RAS, Vladivostok, Russia

Interest in studying upwelling is caused, first of all, by the fact that the areas of sustainable upwelling in comparison with the surrounding waters are biologically more productive. In addition, the presence of water with anomalous temperature affects weather conditions and the climate of the Earth. For the first time an explanation of upwelling was given in the 1940s (Sverdrup, 1942), although it was first mentioned in the scientific literature in 1877.

For a long time, the main source materials for studying upwelling were coastal observations, as a result of which it was treated as a local phenomenon that does not play a special role in the general circulation of water masses. The availability of satellite data allows us to take a fresh look at this problem.

The purpose of our research is to identify the links between the negative anomalies of the surface temperature of the ocean (SSTa) and the content of chlorophyll (CHL-a) as indicators of upwelling. To achieve this goal, satellite images of SOTO (<https://podaac-tools.jpl.nasa.gov/soto/>) were used for the western coast of Vietnam of the South China Sea.

Upwelling indicators	All coast	Northern part	Central part	South part
$(-\Delta T^{\circ}\text{C})$	Spring 2011, 2016 2.9 ⁰ C	Spring 2016 2.9 ⁰ C	Spring 2011 2.9 ⁰ C	Spring 2011 2.9 ⁰ C
CHL_a	Summer 2015, Spring 2016 6.7 мг/м ³	Spring 2016 6.7 мг/м ³	Winter 2014 4.6 мг/м ³	winter 2014 4.6 мг/м ³

As a result:

1. the good consistency of SSTa and CHL_a is shown for both the whole coast of Vietnam and separately for its northern, central and southern parts for the period 2010-2017. But, at the same time, the presence of antiphase is revealed, when the negative water temperature anomalies increase, and the chlorophyll content falls. This phenomenon, as a rule, occurs during the spring period, which is due to the change of the northeast monsoon to the south-west;
2. seasonal variability of upwelling is shown, which is observed, as a rule, in the summer season, less often in spring, occasionally in the autumn and extremely rarely in winter;
3. it was revealed that during the period 2010-2017 upwelling is strongly pronounced in the summer of 2011 and 2015 for the entire coast of Vietnam and its southern part, only in 2011 for

its central part. In the spring it is strongly pronounced of 2016 for the entire coastline and its central part, it is practically not observed in southern part. The northern part is not covered due to the lack of satellite information.

4. The minimum value of the negative temperature anomalies and the maximum content of CHL_a for the study period are determined:

CHARACTERISTICS OF SURFACE BOTTOM SEDIMENTS OF THE SOUTH PART OF CHUKCHI SEA (preliminary results)

**Elena Vologina¹, Michael Sturm², Anatoly Astakhov³, Xuefa Shi⁴, Ivan Kalugin⁵, Andrey
Darin⁵, Limin Hu⁴**

¹ Institute of the Earth's Crust, Irkutsk, Russia

² Swiss Federal Institute of Aquatic Science and Technology, Dübendorf, Switzerland

³ V.I. Il'ichev Pacific Oceanological Institute, FEB RAS, Vladivostok, Russia

⁴ First Institute of Oceanography, SOA, Qingdao, China

⁵ V.S. Sobolev Institute of Geology and Mineralogy, Novosibirsk, Russia

vologina@crust.irk.ru

Bottom sediments recovered by core LV77-5-2 (length – 22 cm in) in the southern part of the Chukchi Sea at 69°42.6610 N and 173°11.9919 W from a water depth of 50 m were studied in detail. The core was lithologically described, dated by ²¹⁰Pb and density and humidity of the deposits were determined. Magnetic susceptibility was measured with a Bartington GT-2 surface sensor. The content of organic carbon (C_{org}) and total nitrogen (N_{tot}) was determined by a CNS gas chromatograph "HEKATECH EuroAE" at Swiss Federal Institute of Aquatic Science and Technology. At the same institute, the concentrations of biogenic silica (SiO_{2biog}) were measured and grain size measurements were performed by a MALVERN-MASTERSIZER®Hydro 2000S. The elemental composition was determined by using a microscanning technique of X-ray fluorescence analysis on synchrotron radiation (XRF SR). Analytical studies of the core were carried out in the center of collective use "Siberian Synchrotron Radiation Center". The unit is part of the accelerator complex of the Institute of Nuclear Physics of the SB RAS (Novosibirsk). Measurement of microelements along the core was carried out at excitation energies of 18 and 24 keV every 0.5 or 1 mm. At each point, 15 to 25 elements with detection limits of ~ 3–5*10⁻⁵ weight % were determined.

The studied sediments are characterized by greenish-gray (interval 0–7 cm) and black (interval 7–20 cm) mud. Remains of shells of mollusks were found at core depths of 12 cm and 20 cm and a pebble within the interval of 8–10 cm. The water content of the deposits decreases with depth. Maximum values (65.2 %) appear at the very top, the lowest (48.7 %) at the bottom of the core. Density values show an increase from 1.25 g/cm³ at the upper 1.5 cm of the core to 1.7 g/cm³ at the lower part.

Magnetic susceptibility varies from 7 · 10⁻⁵ to 41 · 10⁻⁵ SI units, while minimum values are observed within interval 0–2 cm of the core.

The speed of recent sedimentation averaged 0.71 mm/year. Thus, the age of the studied sediments is approximately 320 years.

The grain size composition is mainly homogeneous throughout the core. The silt fraction (2.00–63.0 μm) dominates by 87.9–91.1 %. The content of the clay fraction (0.01–2.00 μm) varies from 6.21 to 7.75 %, and the sand fraction (63.0–2000 μm) is 2.00–5.39 %.

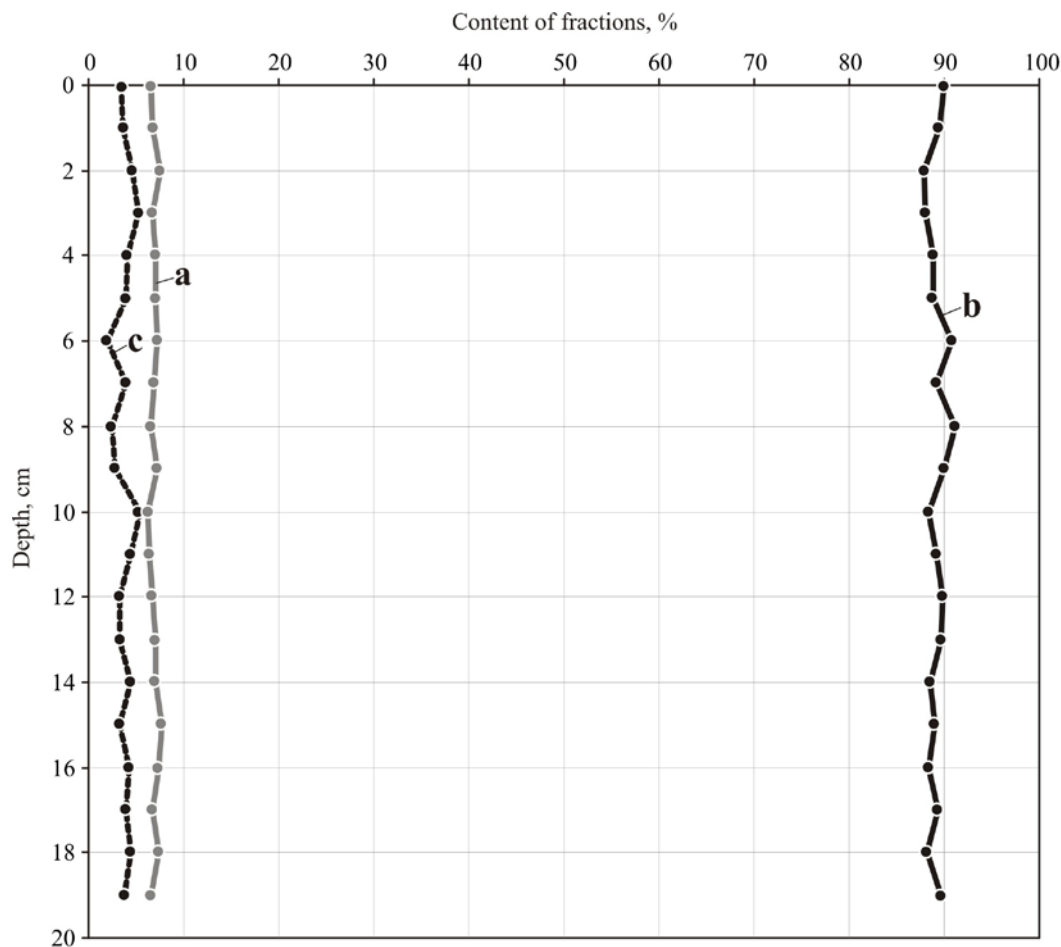


Figure 1. Results of grain size analysis of core LV77-5-2. Content of the fractions: a – clay, b – silt, c – sand.

The biogenic components were analyzed at 1 cm intervals. Biogenic silica ($\text{SiO}_{2\text{biog}}$) (mainly diatoms) varies from 1.71 to 6.36 %. Increased contents are observed in the intervals 0–1 cm (5.01 %) and 8–10 cm (6.36 % and 5.92 %). The content of organic carbon (C_{org}) varies from 1.50 % to 2.22 %. Total nitrogen (N_{tot}) changes from 0.17 % to 0.33 %. C_{org} and N_{tot} are well correlated and have maximum values at 0–2 cm of the core (approximately the last 30 years). The increase of all biogenic components ($\text{SiO}_{2\text{biog}}$, C_{org} and N_{tot}) recorded at the very top of the core, is probably due to the increased biological productivity of the Chukchi Sea, caused by general warmer climate during recent times [1, 2].

XRF SR allowed distinguishing three main groups of elements: A – clastic (K, Rb, Ca, Ti, Mn, Fe); B – aerosol (Zr, Sr, Nb, Y) and C – organic (Br). "Clastic" elements indicate small changes of the composition of the sediment at the turn of 1780–1800. This group reflects dynamics of material transportation by ocean currents. Group B elements show characteristic elements of volcanic aerosols (Zr, Nb, Y) and of Sr, which is known as isomorphous component of Ca-plagioclases. Peaks of Zr, probably mark volcanic eruptions at Kamchatka and Alaska. One peak is

synchronous with the strongest eruption of the Bezymyanny volcano in 1956. The distribution of Br in the sediments is completely independent as this element is correlated with almost all other elements. Regular fluctuations of Br content with a periodicity of about 20 years could be determined.

Expedition work was carried out within the frame work of the Russian-Chinese expedition ASW-2016. This research work was supported by the National Natural Science Foundation of China (grants 41476056, 41611130042 and U1606401), international cooperative projects in Polar Regions (201613), Russian Sciences Foundation (project No 16-17-10109).

REFERENCES:

1. Brohan P., Kennedy J.J., Harris I. et al. Uncertainty estimates in regional and global observed temperature changes: a new dataset from 1850 // J. Geophys. Res. 2006. 111:D12106. doi:10.1029/2005JD006548.
2. Wilson R., D'Arrigo R., Buckley B. et al. A matter of divergence: Tracking recent warming at hemispheric scales using tree ring data // J. Geophys. Res. 2007. 112:D17103. doi:10.1029/2006JD008318.

**THE INFLUENCE OF SEA SURFACE TEMPERATURE IN NOVEMBER ON THE
INCREMENT OF SEA ICE AREA BETWEEN DECEMBER AND THE FOLLOWING
JANUARY IN BERING SEA**

Weibo Wang

Third Institute of Oceanography, SOA, Xiamen, China

wangwb@tio.org.cn

In Bering sea, the 12-months' trends of Sea Ice Area (SIA) from 1979 to 2014 are divided into three phases: the significant increase phase in January-to-April, the slight decrease phase in May-to-October, and the significant decrease phase in December and November, which illustrated two breaks, respectively, from April to May and from December to following January when SIA happens dramatic decrease and increase respectively. In the paper, the two breaks are identified as a result of the significant increase of the daily rates of SIA during the two periods in recent 30 years. The daily rates of SIA are acquired between December and the following January and defined as freezing rate. The freezing rate has a significant negative correlation with SST lagging by 1 month in the regions having northward current including Aleutian Islands and the central continental shelf of Bering Sea, which indicates that a lot of heat carried by northward current curb the formation of sea ice. In recent 20 years, the correlation between both freezing rate and SST is more significant. It is suggested that the northward heat transfer play an important role on the formation of sea ice, which is coordinate effort with atmospheric circulation.

ANALYSIS OF LITHOSPHERIC RHEOLOGICAL STRUCTURE AND DYNAMICS IN THE MARIANA SUBDUCTION ZONE

Shiguo Wu^{1,2}, Lingju Gao³, Jian Zhang³

¹ Key Laboratory of Marine Georesources and Prospecting, Institute of Deep-sea Science and Engineering, Chinese Academy of Sciences, Sanya, China

² Qingdao National Laboratory for Marine Science and Technology, Qingdao, China

³ Key Laboratory of Computational Geodynamics, Chinese Academy of Sciences, Beijing, China

swu@idsse.ac.cn

Mariana subduction zone is the key area of tectonic evolution in the western Pacific Ocean plate edge trench - arc - basin system. The Challenger Deep in the southernmost Mariana trench is the deepest point on the Earth's surface, and the structural convergence point of Mariana trench, Mariana arc, Mariana trough, west Mariana ridge and Parece Vela basin. It is important for understanding Mariana formation evolution to study lithospheric rheological structure and dynamics in Mariana subduction zone. In this work, based on the analysis of gravity and magnetic data, we obtained the rheological characteristics of the equivalent viscous coefficient and the lithosphere strength of the Mariana trench- arc -trough - basin system. We drew the characteristics, changing with depth and the abrupt form of Wadati-Benioff zone under the trench through the calculation of the seismic data. The calculation results are showed as follows: 1) Corresponding to Mariana trench - arc - trough system, the free air gravity anomaly formed an eastward protruding arc anomaly zone, which showed beaded linear characteristics. The abnormal value was high in the middle, and the abnormal value was low at both sides. 2) The lithosphere integrated intensity ratios at different depths reflected that crust on the north and south sides of the trench the upper crust was hard and the lower was soft, and on the middle trench the upper crust was soft and the lower was hard. We calculated the equivalent viscosity coefficients using a given strain rate, and founded that the value in the east was high and the value in the west was low, which illustrated that the deformation of the west side of the crust is more easily than that of the east side of the crust. With large lithosphere strength, high equivalent viscous coefficient, and hard upper crust and soft lower crust rheological characteristics, Challenger Deep provided important conditions for bending, tearing and rapid reversal of the plate subduction area. The analysis of seismicity and gravity profile showed that the lithosphere cumulative stress intensity and effective viscosity coefficient at the Challenger Deep would make the Mariana trench subduction zone bending and cracking or partially turning toward the south and steeping under the action of gravity.

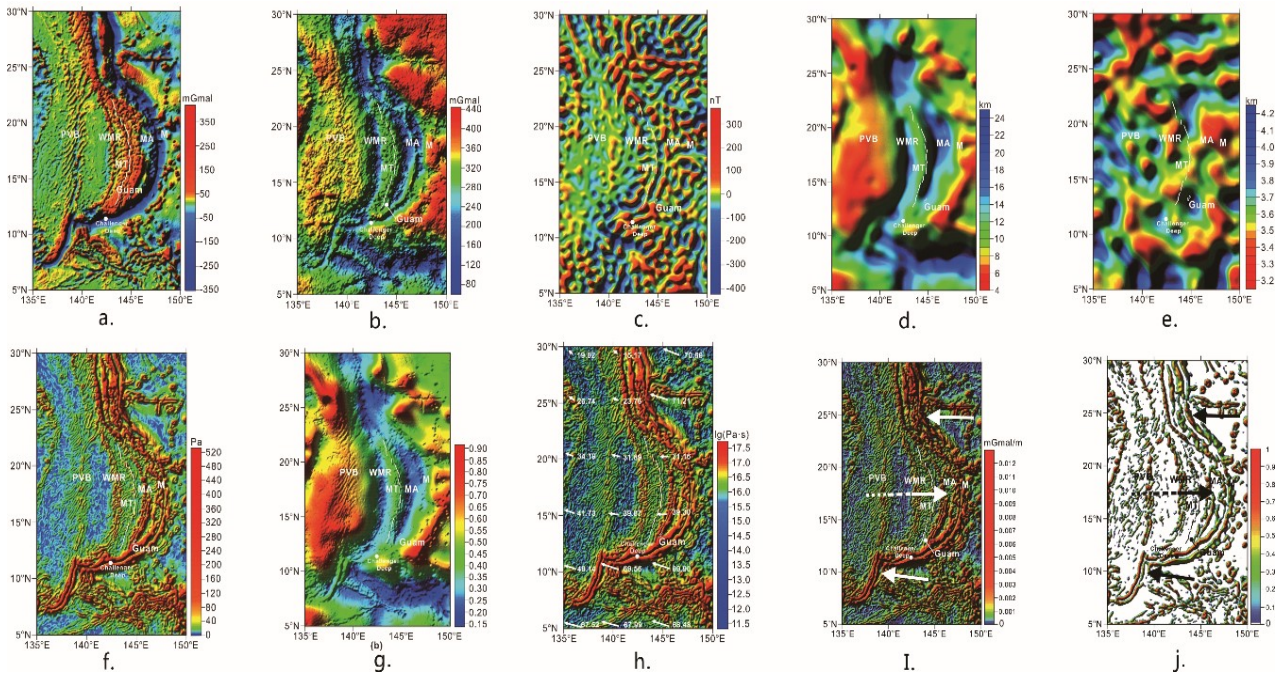


Fig.1 (a) The free-air gravity anomaly; (b) Bugge gravity anomaly; (c) ΔT pole anomaly based on satellite magnetic survey; (d) Depth of Moho; (e) Depth of Curie-surface; (f) Strength of the Lithosphere; (g) The intensity ratios of cumulative stress; (h) The earth's crust coefficients of equivalent viscosity; (i) The total field gradient of the free air gravity anomaly; (j) The normalized gradient in vertical direction for total field of the free air gravity anomaly.

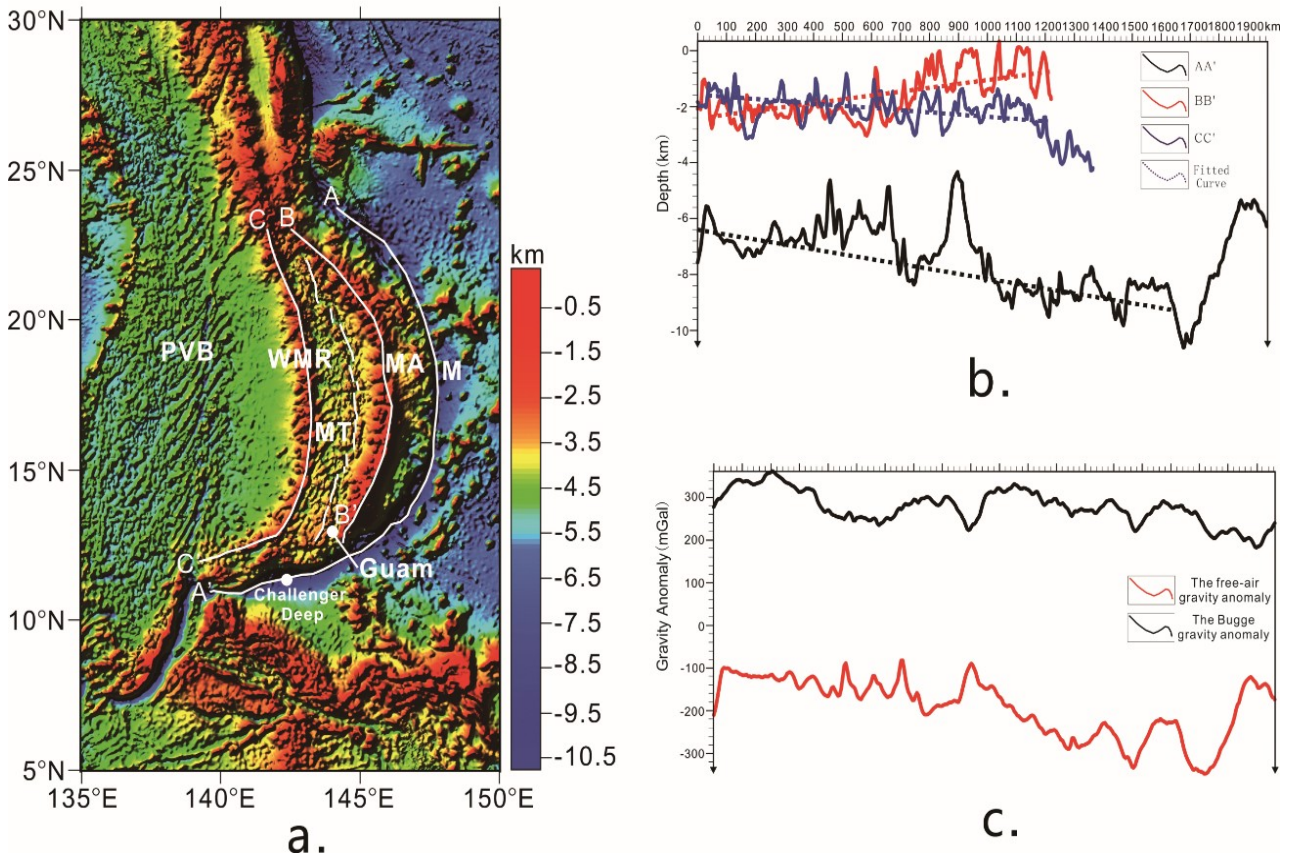


Fig.2 (a) The research profiles location; (b) Sea-floor topographic variation profiles along with Mariana trough, Mariana arc and west Mariana ridge; (c) The free-air gravity anomaly (the red) and Bugge gravity anomaly (the black) profiles.

REFERENCES:

1. Gao L J, Zhang J, Wu S G, Analysis of lithospheric rheological structure and dynamics of the Challenger Deep in Mariana trench[J].Journal of Chinese Academy of Sciences, 2017,34(03):380-388.
2. Xing J, Hao T Y, Hu L T, et al .2016.Characteristics of the Japan and IBM subduction zones:Evidence from gravity and distribution of earthquake sources.Chinese Journal Geophysics, 59(1): 116-140.
3. Gudmundsson O, Sambridge M. A regionalized upper mantle (RUM) seismic model [J]. Journal of Geophysical Research Atmospheres, 1998, 103(B4): 7121-7136.
4. Gvirtzman Z, Stern RJ. Bathymetry of Mariana trench-arc system and formation of the Challenger Deep as a consequence of weak plate coupling [J]. Tectonics, 2004, 23(2):1-15.

RADIOLARIAN RESPONSES OF THE OKHOTSK SEA TO THE ORBITAL AND MILLENNIAL CLIMATE CHANGES OVER THE LAST 135 KYR

Elena Yanchenko, Sergey Gorbarenko

V.I. Il'ichev Pacific Oceanological Institute, FEB RAS, Vladivostok, Russia

yan@poi.dvo.ru

At the present time, particular attention is given to examination of global and regional climatic changes in the past on the millennial scale. The unique geographical position of the OS, longstanding seasonal ice cover and high primary productivity give rise to high sensitivity of the natural system of this sea to the orbital and millennial climatic oscillations.

The study of total radiolarian content (TRC) and species richness (SR) for radiolarian assemblage in core MR 06-04PC-7R from the central Okhotsk Sea (OS) over last 135 kyr (MIS 1-end MIS 6) with previously established age model, position of millennial cycles of climatic changes and records of productivity proxies (total organic carbon (TOC), chlorin, Ba-bio, SiO₂-bio (opal), CaCO₃, ice-rafted debris (IRD) with temporal resolution of about 200 years) [1, 2] was carried out.

The trends of TRC and SR in the radiolarian assemblage change synchronously on the orbital scale and are mainly determined by variations of paleoproductivity and input of organic matter into the water column (Fig.). In turn, the productivity of the OS depends, to a great extent, on changes in the sea ice formation and extension and increases during the MIS 5e (optimum of the Last Interglacial), MIS 3 and MIS 1 with a shorter seasonal sea ice cover and warmer environment condition. Among various productivity proxies considered by us, mainly opal and Ba-bio contents are mostly reflects the variations of TRC and SR of radiolarians. Probably, the supply and decomposition of organic matter in the water column, reflected by the insoluble barite record (Ba-bio) in the sediment, is more important factor in regularity of quantity production of radiolarian (Fig.).

Variations of TRC of radiolarians and their SR on the millennial scale are also controlled by variations of productivity in the photic layer. The millennial productivity minima associated with the cold Greenland/China stadials (GS/CS) resulted in considerable sharp falls in TRC and SR of radiolarians while subsequent increases in productivity during Greenland/China interstadials (GI/CI) caused the smoother growth in TRC and SR of radiolarians. Such a pattern of changes in the species richness and abundance of radiolarians in the time is more similar to variations in $\delta^{18}\text{O}$ of stalagmite carbonates from the China caves [3] than in $\delta^{18}\text{O}$ of Greenland ice core [4]. Probably, TRC and SR are determined predominantly by variability of the winter monsoons in the East Asia affecting the environment and ice cover of the OS.

This research work was supported by the RFBR projects (№16-55-53048 and 16-05-00127), Russian Federation budget (01201363042), the International Cooperation 40, and by Russia-Taiwan project (17-MHT-003).

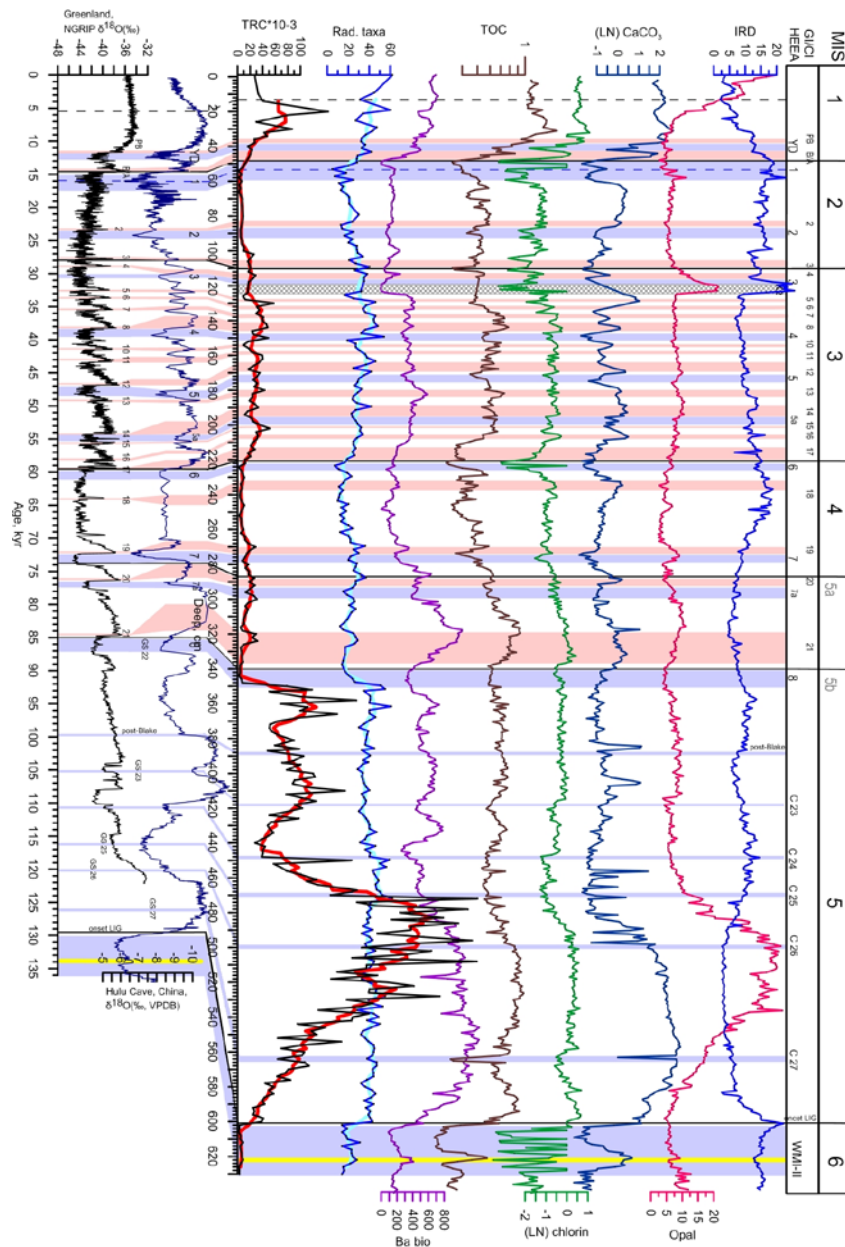


Fig. Total radiolarian content (TRC) ($\text{No}\# \text{ Rad. per. } 1\text{g} \cdot 10^3$) - black/red line; species richness of radiolarian assemblage (SR) ($\text{No}\# \text{ Rad. taxa per. sample}$) - dark/light blue line; Ba-bio, (counts per second); TOC content (%); chlorin content LN(chlor, $\mu\text{g/g}$); CaCO_3 content (%); opal content (%); IRD (% course fraction $>0,063$ mm) from top core (cm). Blue bars shown Heinrich event equivalent anomalies (HEEA) and pink bars – Greenland/Chinese interstadials (GI/CI). Correlation of the OS MIS and millennial events was made according to age model [1, 2].

REFERENSES:

1. Yanchenko E.A., Gorbarenko S.A. 2015. Radiolarian responses of the central Okhotsk Sea to the global orbital and millennial scale climate oscillations over last 90 kyr. *Journal of Asian Earth Sciences* 114 (3). 601-610
2. Sergey Gorbarenko, Tatyana Velivetskaya, Mikhail Malakhov, Aleksandr Bosin. 2017. Glacial terminations and the Last Interglacial in the Okhotsk Sea; Their implication to global climatic changes. *Global and Planetary Change* 152. 51–63
3. Wang Y.J., Cheng H., Edwards R.L. et al. Millennial- and orbital-scale changes in the East Asian monsoon over the past 224,000 years // *Nature*. 2008. Vol. 451. P. 1090–1093.
4. North GRIP (Greenland Ice Core Project Members), 2004. High resolution climate record of the Northern Hemisphere reaching into the last interglacial period. *Nature* 431, 147–151.

SATELLITE REMOTE SENSING OF EXTREME WEATHER

Jingsong Yang, Gang Zheng, Guoqi Han, Dake Chen

State Key Laboratory of Satellite Ocean Environment Dynamics, Second Institute of Oceanography, SOA, Hangzhou,
China

jsyang@sio.org.cn

Tropical cyclones (or typhoons/hurricanes) eyes' centers extracted from SAR images (corresponding to the footprints of typhoons on the sea surface) such as ENVISAT ASAR and RADARSAT SAR images, and from optical images (corresponding to the typhoons on the cloud top) such as Moderate Resolution Imaging Spectroradiometer (MODIS), multi-functional transport satellite (MTSAT) and Fengyun (FY)-2 Chinese meteorological satellite infrared (IR) images by using wavelet-based algorithm and two newly developed algorithms are compared to the tropical cyclone best track (BT) data sets from meteorological agencies such as Joint Typhoon Warning Center (JTWC), Chinese Meteorological Administration (CMA), and the Japan Meteorological Agency (JMA). It is found that the typhoon eyes' centers on the sea surface extracted from SAR images are typically 20-30 km away from those on the cloud top extracted from optical images. It is also found that the three BT data sets are generally closer to the eyes' centers extracted from the SAR images showing sea surface footprints of the typhoon centers than those from the optical images showing cloud top centers of the typhoons.

Storm surges induced by tropical cyclones are often the greatest threat to life and property of coastal areas. HY-2A is the first Chinese ocean dynamic environment monitoring satellite, which was launched in August 2011. The satellite repeats its ground track every 14 days. It plays an important role in global monitoring of sea surface winds (especially extreme winds like typhoons and hurricanes), ocean waves, currents, eddies, and extreme events like storm surges by using its four major payloads, i.e. radar altimetry, microwave scatterometer, scanning microwave radiometer and calibration microwave radiometer. The HY-2A data are obtained from China's National Satellite Ocean Application Service (NSOAS). We use 1 s along-track data with a nominal spatial resolution of about 7 km. The altimetry data are corrected for wet tropospheric (based on the onboard calibration microwave radiometer) and ionospheric path delays, and for ocean, solid earth and pole tides. Several typhoon storm surges were observed by HY-2A satellite altimetry. The storm surge magnitude and the cross-shelf e-folding decay scale are given. The present study shows that the HY-2A satellite altimetry is a useful tool for typhoon storm surges observation.

PERSISTENT EFFECTS OF THE YELLOW RIVER ON THE CHINESE MARGINAL SEAS BEGAN AT LEAST ~880 KA AGO

Zhengquan Yao^{1,2}, Xuefa Shi^{1,2}, Shuqing Qiao^{1,2}, Jianxing Liu^{1,2}, Yanguang Liu^{1,2}, Jihua Liu^{1,2}, Xisheng Fang^{1,2}, Jingjing Gao^{1,2}

¹ Key Laboratory of Marine Sedimentology and Environmental Geology, First Institute of Oceanography, SOA, Qingdao, China

² Laboratory for Marine Geology, Qingdao National Laboratory for Marine Science and Technology, Qingdao, China
yaozq@fio.org.cn; xfshi@fio.org.cn

The Yellow River (or Huanghe and also known as China's Sorrow in ancient times), with the highest sediment load in the world, provides a key link between continental erosion and sediment accumulation in the western Pacific Ocean. However, the exact age of its influence on the marginal sea is highly controversial and uncertain. Here we present high-resolution records of clay minerals and lanthanum to samarium (La/Sm) ratio spanning the past ~1 million years (Myr) from the Bohai and Yellow Seas, the potential sedimentary sinks of the Yellow River. Our results show a climate-driven provenance shift from small, proximal mountain rivers-dominance to the Yellow River-dominance at ~880 ka, a time period consistent with the Mid-Pleistocene orbital shift from 41-kyr to 100-kyr cyclicity. We compare the age of this provenance shift with the available age data for Yellow River headwater integration into the marginal seas and suggest that the persistent influence of the Yellow River on the Chinese marginal seas must have occurred at least ~880 ka ago. This new finding is the first offshore evidence on the drainage history of the Yellow River within an accurate chronology framework.

PRODUCTION CHARACTERISTICS OF BACTERIA AND PHYTOPLANKTON IN THE SEA OF OKHOTSK AND BERING SEA DURING SPRING–SUMMER IN 2000, 2013, 2016 YEARS

**Sergei Zakharkov¹, Yulianna Shambarova¹, Alena Moskovtseva^{1,4}, Elena Shtraikhert¹,
Xuefa Shi², Raisa Gladkich³, Jianjun Zou^{5,6}, Yanguang Liu^{5,6}**

¹ Il'ichev Pacific Oceanological Institute, Vladivostok, Russia

² First Institute of Oceanology, SOA, Qingdao, China

³ Elyakov Pacific Institute of Bioorganic Chemistry, Vladivostok, Russia

⁴ Far Eastern Federal University, Vladivostok, Russia

⁵ Key Laboratory of Marine Sedimentology and Environmental Geology, First Institute of Oceanography, SOA, Qingdao, China

⁶ Laboratory for Marine Geology, Qingdao National Laboratory for Marine Science and Technology, Qingdao, China
zakharkov@poi.dvo.ru

Production of heterotrophic bacteria plays an important role in the carbon turnover in marine ecosystems. While consuming the carbon fixed by phytoplankton in the course of photosynthesis, these microorganisms in turn form the basis of the bacterial feeding chain and become food for filtrating mesozooplankton. The principal parameters characterizing the role of bacterioplankton are its biomass, abundance, and production. Bacteria contribute to the carbon turnover in trophic chains; the total bacterial abundance in the global ocean is as high as 3.1×10^{28} cells [1]. In turn, the level of biological production by bacterioplankton depends on the level of primary phytoplankton production. The levels of primary and bacterial production, as well as the proportion between them, exhibit a pronounced seasonal and geographical variation [2]. Characteristics of bacterioplankton production are also affected by pH of the sea water, which in turn depends on the CO₂ content in the atmosphere.

In spite of the obvious importance of the microbial component of the ecosystem, the body of data describing the distribution and activity of bacterioplankton in the Northern seas of Russia is relatively small, which is due to the isolated location of most of these regions and the relatively short ice-free period [3]. Studies investigating such production characteristics of phyto- and bacterioplankton as chlorophyll a concentration, bacterial abundance, and production, were performed as a part of the RUSALCA Program in 2004, 2009, and 2012. The goal of the present work was to evaluate the production characteristics of bacterioplankton and to analyze their relationship to phytoplankton production and biomass, as well as to substrate concentration in the western part of the Sea of Okhotsk, the Bering Sea, and in the Northwestern Pacific.

Research subjects. To determine the production characteristics of microbial and phytoplankton communities, water samples were collected from the Sea of Okhotsk during an expedition of the RV Professor Gagarinskii from June 2 to June 16, 2000 [4] and from the Bering

Sea and the Northern Pacific Ocean during an expedition of the RV Akademik Lavrent'ev from July 26 to September 3, 2013 [5] and in the above areas in expedition of the RV Akademik Lavrent'ev from July 17 to August 17, 2016. The locations of sample collection sites in the Sea of Okhotsk and the Bering Sea are shown on Figs. A, B, C respectively. List the production characteristics of the microbial and phytoplankton communities and the estimates of dissolved organic matter. Water samples were collected from two to five horizons of the euphotic zone.

Primary phytoplankton production. PP levels were determined using the radiocarbon modification of the light-and-dark-bottle technique [6].

Levels of bacterioplankton production were determined using the radiocarbon method proposed by Romanenko and modified by Sorokin [6]. The method is based on measuring the dark CO₂ assimilation using ¹⁴C.

Assessment of dissolved organic matter was performed by calculating the difference of light absorption by detritus and yellow matter (dissolved organic matter) at the wavelengths of 412 and 443 nm: $adg(412) - adg(443)$ [7].

The study 28th expedition of the RV Professor Gagarinskii in 2000 was performed in June; during this period, PP levels ranged from 51 to 281 mg C m⁻³ day⁻¹ depending on the site. The corresponding BP values ranged from 1 to 8 mg C m⁻³ day⁻¹, amounting to 0.5 to 5.8% PP at the same site. The levels of bacterioplankton production varied depending on the location of the station and the sampling horizon. Generally, BP levels decreased with depth, but on several occasions the samples collected at 100 m were characterized by higher BP than those from subsurface horizons of 1–3 m. The highest productivity of bacterioplankton (55.9 mg C m⁻³ day⁻¹) was observed in the Anan Bay (station 10) at the depth of 1 m. The lowest BP level (0.08 mg C m⁻³ day⁻¹) was registered to the south of Cape Lopatka (station 3) at the depth of 3 m in the 63rd expedition and at station 23 (0.03 mg C m⁻³ day⁻¹) in the 76th expedition in the central part of the Bering Sea. Primary production was measured along with BP at the same sites, mainly in surface waters (1–3 m) and, on two occasions (stations 5 and 12), at the depth of 50 m. The maximal level of phytoplankton production (211 mg C m⁻³ day⁻¹) was registered at station 10 (the Anan Bay) at the depth of 1 m. In this case the ratio between bacterial and primary production (BP/PP).

The maximal BP level was observed in the Anan Bay; the same station was also characterized with a high level of chlorophyll fluorescence. At the same time, the abundance of cultivable bacterial plankton in this location was not the highest, while the location with the maximal bacterioplankton abundance (at the depth of 100 m by the shore of Kamchatka, station 17) exhibited an average level of BP. This probably suggests that BP levels do not depend directly on the abundance of cultivable microbial cells. On the other hand, the high microbial abundance observed at the depth of 100 m at station 17 may be due to the sinking of bacterial cells after the

peak of bacterioplankton development, which usually occurs in this region in July [3], while the samples from this site were collected on August 25. The decrease in bacterioplankton concentration in the course of the expedition can be illustrated by observations performed in the Anan Bay on August 8 and August 11, 2013. The distance between the sites of observation was less than one mile. The measurements of August 11 revealed a significant decrease in the BP and PP levels, in the ratio between these parameters, as well as in the concentration of dissolved organic matter as evaluated by satellite data in comparison to the data from August 8, 2013.

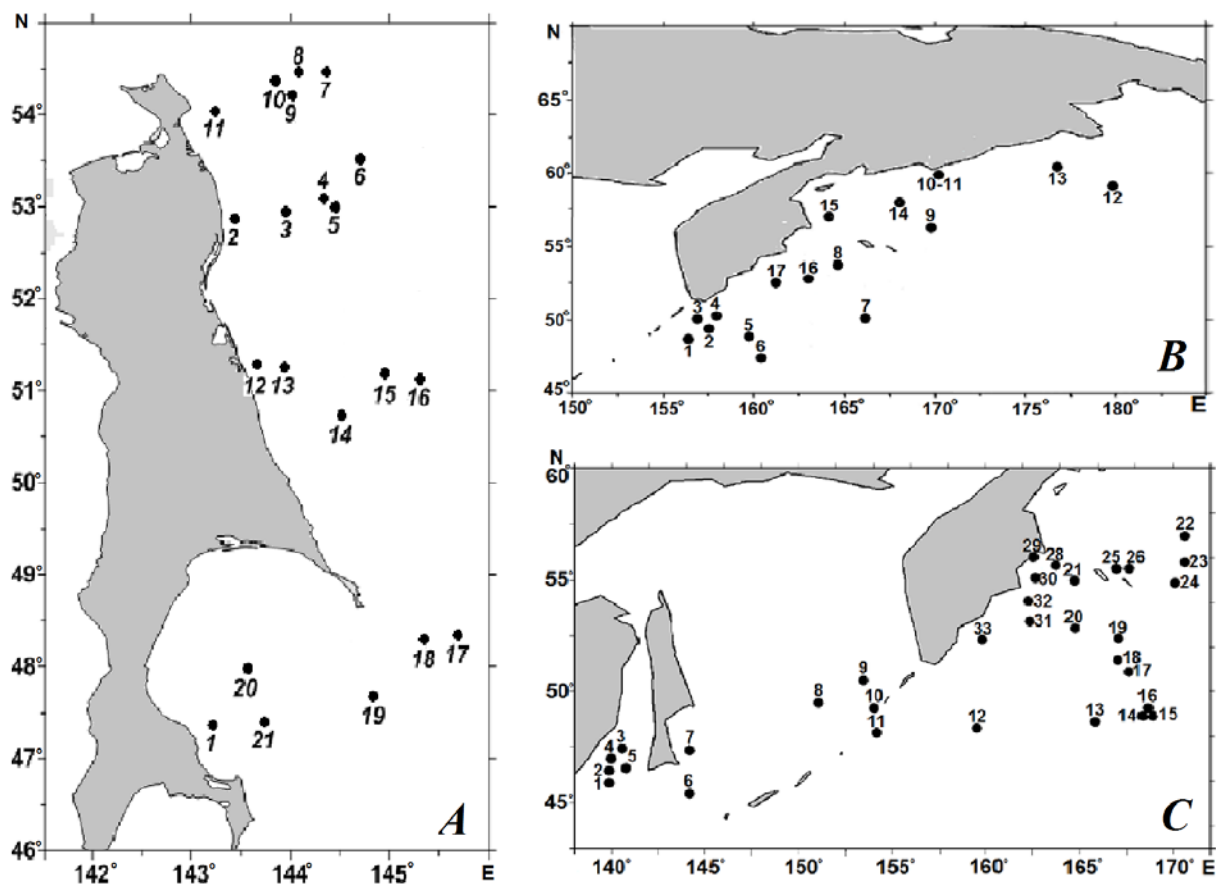


Fig. Location of stations in expeditions: A – 28th expedition of the RV Professor Gagarinskii, B – 63rd expedition of the RV Akademik Lavrent’ev, C – 76th expedition of the RV Akademik Lavrent’ev.

Since in each expedition the number of stations where BP samples were collected on clear days for which satellite data for evaluation of dissolved organic matter were available was limited, it was decided to perform statistical analysis for a combined set of data from the three expeditions. It was found that the coefficient of correlation between the BP level and the dissolved organic matter estimate based on the satellite data was 0.886 (29 points) and was significant with a confidence interval of 99%, even though the expeditions were performed in different times of the year. The common trend of increasing substrate concentration and bacterial production was observed at the stations located close to the shore (Figs. A, B, C). According to the data obtained in our study, PP levels in surface horizons ranged from 12.2 to 211 mg C m⁻³ day⁻¹. The highest PP

values were registered at station 10 (the Anan Bay). The level of BP was the highest in the Anan Bay of the Bering Sea (55.9 mg C m⁻³ day⁻¹) and the lowest in an eddy in the Northwestern Pacific (0.06 mg C m⁻³ day⁻¹). The ratio between bacterial and primary production at different stations ranged from 1.8 to 2600% in the water column and from 0.13 to 43% in the surface layer. We suppose that, after accumulating a larger body of concordant observations concerning the levels of bacterial production and the difference in light absorption at 412 and 443 nm, which characterizes dissolved organic matter, it may be possible to develop a method of evaluating BP levels in different regions and periods of the year based on the satellite data.

REFERENCES:

1. Karner, B.K., DeLong, E.F., and Karl, D.M. Archaeal dominance in the mesopelagic zone of the Pacific ocean, *Nature*, 2001, vol. 409, pp. 507–510.
2. Chen, B., Huang, B., Xie, Y., Guo, C., Song, S., Li, H., and Liu, H., The bacterial abundance and production in the East China Sea: seasonal variations and relationships with the phytoplankton biomass and production, *Acta Oceanol. Sin.*, 2014, vol. 33, no. 9, pp. 166–177.
3. Flint, M.V., Sukhanova, I.N., and Kopylov, A.I., Comparative role of bacteria and phytoplankton in the pelagic organic carbon cycle in the Eastern Bering Sea (Pribilof Islands Area), *Oceanology*, 2003, vol. 43, pp. 48–62.
4. Zakharkov, S.P., Selina, M.S., Vanin, N.S., Shtraikhert, E.A., and Biebov, N., Phytoplankton characteristics and hydrological conditions in the western part of the Sea of Okhotsk in the spring of 1999 and 2000 based on expeditionary and satellite data, *Oceanology*, 2007, vol. 47, pp. 519–530.
5. Zakharkov S.P., Vladimirov A.S., Shtraikhert E.A., X. Shi, Gladkich R.V., Buzoleva L.S., *Microbiology*, 2017, Vol. 68, No. 3, pp. 387–394.
6. Sorokin, Yu.I., *Radioisotopic Methods in Hydrobiology*, Heidelberg: Springer, 1999.
7. Zakharkov, S.P., Shtraikhert, E.A., Shambarova, Y.V., Gordeichuk, T.N., and Shi X. Measuring chlorophyll a concentrations in the Sea of Japan using probe and flow fluorimeters, *Oceanology*, 2016, vol. 56, pp. 444–451.

BENTHIC PROXY OF THE PRODUCTION TREND OF THE YELLOW SEA

**Xuelei Zhang, Zongling Wang, Jihua Liu, Qinsheng Wei, Shiliang Fan, Mingzhu Fu,
Yan Li, Ping Sun, Ping Li, Qinzeng Xu**

Center for Marine Ecology Research, First Institute of Oceanography, SOA, Qingdao, China

zhangxl@fio.org.cn

The Yellow Sea is a semi-enclosed shallow shelf and is vulnerable to eutrophication pressures from the neighboring lands. To date, it is difficult to resolve the history of production in the Yellow Sea, largely due to lack of long term systematic observation in the region. We presents an analysis of sediment records of the key bioactive elements C, N and P at three sites locating in the north, middle and south of the Southern Yellow Sea. The sediment contents of total organic carbon (TOC) and total nitrogen (TN) presented an overall increasing feature over the last century; the molar ratios C/N and C/P also presented significant increases since six decades ago. The low C/N ratios (<8) in the middle and north of the Southern Yellow Sea also indicated that the sediment organics derived from the sea. The contents of TOC, TN and TP in the surface sediment were mostly positively correlated with contents of these elements except for TP and primary productivity in the overlying water column of Southern Yellow Sea. The trends of historical changes of sediment contents of TN and TP and N/P molar ratio were consistent with the observed increase of nutrients in the water column of 36°N in the Yellow Sea since late 1970s/late 1980s and the trends of TOC and TN contents also paralleled with the decadal increases of chlorophyll a content, zooplankton biomass and macrobenthic biomass. The results indicated that the Yellow Sea has received more nutrient inputs from the neighboring lands, which stimulated the sea's production toward a higher level through bottom-up effects.

SEDIMENTARY OXYGENATION VARIATIONS IN THE OKINAWA TROUGH OVER THE LAST GLACIAL PERIOD: IMPLICATIONS FOR THE VENTILATION OF NPIW

Jianjun Zou^{1,2}, Xuefa Shi^{1,2}

¹Key Laboratory of Marine Sedimentology and Environmental Geology, First Institute of Oceanography, SOA, Qingdao, China

²Laboratory for Marine Geology, Qingdao National Laboratory for Marine Science and Technology, Qingdao, China
zoujianjun@fio.org.cn

In this study, we investigate a suite of sediment geochemical proxies (total organic carbon and carbonate contents, carbon to nitrogen ratio, aluminium and redox-sensitive elements) to reconstruct the history of sedimentary oxygenation in the northern Okinawa Trough (OT) over the last 50 thousand years (ka). Our data support the presence of oxygen-deficient deep waters during the late deglacial and Preboreal phases (15–9.5 ka), but oxygenated water column during the Heinrich Stadial 1 (HS1) and the Last Glacial Maximum (LGM). In contrast, increased sedimentary oxygenations are evident during the late glacial period and since 8.5 ka. Fluctuations of sedimentary oxygenation were widespread and apparently coherent over the entire North Pacific basin, reflecting broad effects of North Pacific Intermediate Water (NPIW) ventilation and export productivity. Intensified Kuroshio, however, improved the sedimentary oxygenation since 8.5 ka. We found the correspondence between changes in deglacial sedimentary oxygenation in the OT and Atlantic Meridional Overturning Circulation through the NPIW ventilation. The mechanism behind Atlantic-Pacific ventilation seesaw seems to be attributed to the perturbation of sea ice formation in high latitude North Pacific through atmospheric teleconnection.

This work is granted by the national program on global change and Air Sea Interaction (GASI-GEOGE-04, by the National Natural Science Foundation of China (Grant No: 41476056, 41420104005, U1606501, 41611130042).

REEs GEOCHEMISTRY OF SURFACE SEDIMENTS IN THE CHUKCHI AND EAST SIBERIAN SEAS

Valentina Sattarova¹, Kirill Aksentov¹, Anatoly Astakhov¹, Xuefa Shi²

1. V.I. Il'ichev Pacific Oceanological Institute, Vladivostok, Russia

2. First Institute of Oceanography, SOA, Qingdao, China

sval_80@poi.dvo.ru

Rare earth elements (REE) are a unique set of elements. REEs content and their relative distribution in sediments and sedimentary rocks are powerful tools for the determining geological conditions and processes. Two elements (Ce and Eu) distinguish themselves among this group; they are changing their oxidation states under oxidizing and reducing conditions. In addition, the close chemical properties of REE lead to a slow change in their composition under the influence of natural processes, leading to the reflection of the sources of matter, as well as the physico-chemical characteristics of the processes that are going on. Respectively, the study of REEs is of increasing interests to geochemists and geologists.

The Chukchi and East Siberian seas are least studied due to the harsh climatic conditions and the duration of the ice period. The Chukchi Sea plays an important role in the exchange of substance and energy between the Arctic Ocean and the Pacific Ocean, and is also sensitive to changes of the global climate. Few previous studies of REEs in sediments from these seas have been carried out. Chen et al. [1] analyzed 26 surface samples from the Chukchi Sea for rare earth elements and found higher concentrations in fine-grained sediments with shale-normalized REE patterns that were consistent with terrigenous components subjected to only weak chemical weathering. Yang et al. [2] studied the correlation between REEs in lagoon sediments and climate change in the region of Barrow in Alaska. Concentrations of La, Ce, Nd in surface sediments from East Siberian Sea were showed in Viscosi-Shirley et al. [3].

In this study, we determined all REEs spectrum in the surface sediments from the Polar Regions by the example of the Chukchi and East Siberian seas. On the basis of these data demonstrated the features of their distribution and considered the relationship of lanthanides with organic matter and other chemical elements and parameters.

Surface sediments were collected during the expeditions 46 and 52 on R/V “Professor Khromov” (2002, 2004), “Sever” (2006) and 77 on R/V “Akademik M.A. Lavrentyev” (2016). Determination of trace and REE contents in the samples was performed at the Common Use Center of the Far East Geological Institute, FEB RAS, by ICP-MS using an “Agilent 7500c” quadrupole mass-spectrometer (Agilent Technologies, USA). To correct for instrumental drift and matrix effects, 10^{-7} % of added ^{115}In was used as an internal standard. Other major elements were analyzed by ICP-AES using an “ICAP6500 Duo” spectrometer (Thermo Electron Corporation, USA). To correct for instrumental drift and matrix effects, 10^{-4} % of added cadmium solution was used as an

internal standard. In order to check data quality, Russian Geological Samples of oceanic sediment standards OOPE 401 (calcareous ooze) and OOPE 101 (terrigenous clay) were measured.

The spatial distribution of REEs in surface sediments is plotted in Fig. 1. The REEs concentrations in the Chukchi Sea range from 62 to 169 mg/kg. The average REEs content in the surface sediments is 113 mg/kg.

The concentrations of the lanthanide in bottom sediments from the East Siberian Sea are higher as distinct from ones in the Chukchi Sea and consist from 108 mg/kg to 200 mg/kg, averaging 166 mg/kg (Fig. 1).

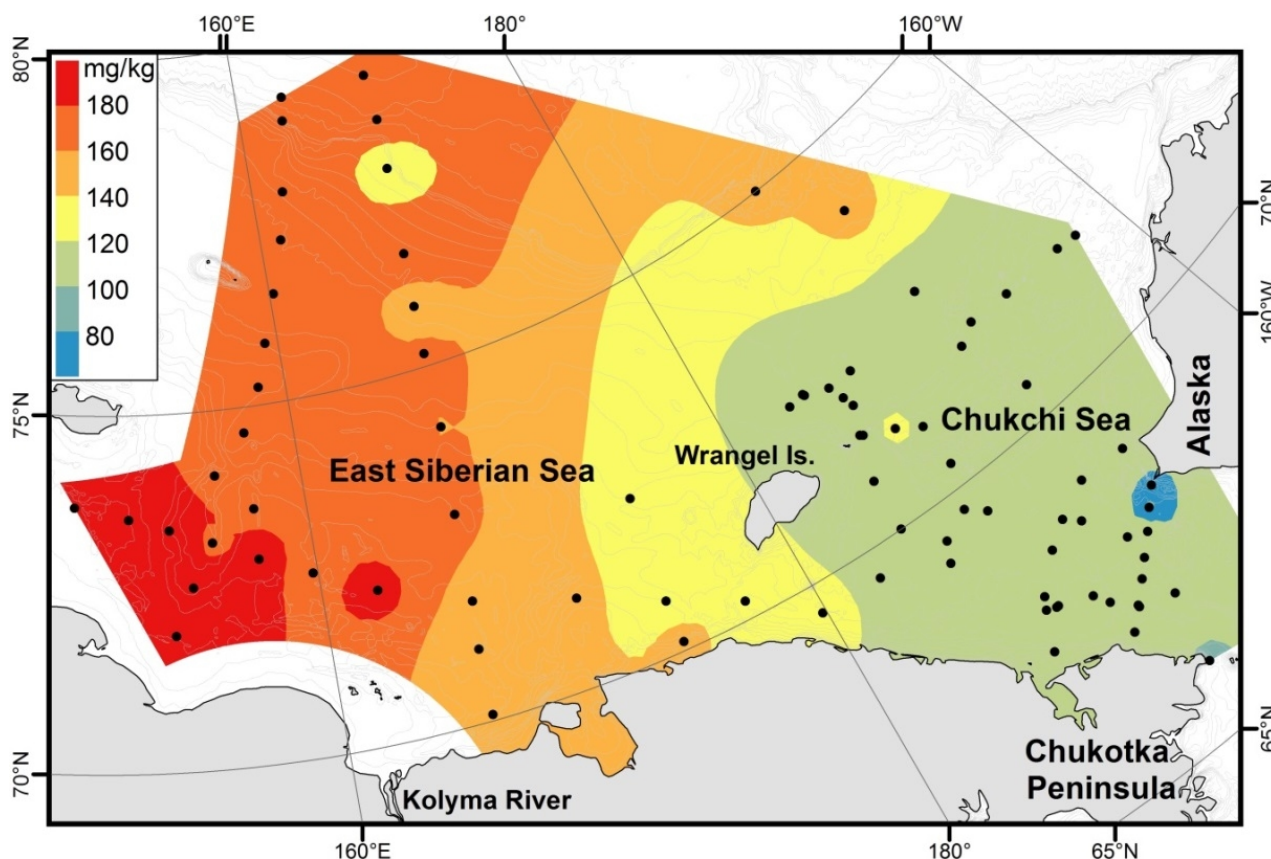


Fig. 1. Map of the study areas and REEs distribution in surface sediments.

To clarify the REEs distribution in the sediments we normalized the REEs content in samples to North American Shale Composite NASC [4]. The distribution shale-normalized REEs pattern of all sediment samples from the Chukchi Sea are similar and characterized by the slightly enriches light and medium REEs (Fig. 2). The LREE/HREE ratio varies from 1.27 to 1.76. All REEs patterns show weak positive anomalies of Ce and Eu ($Ce_{an} = 0.89-1.08$, averaging 1.02; $Eu_{an} = 0.96-1.18$, averaging 1.03).

The shale-normalized REEs pattern of sediments from the East Siberian Sea distinguished from Chukchi sediments by distribution of light REE (La, Ce). Value Ce_{an} has the range from 0.91 to 1.01, averaging 0.96; value Eu_{an} has variation range of 0.88 - 1.07, averaging 0.98. The LREE/HREE ratio ranges from 1.31 to 1.80.

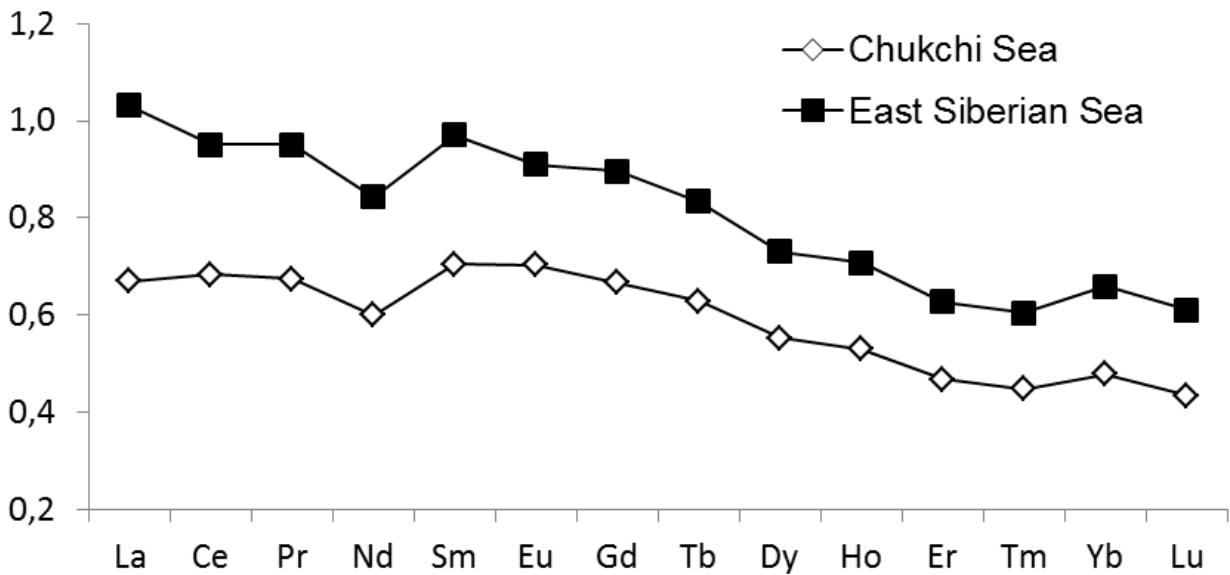


Fig. 2. Mean shale-normalized REEs distribution of sediments in the Chukchi and East Siberian seas.

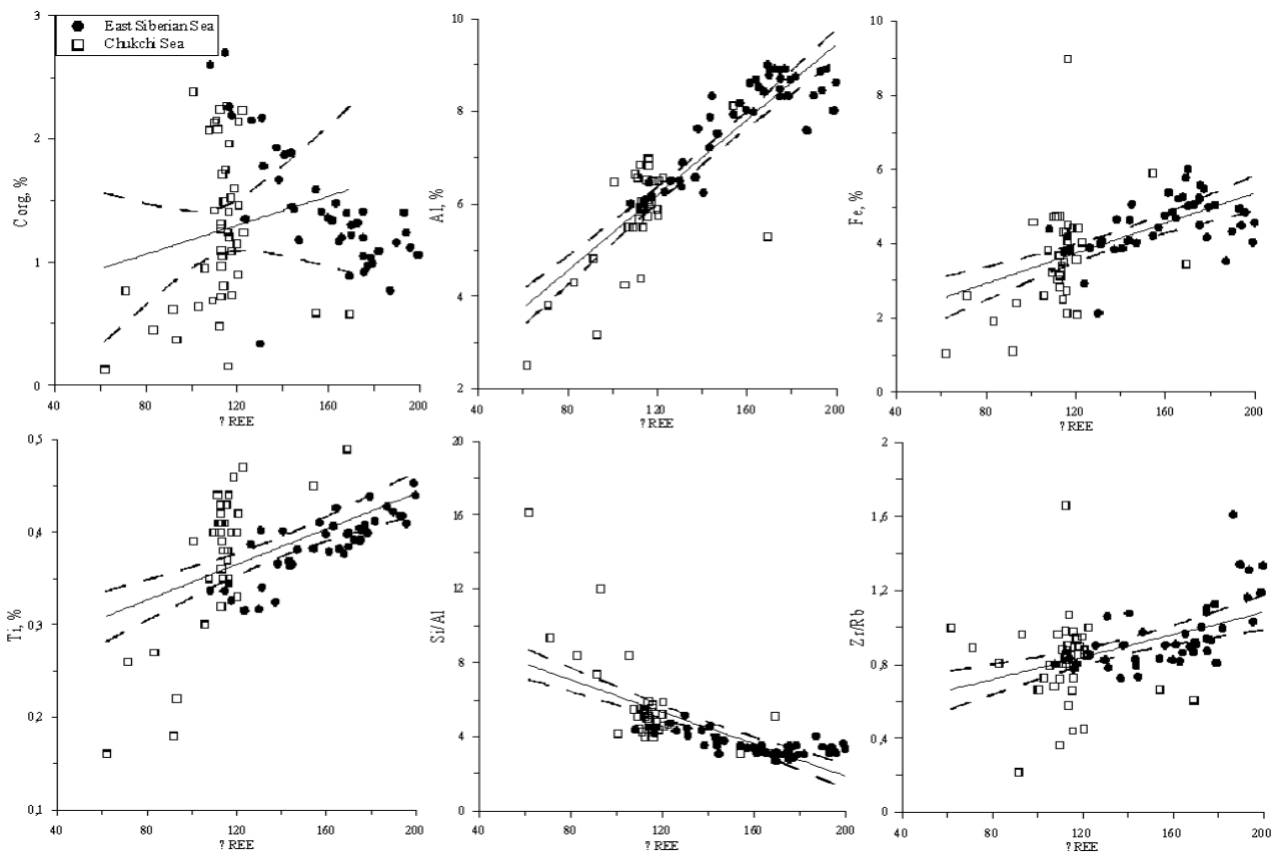


Fig. 3. Correlation between Σ REEs and other elements, lithological indices in the sediments from the Chukchi and East Siberian seas.

Accumulation in the bottom sediments of light REE is related with more higher migration rates for soluble complex compounds of heavy lanthanides compared with ones for light REE compounds [5].

To elucidate the geochemical behavior of REEs, we considered their correlations with other elements and lithological indices. It is seen that the REE contents depend on the concentrations of

Al, Fe, Ti, and show no dependence on the C_{org} content (Fig. 3). The influence of distributive provinces can be observed in a positive relationship with the Zr/Rb ratio, which is an indicator of the content of heavy minerals. The revealed correlation the contents of REEs and those of Al, Fe and Ti is probably due to the properties of lanthanide are accumulated by the iron hydroxides.

The work was supported by the Russian Science Foundation (Project no. 16-17-10109).

REFERENCES:

1. Chen, Z., Gao, A., Liu, Y., Sun, H., Shi, X., Yang, Z. REE geochemistry of surface sediments in the Chukchi Sea // *Science in China*. 2003. V. 46. N 6. P. 603-611.
2. Yang, W.L., Mao, X.Y., Dai, X.X. et al. REE characteristics and environmental significance in Core 96-7-1 in Elson Lagoon in the region of Barrow in the Arctic // *Chinese Journal of Polar Research* (in Chinese). 2001. V. 13. N 2. P. 91-106.
3. Viscosi-Shirley, C., Mammone, K., Piasias, N., Dymond, J. Clay mineralogy and multi-element chemistry of surface sediments on the Siberian-Arctic shelf: implications for sedimen provenance and grain size sorting // *Continental Shelf Research*. 2003. V. 23. P. 1175-1200.
4. Gromet, L.P., Dymek, R.F., Haskin, L.A., Korotev, R.L. The "North American Shale Composite". Its Compilation, Major and Trace Element Characteristics // *Geochim. Cosmochim. Acta*, 1984. V. 48. P. 2469–2482.
5. Dubinin, A.V. Rare earth element geochemistry in the ocean. 2006. Moscow. Nauka. 360 pp. (in Russian).

CONTENTS:

<i>Antonina Artemova, Valentina Sattarova, Yuriy Vasilenko</i> . Diatom distribution and geochemical evidence in the Holocene Kurile basin sediments (Sea of Okhotsk).....	6
<i>Anatoly Astakhov, Yanguang Liu, Andrey Dar'in, Ivan Kalugin, Aleksandr Bosin, Elena Vologina</i> . Ice conditions of the Last Centuries in the northern Chukchi Sea: reconstructions using detailed variation of chemical composition in shelf sediments	12
<i>Nadezhda Astakhova</i> . Gold, silver and platinum in ferromanganese crusts from marginal seas of the Northwest Pacific	16
<i>Alexander Charkin, Michiel Rutgers van der Loeff, Natalia Shakhova, Örjan Gustafsson, Oleg Dudarev, Maxim Cherepnev, Anatoly Salyuk, Andrey Koshurnikov, Eduard Spivak, Alexey Gunar, Alexey Ruban, Igor Semiletov</i> . Discovery and characterization of submarine groundwater discharge in the Buor-Khaya gulf, Laptev Sea.....	19
<i>Yuan Chi, Honghua Shi</i> . Evaluation on island ecological vulnerability and its spatial heterogeneity.....	20
<i>Alexander Derkachev, Sergey Gorbarenko, Maxim Portnyagin, Nataliya Nikolaeva, Xuefa Shi, Yanguang Liu</i> . New data on tephrostratigraphy of Holocene-Pleistocene deposits from the north-west Pacific (on the basis of the materials of 76th Cruise of the R/V "Akademik M.A. Lavrentyev").....	21
<i>O. Dudarev, A. Charkin, I. Semiletov, N. Shakhova, D. Chernykh, A. Ruban, T. Tesi, O. Gustafsson</i> . Sedimentation environments on the Laptev Sea outer shelf (northern polygon).....	23
<i>Wei Gao, Ping Li, Jie Liu</i> . Sedimentary environment and framework characteristics of Diaokou lobe in the modern Yellow River delta	27
<i>Y. Golozubova, L. Buzoleva, E. Bogatyrenko</i> . Microbiological diversity of proteobacterias from surface water of the Golden Horn.....	30
<i>Sergey Gorbarenko, Xuefa Shi</i> . Advances in the research of paleoceanography and climate changes in the Northern Pacific and marginal seas as a result of the Chinese-Russian cooperation during last decade.....	32
<i>Xiqiu Han</i> . Reconstruction of the paleo-bottom water temperatures using seep carbonates.....	37
<i>Limin Hu, Xuefa Shi, Yanguang Liu, Jianjun Zou, Kirsten Fahl, Xun Gong</i> . The sedimentary response of organic matter to natural forcing in the Bering Sea: sea-ice variability and regime shift for the Past Century.....	38
<i>Ningjing Hu, Peng Huang, Jihua Liu, Xuefa Shi, Hui Zhang</i> . Sr, Nd and Pb isotopes as tracers of the middle Okinawa Trough detrital sediments: paleoenvironmental implication.....	39
<i>Viktor Kalinchuk</i> . Measurements of mercury concentrations in air and seawater during the First Russian-Chinese Arctic Research Expedition aboard the R/V "Akademik M.A. Lavrentev".....	40
<i>Dmitry Kaplunenko, Vyacheslav Lobanov, Pavel Tischenko, Sergey Sagalaev, Maria Shetsova, Xuefa Shi, Yanguang Liu</i> . The unique oceanographic measurements of climatic effects observed during the joint Russian-Chinese cruises of 2010-2016 to the North-East Asian marginal seas from surface to bottom.....	43
<i>Victor Karnaukh, Xuefa Shi, Evgeny Sukhoveev, Andrey Koptev</i> . The Late Neogene (?) volcanic activity on the Pervenets Rise: combination of high resolution seismic profiling and multibeam survey.....	44
<i>Ping Li, Yuanqin Xu, Lejun Liu, Hang Zhou, Wei Gao, Jie Liu</i> . Sedimentary structures and chemical elements distribution of the submarine landslide in the northern continental slope, South China Sea.....	46
<i>Jianxing Liu, Xi Mei, Xuefa Shi, Qingsong Liu</i> . Widespread occurrence of greigite (Fe ₃ S ₄) in the sediments of the central South Yellow Sea: implications for mid-Pleistocene palaeoenvironmental changes.....	47

<i>Jie Liu, Ping Li, Wei Gao, Xiao Liu</i> . Marine sedimentary environment evolution of the southern Laizhou Bay under the impact of port projects.....	48
<i>Galina Malakhova, Sergey Gorbarenko, Xuefa Shi, Yanguan Liu, Jianjun Zou</i> . Diagenesis of magnetic minerals in the sediments of the Japan Sea (Yamato Rise) for the last 78 ka and its effect on the geomagnetic and climatic signals.....	52
<i>Leonid Mitnik, Maia Mitnik, Vladimir Kuleshov</i> . Passive microwave sensing of the Northwest Pacific tropical zone from the current and next generation satellites.....	56
<i>Vadim Navrotsky</i> . The World Ocean as the main driver of Climate Change.....	60
<i>Tatiana V. Nikulina, Tatiana A. Mogilnikova</i> . Features of the phytoplankton communities in the Sakhalin Island coastal zone and characteristic of potential toxic algal species in the summer-autumn period 2015.....	61
<i>Anatoly Obzhirov</i> . Gasgeochemical indicators geological processes on the costal and sea.....	62
<i>Aijun Pan</i> . Local wintertime ventilation in the central North Pacific.....	64
<i>Irina Pipko, Svetlana Pugach, Irina Repina, Oleg Dudarev, Alexander Charkin, Igor Semiletov</i> . Distribution and air-sea fluxes of carbon dioxide on the Chukchi Sea shelf.....	65
<i>Sergei Pletnev, Yonghua Wu, Alexndra Romanova, Vladimir Annin, Olga Vereshchagina, Igor Utkin</i> . A history of methane release in southwestern part of the Okhotsk Sea during the last 10 000 years (foraminifera, $\delta^{13}\text{C}$, $\delta^{18}\text{O}$, ^{14}C).....	66
<i>Vladimir Ponomarev, Elena Dmitrieva, Svetlana Shkorba, Aleksandr Karnaukhov</i> . Climate regime change in the land-ocean-atmosphere system at the turn of 20-21 Centuries.....	69
<i>Sergey Prants</i> . How eddies gain, retain and release water: the Lagrangian approach.....	73
<i>Olga Psheneva, Tiegang Li, Sergey Gorbarenko, Xuefa Shi, Yanguang Liu, Jianjun Zou</i> . Bottom water condition changes in the NW Pacific during the Last Glacial Maximum- Holocene according to benthic foraminifera.....	74
<i>Shuqing Qiao, Xuefa Shi, Lin Zhou, Limin Hu, Gang Yang, Yanguang Liu, Zhengquan Yao</i> . Sediment accumulation and budget in the Bohai Sea, Yellow Sea and East China Sea.....	78
<i>Xiangwen Ren, James R. Hein, Li Li, Zanzhong Yang, Na Xing, Aimei Zhu, Xuefa Shi</i> . Controls on the concentration of Co in ferromanganese crusts from the Magellan seamounts, West Pacific.....	79
<i>Vladimir S'edin, Yury Mel'nichenko, Evgeny Terekhov</i> . Features of the geological structure of Marginal seas of the East Asia.....	80
<i>Kseniia Shcherbakova, Denis Kosmach, Elena Panova, Igor Semiletov, Natalia Shakhova, Örjan Gustafsson</i> . Initial results on methane isotopic composition in the East Siberian seas and Ob River.....	82
<i>Xuefa Shi, Jianjun Zou, Sergey Gobarenko</i> . Variations in sedimentary deposits and environment in the NW Pacific during the late Quaternary.....	83
<i>Hongjun Song, Rubao Ji, Yun Li, Andrew R. Solow</i> . Derive chlorophyll distributional pattern from 'gappy' satellite data in the Arctic Ocean: a statistical approach.....	84
<i>Ira Tsoy, Mariia Obrezkova, Anatoly Astakhov, Xuefa Shi, Limin Hu</i> . Diatoms as indicators of the Late Holocene environmental changes in the East Siberian and Chukchi seas.....	85
<i>Yuriy Vasilenko, Sergey Gorbarenko, Aleksandr Bosin, Xuefa Shi, Tatyana Khusid, Jianjun Zou, Yanguang Liu, Mikhail Savenko</i> . The sea ice conduction in the eastern Sea of Okhotsk during the deglaciation and Holocene.....	88
<i>Galina Vlasova, Svetlana Marchenko, Natalya Rudykh</i> . SSTa and CHL_a_ as indicators of upwelling along the coast of Vietnam.....	92
<i>Elena Vologina, Michael Sturm, Anatoly Astakhov, Xuefa Shi, Ivan Kalugin, Andrey Darin, Limin Hu</i> . Characteristics of surface bottom sediments of the south part of Chukchi Sea (preliminary results).....	94
<i>Weibo Wang</i> . The influence of sea surface temperature in November on the increment of sea ice area between December and the following January in Bering Sea.....	97

<i>Shiguo Wu, Lingju Gao, Jian Zhang</i> . Analysis of lithospheric rheological structure and dynamics in the Mariana subduction zone.....	98
<i>Elena Yanchenko, Sergey Gorbarenko</i> . Radiolarian responses of the Okhotsk Sea to the orbital and millennial climate changes over the last 135 kyr.....	101
<i>Jingsong Yang, Gang Zheng, Guoqi Han, Dake Chen</i> . Satellite remote sensing of extreme weather.....	103
<i>Zhengquan Yao, Xuefa Shi, Shuqing Qiao, Jianxing Liu, Yanguang Liu, Jihua Liu, Xisheng Fang, Jingjing Gao</i> . Persistent effects of the Yellow River on the Chinese marginal seas began at least ~880 ka ago.....	104
<i>Sergei Zakharkov, Yulianna Shambarova, Alena Moskovtseva, Elena Shtraikhert, Xuefa Shi, Raisa Gladkich, Jianjun Zou, Yanguang Liu</i> . Production characteristics of bacteria and phytoplankton in the Sea of Okhotsk and Bering Sea during spring–summer in 2000, 2013, 2016 years.....	105
<i>Xuelei Zhang, Zongling Wang, Jihua Liu, Qinsheng Wei, Shiliang Fan, Mingzhu Fu, Yan Li, Ping Sun, Ping Li, Qinzeng Xu</i> . Benthic proxy of the production trend of the Yellow Sea.....	109
<i>Jianjun Zou, Xuefa Shi</i> . Sedimentary oxygenation variations in the Okinawa Trough over the Last Glacial Period: implications for the ventilation of NPIW.....	110
<i>Valentina Sattarova, Kirill Aksentov, Anatoly Astakhov, Xuefa Shi</i> . REEs geochemistry of surface sediments in the Chukchi and East Siberian seas.....	111

Научное издание

ОКЕАНОЛОГИЧЕСКИЕ ПРОЦЕССЫ И ИЗМЕНЕНИЯ КЛИМАТА

3-й международный российско-китайский симпозиум по морским наукам

21-23 сентября 2017 г., Владивосток, Россия

Материалы докладов

Материалы докладов печатаются в авторской редакции

Составитель оригинал-макета: Е.А. Янченко

Подписано к печати 14.09.2017 г.

Сетевое (on-line) электронное издание

Тихоокеанский океанологический институт им. В.И. Ильичева

690041, г. Владивосток, ул. Балтийская, 43

Тел. (423)2311-400, факс (423) 2312-573, email: opcc-2017@poi.dvo.ru